

3/82

CMCRCZ 11 (3), 181-267 (1982)

ΧΗΜΙΚΑ ΧΡΟΝΙΚΑ

ΝΕΑ ΣΕΙΡΑ

CHIMIKA CHRONIKA

NEW SERIES

**AN INTERNATIONAL EDITION
OF THE GREEK CHEMISTS ASSOCIATION**

MANAGING COMMITTEE

Irene DILARIS, Yannis GAGLIAS, Vassilios M. KAPOULAS, Vassilios LAMBROPOULOS,
Georgia MARGOMENOU - LEONIDOPOULOU, Panayotis PROUNTZOS, George SKALOS

Ex-officio Members: Panayotis PAPAPOPOULOS (Asst. Gen. Secretary of G.C.A.),
Stelios CHATZIYANNAKOS (Treasurer of G.C.A.).

EDITORS - IN - CHIEF

V.M. KAPOULAS G. SKALOS G. MARGOMENOU - LEONIDOPOULOU

EDITORIAL ADVISORY BOARD

N. ALEXANDROU <i>Org. Chem., Univ. Salonica</i>	E. KAMPOURIS <i>Polymer. Chem., Tech. Univ. Athens</i>	G. PNEUMATIKAKIS <i>Inorg. Chem., Univ. Athens</i>
A. ANAGNOSTOPOULOS <i>Inorg. Chem., Tech. Univ. Salonica</i>	M.I. KARAYANNIS <i>Anal. Chem., Univ. Ioannina</i>	C.N. POLYDOROPOULOS <i>Phys/Quantum Chem., Univ. Ioannina</i>
D. BOSKOS <i>Org. Chem., Tech., Univ. Salonica</i>	N. KATSANOS <i>Phys. Chem., Univ. Patras</i>	K. SANDRIS <i>Organic Chem., Tech. Univ. Athens</i>
P. CATSOULACOS <i>Pharm. Chem., Univ. Patras</i>	A.KEHAYOGLOU <i>Org. Chem. Tech., Univ. Salonica</i>	M.J. SCOULLOS <i>Env./Mar. Chem., Univ. Athens</i>
G.D. COUMOULOS <i>Physical Chemistry Athens</i>	D. KIOUSSIS <i>Petrochemistry, Univ. Athens</i>	C.E. SEKERIS <i>Mol. Biology, N.H.R.F., Athens</i>
C.A. DEMOPOULOS <i>Biochemistry, Univ. Athens</i>	A. KOSMATOS <i>Org. Chem., Univ. Ioannina</i>	G.A. STALIDIS <i>Phys. Chem., Univ. Salonica</i>
C.E. EFSTATHIOU <i>Anal. Chem., Univ. Athens</i>	P. KOUROUNAKIS <i>Pharm. Chem., Univ. Salonica</i>	Ch. STASSINOPOULOU <i>N.R.C. «Democritos», Athens</i>
A.E. EVANGELOPOULOS <i>Biochemistry, N.H.R.F., Athens</i>	S.B. LITSAS <i>Bioorg. Chem., Arch. Museum, Athens</i>	A. STASSINOPOULOS <i>Argo AEBE Athens</i>
S. FILIANOS <i>Pharmacognosy, Univ. Athens</i>	G. MANOUSSAKIS <i>Inorg. Chem., Univ. Salonica</i>	A. STAVROPOULOS <i>Ind. Technol., G.S.I.S., Piraeus</i>
D.S. GALANOS <i>Food Chem., Univ. Athens</i>	I. MARANGOSIS <i>Chem. Mech., Tech. Univ. Athens</i>	I.M. TSANGARIS <i>Inorg. Chem., Univ. Ioannina</i>
A.G. GALINOS <i>Inorg. Chem., Univ. Patras</i>	I. NIKOKAVOURAS <i>Photochem., N.R.C. «D», Athens</i>	G. TSATSARONIS <i>Food Technol., Univ. Salonica</i>
P. GEORGAKOPOULOS <i>Pharm. Techn., Univ. Salonica</i>	D.N. NICOLAIDES <i>Org. Chem., Univ. Salonica</i>	G.A. TSATSAS <i>Pharm. Chem., Univ. Athens</i>
I. GEORGATSOS <i>Biochemistry, Univ. Salonica</i>	C.M. PALEOS <i>N.R.C. «Democritos», Athens</i>	A.K. TSOLIS <i>Chem. Technol., Univ. Patras</i>
M.P. GEORGIADIS <i>Org./Med. Chem., Agr. Univ. Athens</i>	V. PAPAPOPOULOS <i>N.R.C. «Democritos» Athens</i>	G. VALCANAS <i>Org. Chem., Tech. Univ. Athens</i>
N. HADJICHRISTIDIS <i>Polymer Chem., Univ. Athens</i>	G. PAPAGEORGIOU <i>Biophysics, N.R.C. «D», Athens</i>	A.G. VARVOGLIS <i>Org. Chem., Univ. Salonica</i>
T.P. HADJIIOANNOU <i>Anal. Chem., Univ. Athens</i>	V.P. PAPAGEORGIOU <i>Nat. Products, Tech. Univ. Salonica</i>	G.S. VASSILIKIOTIS <i>Anal. Chem., Univ. Salonica</i>
E. HADJLOUDIS <i>Photochem., N.R.C. «D», Athens</i>	S. PARASKEVAS <i>Org. Chem., Univ. Athens</i>	S. VOLIOTIS <i>Instrum. Analysis, Univ. Patras</i>
D. JANNAKOUDAKIS <i>Phys. Chem., Univ. Salonica</i>	G. PHOKAS <i>Pharmacognosy, Univ. Salonica</i>	E.K. VOUDOURIS <i>Food Chem., Univ. Ioannina</i>
N.K. KALFOGLOU <i>Polymer Sci., Univ. Patras</i>	S. PHILIPAKIS <i>N.R.C. «Democritos», Athens</i>	I. VOURVIDOU - FOTAKI <i>Org. Chem., Univ. Athens</i>
		I.V. YANNAS <i>Mech. Eng., M.T.I., U.S.A.</i>

Correspondence, submission of papers, subscriptions, renewals and changes of address should be sent to *Chimika Chronika, New Series*, 27 Kaningos street, Athens, Greece. The Guide to Authors is published in the first issue of each volume, or sent by request. Subscriptions are taken by volume at 500 drachmas for members and 1.000 drachmas for Corporations in Greece and 28 U.S. dollars to all other countries except Cyprus, where subscriptions are made on request.

Printed in Greece by ATHANASOPOULOS-PAPADAMIS-ZACHAROPOULOS, G.P.

76, EMM. BENAKI ATHENS (145)

Υπεύθυνος σύμφωνα με το νόμο: Παναγιώτης Ξυδάλης, Κάνιγγος 27, Αθήνα (147).

CONTENTS

The conductance and association behavior of alkali bromides in isopropanol-water mixtures (<i>in English</i>) by D.A. Jannakoudakis, G.C. Ritzoulis, J. Roubis	183
Kinetic study of the oxidation of benzoic acid hydrazide by mercury (II) acetate (<i>in English</i>) by Demetrius A Haristos and Doukeni E. Missopolinou	193
The conductance and association behavior of the sodium benzenesulfonate in dioxane-water mixtures (<i>in English</i>) by D.K. Panopoulos, D.A. Jannakoudakis	201
The determination of residual solvents in plastics packaging materials in relation to off odors developed in packaged bakery products (<i>in English</i>) by M.G. Kontominas and E. Voudouris	215
A Dirac-like equation (<i>in English</i>) by P.J. Lemos	225
Synthesis and structure elucidation of a new series of (triphenylphosphine) (N-alkyldithio- carbamate) (nitrosyl) nickel complexes (<i>in English</i>) by C.A. Tsipis, D.Ph. Kessissoglou and G.E. Manoussakis	235
Fluorescent properties of aromatic complexes with rare earths and other elements of the IIIa group (<i>in English</i>) by G. Kallistratos, U. Kallistratos and H. Mündner	249

THE CONDUCTANCE AND ASSOCIATION BEHAVIOR OF ALKALI BROMIDES IN ISOPROPANOL-WATER MIXTURES

D.A. JANNAKOUDAKIS, G.C. RITZOULIS, J. ROUBIS

University of Thessaloniki, Laboratory of Physical- Chemistry, Thessaloniki, Greece

(Received December 15, 1979)

Summary

In this work the conductance of the bromide salts of Sodium, Potassium, Rubidium and Caesium in isopropanol-water solvent mixtures at 25°C is studied. The experimental data were analysed by means of Fuoss-Onsager-Skinner conductometric equation and the values of limiting conductance, the association constant and the ion size parameter at various concentrations in isopropanol, in a region of dielectric constants $24 < D < 72$, are calculated.

It is found that the increase of the isopropanol's concentration in the mixture, leads to a decrease of the limiting conductance, while the association of the ions is increasing.

It is also found that the limiting conductance increases together with the crystallographic radii.

The variation of the Walden products of NaBr, KBr, RbBr, CsBr in isopropanol-water mixtures is also examined.

Key words : equivalent conductance.

Introduction

Previous conductometric measurements for alkali metal salts in various solvents and solvent mixtures showed that the ionic conductance decreases in the order $Cs > Rb > K > Na$. The differences are higher in water and lower in nitrobenzene and dimethylsulfoxide.¹

Because the ionic conductance of alkali metals increases with the size of an ion, it is logical to assume that the smaller ions are less conductive than the larger ones because the former are solvated stronger than the latter.

From the literature it is known that in solutions of symmetrical electrolytes having unequal ion-size, specific ion-solvent interactions take place when at least one component is polar. Conductometric measurements for alkali metal salts in water- ethanol mixtures have shown that the association of these salts increases as the crystallographic radii of the cation increase. Kay and co-workers have found

that the CsCl, in spite of the greater size of the cation, is more associated than KCl in ethanol- water mixtures. The same order was found by Kay for alkali halides in various hydrogen -bonded solvents; namely, association increases $\text{Li} < \text{Na} < \text{K} < \text{Rb}$.

In this work we examine the conductometric behavior of alkali metal ions in isopropanol - water mixtures in order to find out if the above mentioned order still remains for this system, for the isopropanol is a sec-alcohol having relatively high viscosity and low dielectric constant.

We used the salts NaBr, KBr, RbBr, CsBr which have a common ion in order to be able to make comparison of conductometric properties between the various metal ions.

Experimental

The salts NaBr, KBr, RbBr, CsBr under investigation were obtained from Merk grade Suprapur after recrystallisation from conductivity water and drying.

The isopropanol (puriss p.a.) was used after two distillations. The value of specific conductivity was found to be 5×10^{-8} mho cm^{-1} .

The resistances of the electrolytic solutions were measured by a precise conductance bridge, Beckman Model RC-18A, using a frequency of 3000 c/sec. Basically this bridge consists of an alternating current Weston Bridge and an oscilloscope for the determination of the balancing point.

The conductance cell used was similar to that described by Dagget Bair and Kraus.²

The determination of the cell constant was carried out by measuring the resistances of Potassium Chloride in aqueous solutions using the equation of Lind, Zwolenick, Fuoss.³ The cell constant was found equal to 0.868_5 cm^{-1} .

For each series of measurements the following procedure has been used.

About 300 ml of freshly prepared solvent was run into the cell against a counter current of nitrogen. The cell was then closed, weighed and placed in the thermostat. After thermal stabilisation nitrogen is introduced in the cell through a special device stirring in the meanwhile the cell contents. The nitrogen flow and the stirring is stopped, and the solvent resistance is measured. The same procedure is repeated for the measurement of the resistance of each solution.

The various solutions of the salts under examination were prepared by the following procedure. An approximately 0.03M stock solution of the salt was prepared for the respective solvent mixtures. Certain quantities of this solution were added in the conductance cell and the resistances were measured.^{4,5}

Before each run the cell was cleaned with fuming nitric acid and rinsed thoroughly with conductivity water.

The densities were measured at $25 \pm 0.01^\circ\text{C}$ using a Sprengel type pycnometer and the viscosities, at the same temperature, using an Ubbelohde viscometer which was calibrated with conductivity water with specific conductivity of $1 - 2 \times 10^{-6}$ mho cm^{-1} .

The value of the viscosity for the isopropanol was $\eta = 2.07 \times 10^{-2}$ poise in agreement with that reported in the literature.

The dielectric constants D of various solvent mixtures were measured by means of a Dipolmeter Type DM 01, (which operation is based on heterodyne principle). The Dielectric constant of our isopropanol was 19.45, in excellent agreement with the value 19.41 quoted by Dunnhauser and Bahe.⁶

Results and Discussion

The values of the viscosities and the dielectric constants of the isopropanol - water solvent mixtures used are listed in Table I. The solvent compositions given in this table are expressed in weight per cent isopropanol.

TABLE I : Physical Properties of Isopropanol-Water Mixtures at 25°C.

i-prOH w/w %	$\eta \cdot 10^2$ poise	D
10	1.390	72.35
20	2.038	65.80
40	2.891	49.96
60	3.005	35.43
80	2.543	24.21

Experimental values for the equivalent conductance Λ , the concentration c (equivalent per liter) of the salts examined in the various isopropanol solvent mixtures are listed in Tables II, III, IV, and V.

During the estimations of Λ , solvent corrections are made. The column $\Delta\Lambda$ lists the differences of the experimental Λ values from the best fits of Fuoss-Onsager-Skinner equation that will be discussed.

The analysis of the conductance data were made by means of the Fuoss-Onsager-Skinner equations^{7,8}

$$\Lambda = \Lambda_0 - Sc^{1/2}\gamma^{1/2} + E'c\gamma \ln(6E_1c\gamma) + Lc\gamma - K_A c f^2 \Lambda \quad (1)$$

$$\Lambda = \Lambda_0 - Sc^{1/2} + E'c \ln(6E'c) + Lc \quad (2)$$

Equation (1) was applied for the cases of associated electrolytes. Equation (2) was used for the cases of non-associated electrolytes. The various symbols appearing in the above equation have the following significance. Λ is the equivalent conductance, Λ_0 is the limiting equivalent conductance, $S = \alpha\Lambda_0 + \beta$ is the Fuoss-Onsager constant, L is a constant which is an explicit function of the «ion size» parameter \bar{a} , f is the activity coefficient γ is the fraction of the salts present as free ions and K_A is the association constant.

The calculations of the parameters were done on a Univac 1100 by means of a program which finds the values of Λ_0 , K_A , \bar{a} which minimize^{7,9} the sum $\Sigma(\Delta\Lambda)^2$, where

TABLE II : Equivalent Conductance of Sodium Bromide in Isopropanol-Water Mixtures at 25°C.

10% i-PrOH (w/w)			20% i-PrOH (w/w)			40% i-PrOH (w/w)			60% i-PrOH (w/w)			80% i-PrOH (w/w)		
$c \cdot 10^4$ gm.equiv. lit ⁻¹	Λ mho.cm ² .equiv. ⁻¹	$\Delta\Lambda$	$c \cdot 10^4$ gm.equiv. lit ⁻¹	Λ mho.cm ² .equiv. ⁻¹	$\Delta\Lambda$	$c \cdot 10^4$ gm.equiv. lit ⁻¹	Λ mho.cm ² .equiv. ⁻¹	$\Delta\Lambda$	$c \cdot 10^4$ gm.equiv. lit ⁻¹	Λ mho.cm ² .equiv. ⁻¹	$\Delta\Lambda$	$c \cdot 10^4$ gm.equiv. lit ⁻¹	Λ mho.cm ² .equiv. ⁻¹	$\Delta\Lambda$
8.2228	86.07	-0.07	9.1398	61.88	-0.09	3.5144	40.89	0.09	5.7815	30.47	-0.03	4.5022	24.34	-0.08
12.138	85.67	-0.03	17.984	61.42	-0.14	6.9155	40.71	-0.02	11.376	29.92	-0.02	8.8592	23.43	-0.01
15.931	85.32	0.01	26.549	61.04	-0.12	10.208	40.53	-0.06	16.793	29.51	-0.01	13.077	22.76	0.02
19.608	85.06	0.02	34.854	60.76	-0.12	13.398	40.36	-0.06	22.042	29.20	-0.02	17.164	22.24	0.03
23.176	84.82	0.05	42.887	60.51	-0.10	16.490	40.20	-0.05	27.128	28.92	-0.01	21.125	21.81	0.03
29.989	84.39	0.11	50.684	60.30	-0.08	19.489	40.06	-0.03	32.061	28.67	0.00	24.966	21.44	0.03
36.415	84.17	0.03	58.249	60.12	-0.07	22.398	39.94	-0.02	36.846	28.46	0.00	28.693	21.12	0.03
42.484	83.94	0.01	65.591	59.95	-0.04	25.221	39.85	-0.03	41.490	28.28	0.00	32.310	20.83	0.02
48.225	83.77	-0.03	72.721	59.79	-0.01	27.962	39.76	-0.02	46.000	28.11	0.01	35.822	20.59	0.02
53.664	83.59	-0.05	79.647	59.65	0.01	30.626	39.65	0.00	54.639	27.81	0.03	39.233	20.36	0.00
58.824	83.42	-0.05	86.378	59.53	0.03	33.214	39.57	0.01	58.778	27.67	0.03	42.549	20.16	0.01
			92.921	59.40	0.07	35.730	39.49	0.03	62.804	27.55	0.02	45.772	19.97	0.02

TABLE III : Equivalent Conductance of Potassium Bromide in Isopropanol-Water Mixtures at 25°C.

10% i-prOH (w/w)			20% i-prOH (w/w)			40% i-prOH (w/w)			60% i-prOH (w/w)			80% i-prOH (w/w)		
$c \cdot 10^4$ gm.equiv. lit ⁻¹	Λ mho.cm ² .equiv. ⁻¹	$\Delta\Lambda$	$c \cdot 10^4$ gm.equiv. lit ⁻¹	Λ mho.cm ² .equiv. ⁻¹	$\Delta\Lambda$	$c \cdot 10^4$ gm.equiv. lit ⁻¹	Λ mho.cm ² .equiv. ⁻¹	$\Delta\Lambda$	$c \cdot 10^4$ gm.equiv. lit ⁻¹	Λ mho.cm ² .equiv. ⁻¹	$\Delta\Lambda$	$c \cdot 10^4$ gm.equiv. lit ⁻¹	Λ mho.cm ² .equiv. ⁻¹	$\Delta\Lambda$
4.4148	103.43	0.01	4.6614	73.84	0.08	9.5514	47.36	-0.06	6.0306	33.50	-0.07	3.2660	26.10	-0.03
8.6872	102.8	0.01	9.1724	73.52	-0.03	18.794	46.76	-0.01	11.866	32.84	-0.04	6.4266	25.20	0.00
12.824	102.46	0.02	13.540	73.19	-0.02	27.744	46.37	-0.02	17.517	32.37	-0.04	9.4869	24.53	0.01
16.831	102.12	0.03	17.771	72.94	-0.03	36.415	46.04	-0.01	22.991	31.97	-0.02	12.451	24.00	0.01
20.815	101.87	0.00	21.872	72.75	-0.06	44.818	45.79	-0.02	28.297	31.65	-0.02	15.325	23.55	0.02
24.482	101.61	0.02	25.849	72.52	-0.02	52.967	45.54	0.00	33.442	31.37	-0.02	18.111	23.16	0.02
28.136	101.42	0.00	33.452	72.21	-0.03	60.872	45.34	0.01	38.433	31.13	-0.02	23.438	22.54	0.00
31.682	101.21	0.01	40.620	71.91	0.00	68.545	45.15	0.03	43.278	30.91	-0.02	28.460	22.02	0.00
35.126	101.03	0.02	47.390	71.71	-0.01	75.996	44.97	0.06	47.982	30.71	-0.01	33.204	21.60	0.00
41.723	100.74	0.00	53.795	71.54	-0.03	83.234	44.82	0.08	52.552	30.53	-0.01	37.691	21.24	0.00
44.884	100.58	0.02	59.862	71.35	0.00	90.269	44.67	0.11	56.993	30.37	-0.01	41.942	20.93	0.00
47.958	100.45	0.03	65.618	71.20	0.00	97.106	44.94	-0.26	61.311	30.27	0.06	45.975	20.67	-0.01
50.949	100.33	0.03							65.510	30.08	0.00			
53.861	100.23	0.02							69.596	29.95	0.00			
56.695	100.12	0.03							73.573	29.83	0.00			
									77.445	29.72	0.00			

TABLE IV : Equivalent Conductance of Rubidium Bromide in Isopropanol-Water Mixtures at 25°C.

10% i-prOH (w/w)			20% i-prOH (w/w)			40% i-prOH (w/w)			60% i-prOH (w/w)			80% i-prOH (w/w)		
$c \cdot 10^4$ gm.equiv. lit ⁻¹	Λ mho.cm ² .equiv. ⁻¹	$\Delta\Lambda$	$c \cdot 10^4$ gm.equiv. lit ⁻¹	Λ mho.cm ² .equiv. ⁻¹	$\Delta\Lambda$	$c \cdot 10^4$ gm.equiv. lit ⁻¹	Λ mho.cm ² .equiv. ⁻¹	$\Delta\Lambda$	$c \cdot 10^4$ gm.equiv. lit ⁻¹	Λ mho.cm ² .equiv. ⁻¹	$\Delta\Lambda$	$c \cdot 10^4$ gm.equiv. lit ⁻¹	Λ mho.cm ² .equiv. ⁻¹	$\Delta\Lambda$
4.1097	105.79	-0.03	6.5006	75.53	-0.04	4.3764	48.83	-0.03	4.1038	34.45	0.00	4.9602	25.67	-0.05
8.0869	105.41	0.05	12.791	74.92	-0.05	8.6116	48.41	-0.03	8.0752	33.84	0.02	9.7605	24.47	-0.04
11.937	105.14	0.00	18.882	74.61	0.00	12.712	48.07	0.01	11.920	33.38	0.03	14.408	23.58	-0.02
15.668	104.81	-0.03	24.783	74.33	-0.03	16.685	47.81	0.02	15.645	33.01	0.04	18.910	22.90	-0.03
19.284	104.52	-0.01	30.503	74.06	-0.01	20.535	47.59	0.03	19.256	32.72	0.03	23.275	22.34	-0.03
22.790	104.30	-0.01	36.049	73.84	-0.01	24.269	47.42	0.02	22.757	32.48	0.00	27.506	21.87	-0.03
29.493	103.96	0.01	41.429	73.62	0.01	31.407	47.13	0.00	29.450	32.06	0.00	35.597	21.12	-0.05
35.813	103.64	0.01	46.651	73.45	0.01	38.137	46.89	-0.02	35.761	31.71	0.00	43.225	20.53	-0.05
41.782	103.37	0.01	51.722	73.29	0.02	44.493	46.67	-0.01	41.722	31.44	-0.02	50.429	20.05	-0.04
47.428	103.11	0.00	56.648	73.16	0.01	50.506	46.49	0.03	47.360	31.18	0.00	57.244	19.65	-0.02
52.777	102.88	0.03	61.438	73.01	0.03	56.202	46.30	0.00	52.701	30.98	-0.01	63.700	19.29	0.02
57.852	102.70	0.03	66.090	72.89	0.03	61.606	46.15	0.00				69.825	18.99	0.06

TABLE V : Equivalent Conductance of Caesium Bromide in Isopropanol-Water Mixtures at 25°C.

$c \cdot 10^4$ gm.equiv. lit ⁻¹	Λ mho.cm ² .equiv. ⁻¹	$\Delta\Lambda$	$c \cdot 10^4$ gm.equiv. lit ⁻¹	Λ mho.cm ² .equiv. ⁻¹	$\Delta\Lambda$	$c \cdot 10^4$ gm.equiv. lit ⁻¹	Λ mho.cm ² .equiv. ⁻¹	$\Delta\Lambda$	$c \cdot 10^4$ gm.equiv. lit ⁻¹	Λ mho.cm ² .equiv. ⁻¹	$\Delta\Lambda$	$c \cdot 10^4$ gm.equiv. lit ⁻¹	Λ mho.cm ² .equiv. ⁻¹	$\Delta\Lambda$
10% i-PrOH (w/w)			20% i-PrOH (w/w)			40% i-PrOH (w/w)			60% i-PrOH (w/w)			80% i-PrOH (w/w)		
6.6994	105.74	0.06	6.5593	75.83	-0.04	6.3875	48.64	-0.04	7.9898	33.84	-0.02	4.6435	25.65	0.00
12.985	105.01	0.12	12.907	75.23	0.00	12.569	48.10	-0.02	15.722	33.01	0.00	9.1373	24.39	0.02
19.169	104.65	-0.00	19.053	74.86	-0.02	18.554	47.69	-0.00	23.208	32.41	0.01	13.488	23.49	0.00
25.160	104.30	-0.03	25.007	74.58	-0.08	24.352	47.38	0.00	30.461	31.92	0.02	17.703	22.77	0.01
30.966	103.97	-0.03	30.778	74.32	-0.10	29.975	47.11	0.00	37.491	31.52	0.02	21.789	22.17	0.02
36.596	103.68	-0.02	36.374	74.08	-0.10	35.422	46.88	0.00	44.307	31.17	0.02	25.750	21.69	0.00
47.360	103.26	-0.07	47.073	73.63	-0.07	45.840	46.51	-0.01	57.339	30.61	0.00	33.324	20.90	-0.03
57.509	102.88	-0.07	57.160	73.29	-0.07	55.663	46.17	0.01	69.626	30.13	0.01	40.465	20.26	-0.01
67.094	102.58	-0.08	66.687	72.97	-0.03	64.940	45.92	0.00	81.230	29.76	0.00	47.209	19.76	-0.02
76.161	102.26	-0.03	75.698	72.73	-0.04	73.716	45.69	-0.01	92.207	29.43	0.00	53.589	19.35	-0.03
84.750	101.93	0.06	84.236	72.53	-0.06	82.030	45.49	-0.01	102.60	29.16	0.00	59.633	18.99	-0.02
92.899	101.68	0.10	92.335	72.33	-0.05	89.917	45.29	-0.01	112.47	28.91	0.01	65.367	18.62	-0.07

$$\Delta\Lambda_i = \Delta\Lambda_{\text{obs}} - \Delta\Lambda_{\text{calc}}$$

For the cases where there is no association, the calculations of parameters Λ_o and \bar{a} were done using equation (2).

TABLE VI : Conductance Parameters of Sodium Bromide in Isopropanol-Water Mixtures at 25°C.

i-prOH w/w (%)	Λ_o	K_A	\bar{a}	σ_Λ	$\Lambda_o \cdot \eta$
10	87.78	—	3.8	0.05	1.220
20	63.18	—	4.8	0.09	1.285
40	41.78	—	5.1	0.04	1.255
60	31.76	—	3.2	0.02	0.807
80	26.20	16.0	3.1	0.03	0.666

TABLE VII : Conductance Parameters of Potassium Bromide in Isopropanol-Water Mixtures at 25°C.

i-prOH w/w (%)	Λ_o	K_A	\bar{a}	σ_Λ	$\Lambda_o \cdot \eta$
10	104.86	—	3.7	0.02	1.457
20	75.04	—	3.7	0.03	1.529
40	48.74	—	3.7	0.09	1.409
60	34.92	4.0	3.3	0.03	1.409
80	27.92	44.0	3.3	0.01	0.710

TABLE VIII : Conductance Parameters of Rubidium Bromide in Isopropanol-Water Mixtures at 25°C.

i-prOH w/w (%)	Λ_o	K_A	\bar{a}	σ_Λ	$\Lambda_o \cdot \eta$
10	107.34	—	4.5	0.07	1.492
20	76.82	—	3.7	0.02	1.565
40	49.80	—	3.1	0.01	1.439
60	35.58	4.5	2.9	0.02	1.065
80	28.19	70.0	3.5	0.03	0.717

TABLE IX : Conductance Parameters of Caesium Bromide in Isopropanol-Water Mixtures at 25°C.

i-prOH w/w (%)	Λ_o	K_A	\bar{a}	σ_Λ	$\Lambda_o \cdot \eta$
10	107.54	—	3.9	0.06	1.494
20	77.16	—	3.3	0.06	1.572
40	49.89	3.0	4.1	0.01	1.440
60	35.63	6.0	2.9	0.01	1.070
80	28.28	86.0	3.3	0.01	0.719

In Tables VI, VII, VIII and IX, the results of the above analysis are given. From the values of these tables it is shown that Λ_o increases with the decrease of the viscosity of the solution. The product of the limiting conductance and the solvent viscosity should be constant for all solvents for a given salt :

$$\Lambda_o \eta = \left(\frac{X_e}{1800\pi} \right) \left(\frac{1}{r_+} + \frac{1}{r_-} \right)$$

where r_+ and r_- are the radii of solvent ions. In all cases examined it was shown that the values of the product $\Lambda_o \eta$ are increasing as the dielectric constant of the solvent mixtures increases at about 20% (or $D=60$) and then they decrease.

An analogous variation of the product $\Lambda_o \eta$ is shown by other investigators for various salts in alcohol-water mixtures.^{10,11,12} Generally it is shown that a maximum in the product $\Lambda_o \eta$ appears which moves to higher values as the number of carbon atoms in the alcohol molecule increases.

The appearance of the maximum is due to the fact that the addition of alcohol in water affects the structure of water and this influences gets stronger as the amount of alcohol increases. Thus, although small amounts of alcohol do not disturb greatly the structural equilibrium of water, the addition of larger amounts of alcohol breaks down the water structure as water molecules are replaced by alcohol molecules. The ions in the solutions are solvated by the polar molecules of the water but in low alcohol contents, the alcohol does not take part in the solvation effect. In the cases of high alcohol contents, molecules of water are replaced by water molecules in the solvated ion.

In all concentrations of the isopropanol-water mixtures used the limiting conductance increases with the crystallographic radius of the cation. This effect is more intense for the first three salts, but differences of Λ_o between Rband Cs are small. The salts of Sodium do not show any association at the whole concentrations range of solvent mixtures used but for the rest of the salts the association appears from a concentration about 60% (w/w). For the greater concentrations of isopropanol association increases with the increase of isopropanol. This effect is due to the decrease of the dielectric constant as well as the smaller solvation.

For the bromide salts of Sodium, Potassium, Rubidium and Caesium the association increases with the crystallographic radius, of cation.

The most likely explanation for the correlation is that as the sizes of an ion increases, so does the probability of an intimate collision between a cation and anion, and because the ion-pair so formed does not contribute to the conductance of the solution, until the bombardment of the solvent molecules causes their separation.

Περίληψη

Αγωγιμομετρική συμπεριφορά και σύζευξη στα βρωμιούχα άλατα των αλκαλιμετάλλων σε μικτά διαλυτικά συστήματα ισοπροπανόλης - νερού

Στην εργασία αυτή μελετάται η αγωγιμότητα των βρωμιούχων αλάτων του Νατρίου, Καλίου, Ρουβιδίου και Καισίου σε μικτά διαλυτικά συστήματα ισοπροπανόλης-νερού στους 25°C.

Τα πειραματικά αποτελέσματα αναλύονται με τις εξισώσεις των Fuoss-Onsager-Skinner. Δίδονται οι τιμές της ισοδύναμης αγωγιμότητας άπειρης αραιώσης, της σταθεράς συζεύξεως και της παραμέτρου του ιονικού μεγέθους σε διάφορες περιεκτικότητες ισοπροπανόλης.

Βρέθηκε ότι αύξηση της περιεκτικότητας της ισοπροπανόλης έχει σαν αποτέλεσμα την ελάττωση της ισοδύναμης αγωγιμότητας άπειρης αραιώσης και την αύξηση του βαθμού συζεύξεως των ιόντων.

Διαπιστώθηκε ακόμα ότι η ισοδύναμη αγωγιμότητα άπειρης αραιώσης, για την ίδια περιεκτικότητα ισοπροπανόλης, ανέρχεται με την αύξηση της κρυσταλλογραφικής ακτίνας των κατιόντων.

References

1. Elton Price: «Solvation of Electrolytes and Solution Equilibria» in J.J. Lagowski *The Chemistry of Non-Aqueous Solvents* Vol 1 Academic Press N.Y. 1966.
2. Dagget H.M., Bair E.J., Kraus C.A.: *J. Am. Chem. Soc.* **73**, 799 (1951).
3. Lind J.E., Zwolnik J.J., Fuoss R.M.: *J. Am. Chem. Soc.* **81**, 1557 (1959).
4. Jannakoudakis D.A., Ritzoulis G.C.: *Chimika Chronika New Series* **7**, 11-19 (1978).
5. Prue J.E., Sherrington R.J.: *Trans. Faraday Soc.* **57**, 1795 (1961).
6. Dannhauser W., Bahe L.W.: *J. Chem. Phys.* **40**, 3058 (1964).
7. Fuoss R.M., Onsager L., Skinner J.T.: *J. Phys. Chem.* **69**, 2581 (1965).
8. Barthel J.: *Angewandte Chemie* **7**, 253 (1968).
9. Fuoss R.M.: *The Conductance of Symmetrical Electrolytes* in Conway B.E., Baradas R.G.: *Chemical Physics of Ionic Solutions*, p 463, Wiley, New York, 1966.
10. Accascina, DeLisi R., Goffredi M.: *Electrochim. Acta* **15**, 1209 (1970).
11. Brodwater T.L., Kay R.L.: *J. Phys. Chem.* **74**, 3802 (1970).

KINETIC STUDY OF THE OXIDATION OF BENZOIC ACID HYDRAZIDE BY MERCURY (II) ACETATE

DEMETRIUS A. HARISTOS and DOUKENI E. MISSOPOLINO

Laboratory of Inorganic Chemistry, School of Science, and Laboratory of Physical Chemistry, Polytechnic School, Aristotelian University of Thessaloniki, Greece.

(Received February 22, 1982)

Summary

The kinetics of the oxidation of benzoic acid hydrazide by mercury (II) acetate is studied at different temperatures and in several acid and salt concentrations. Further evidence for the detection of the substituent effect is given by using ring monosubstituted benzoic acid hydrazides.

The reaction is of the first order in each reactant but does not show any significant influence with changes in the acid concentration for the pH range of 4.5 to 5.5 and in salt concentration from $5 \cdot 10^{-3}$ to 1.0 M. The inductive and resonance effect of the substituent do not influence the reaction rate.

The amino-group nitrogen is the donor in the complex formation with the Hg(II). The mechanism of the main reaction contains one electron transfer. The electron is transferred to the mercury(II) by the amino-group nitrogen while the cleavage of the C-N bond results the formation of the hydrazyle radical (\dot{N}_2H_3). It is also suggested the possibility of a four electron mechanism containing the intermediate formation of the diimide $C_6H_5CO-N=NH$.

Key words : benzoic acid hydrazide, mercury(II) acetate, oxidation, optical density, reaction rate, acidity, ionic strength, inductive and resonance effect.

Abbreviations : HBAH: benzoic acid hydrazide, XBAH: ring monosubstituted benzoic acid hydrazide (X = p-F, m-Cl, p-Cl, m-Br, p-Br, p-I, m-CH₃O, p-CH₃O and m-NO₂), Hg(OAc)₂: mercury(II) acetate.

Introduction

This paper deals with the redox system of benzoic acid hydrazide-mercury(II) acetate and especially refers to the stoichiometry, the order and the mechanism of the reaction.

The formation of complex compounds of hydrazides with mercury(II) ions is already known^{1,2} but nothing has been published concerning the oxidative action of mercury(II) on hydrazides.

Further evidence of some aspects of the present investigation is given by using ring monosubstituted benzoic acid hydrazides as the reductive agents.

Experimental

Reagents and instruments

The hydrazides used were prepared and identified as it has been mentioned in earlier papers^{3,4}.

The $\text{Hg}(\text{OAc})_2$ was Merck pro. analysi recrystallized from water. The stock solutions of it were checked by determining the mercury as mercuric sulphide⁵. The effect of ionic strength was studied in the range of 5.10^{-3} to 1.0 M with BDH analytical grade NaClO_4 .

The measurements of optical density vs time at constant wave length were scanned at 245 nm which lies in the $\pi \rightarrow \pi^*$ excitation^{6,7} of the system (Fig. 1).

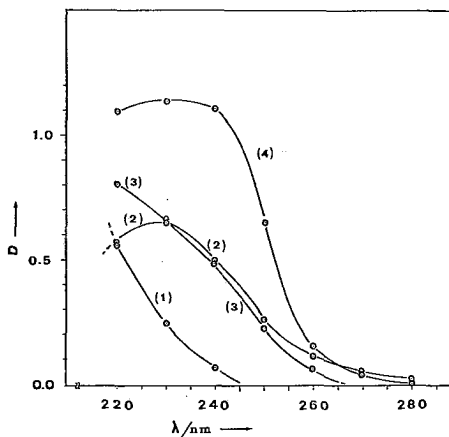


FIG. 1 : Optical density plots vs λ at $T=8^\circ\text{C}$, $\text{pH}=5.12 \pm 0.03$ and $I=1.10^{-2}$ M for the solutions: (1) $\text{Hg}(\text{OAc})_2$ ($C=4.10^{-4}$ M), (2) HBAH ($C=8.10^{-5}$ M), (3) mixture of HBAH ($C=8.10^{-5}$ M) and $\text{Hg}(\text{OAc})_2$ ($C=4.10^{-4}$ M) before the reaction and (4) the same mixture after the end of the reaction.

The measurements of the reaction rates were taken at the temperatures of 25° , 35° , 45° and 55°C in the pH range of 4.5 to 5.5 in acetate buffers⁸.

The identification and the determination of the reaction products were carried out in solutions of the following initial concentration :

$$|\text{Hg}(\text{OAc})_2| = 1.10^{-2} - 1.10^{-3}\text{M} \text{ and } |\text{HBAH}| = 1.10^{-3} - 1.10^{-4}\text{M}.$$

The $\text{Hg}(\text{I})$ was calculated by determining the non reacted $\text{Hg}(\text{II})$ after the end of the reaction in solutions containing an excess of $\text{Hg}(\text{OAc})_2$. Separation of $\text{Hg}(\text{I})$ from $\text{Hg}(\text{II})$ was achieved by addition of hydrochloric acid and filtration.

The determination of the order of the reaction was carried out by application of the isolation method⁹ (Fig. 2).

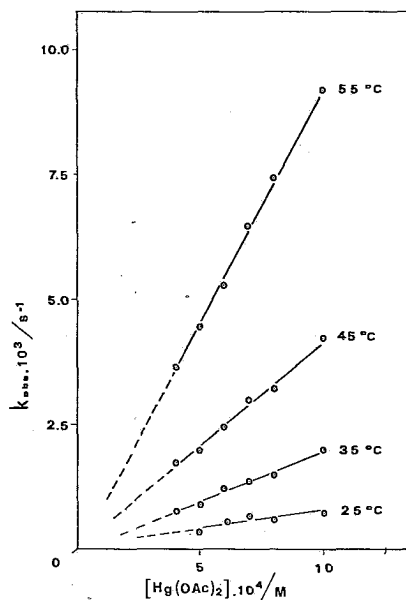
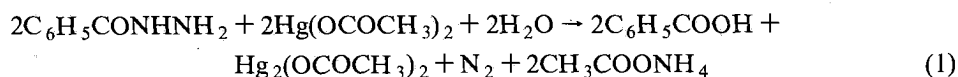


FIG. 2 : Dependence of k_{obs}/s^{-1} on $Hg(OAc)_2/M$ concentrations for constant $[HBAH] = 8.10^{-3}M$ at various temperatures, $pH = 5.12 \pm 0.03$, $I = 1.10^{-2} M$, $\lambda = 245 nm$.

Results and discussion

The results of the determination of the reaction products between HBAH and $Hg(OAc)_2$ predict that the stoichiometry is satisfactorily given by the one electron transfer mechanism.



A small part of the reaction seems to follow the four electron mechanism. The latest has been suggested by the slightly larger quantity of N_2 and smaller quantity of NH_3 found than those calculated. This could be attributed either to secondary reactions on \dot{N}_2H_3 radical,^{10,11} coming out from the cleavage of the C-N bond³ or to the decomposition of a diimide formed as an intermediate product^{12,13} of the oxidation.

The results of the isolation method showed that there is a good linear correlation between the k_{obs}/s^{-1} values and the $Hg(OAc)_2$ concentrations (Fig. 2). According to these the overall reaction follows the kinetics of the second order reactions :

$$\text{Rate} = k[\text{HBAH}][\text{Hg}(\text{OAc})_2] \quad (2)$$

Calculations of the $k/\text{mol}^{-1}\text{s}^{-1}$ values are achieved by application of the second order reactions integrated rate expression.

Influence of acid and salt concentration

The effect of acidity on the oxidation rates was studied at different temperatures and at constant ionic strength 1.10^{-2} M (Table I). The results showed that the reaction was not significantly affected by changes in acid concentrations¹⁴ between the pH values of 4.5 and 5.5. The reaction rate decreases gradually for pH values lower than 4.5. In this pH range the protonation of amino-group takes place^{7,15} and thus, it is prevented the association of the hydrazide with the Hg(II). At pH values higher than 5.5 the reaction rate seems to increase. Meanwhile, considerable deviations of the calculated k values as well as the presence of hydrolysis products of $\text{Hg}(\text{OAc})_2$ ^{16,17} suggest a more complicated mechanism. The changes of the salt concentration did not show any significant effect on the reaction rate.

A sufficient explanation of the above experimental results is as follows: The polar form of the hydrazide includes a negative charge on the carbonyl oxygen. This polar center can attract an H^+ and, in case of association of Hg(II) with the carbonyl-group, the reaction rate could be influenced with changes in acid concentrations. The absence of any significant influence indicates that the carbonyl-group does not participate in the formation of any complex compound with Hg(II). As well, the reaction could be influenced with changes in salt concentrations, if there was even a partly ionic character in each reactant. As a conclusion, the formation of the N-Hg(II) bond seems to be favourable.

From the data of the table I at the pH range 4.5 - 5.5 the following rate constant values are calculated: $k = 0.78 \pm 0.01 \text{ mol}^{-1}\text{s}^{-1}$ at 25°C , $k = 1.99 \pm 0.04 \text{ mol}^{-1}\text{s}^{-1}$ at 35°C , $k = 4.17 \pm 0.04 \text{ mol}^{-1}\text{s}^{-1}$ at 45°C , $k = 9.23 \pm 0.05 \text{ mol}^{-1}\text{s}^{-1}$ at 55°C . These k values are in a very good agreement with those coming out of the data of Fig. 2. The activation energy calculated¹⁸ from the above values of k , is E_a 66.5 kJ mol^{-1} .

Substituent effect

Nine ring monosubstituted benzoic acid hydrazides (abbreviated as HBAH) were used in the purpose of studying the influence of the substituent on the reaction rate.

Measurements of the reaction rates were done in the pH range of 4.6 to 5.3 and at constant ionic strength 1.10^{-2} M. The $k/\text{mol}^{-1}\text{s}^{-1}$ values at the temperatures of 45° and 55°C are given in the table II. It is obvious that these values are almost the same. The inductive and resonance effects¹⁹ of the substituents could influence the electron density of the carbonyl oxygen only. Amino-group is far enough to be influenced. This result is in accordance with the negligible effect of acidity and of ionic strength.

As a conclusion the carbonyl-group seems to act neither as a donor in an association bond with Hg(II) nor as a bridge in the electron transfer reaction.

TABLE I : Effect of Temperature on the Rate Constant at pH range 4.06-5.62 and at constant ionic strength 1.10^{-2} M.

25°C			35°C			45°C			55°C		
pH	k	log k	pH	k	log k	pH	k	log k	pH	k	log k
4.33	0.55	-0.2596	4.12	1.25	0.0969	4.06	2.65	0.4233	4.12	5.49	0.7396
4.50	0.68	-0.1678	4.22	1.52	0.1818	4.19	3.18	0.5024	4.25	6.14	0.7882
4.64	0.74	-0.1308	4.42	1.78	0.2504	4.31	3.98	0.5999	4.40	7.34	0.8657
4.78	0.82	-0.0862	4.60	1.98	0.2967	4.51	4.18	0.6212	4.52	9.21	0.9640
4.98	0.74	-0.1308	4.82	1.88	0.2742	4.65	4.09	0.6117	4.71	9.28	0.9676
5.12	0.77	-0.1135	4.98	2.06	0.3159	4.79	4.17	0.6201	4.82	9.04	0.9562
5.24	0.80	-0.1069	5.12	1.97	0.2945	4.93	4.24	0.6274	4.94	9.42	0.9741
5.45	0.79	-0.1024	5.24	2.14	0.3096	5.11	4.15	0.6181	5.14	9.12	0.9600
5.62	0.86	-0.0655	5.38	1.94	0.2878	5.28	4.35	0.6385	5.31	9.07	0.9576
			5.54	2.20	0.3424	5.46	4.43	0.6464	5.44	9.40	0.9731
						5.56	4.57	0.6500	5.58	9.34	0.9704

TABLE II : Rate Constants of the oxidation of ring monosubstituted benzoic acid hydrazides by $\text{Hg}(\text{OAc})_2$ at pH range 4.6-5.3, at constant ionic strength 1.10^{-2} M and at two different temperatures.

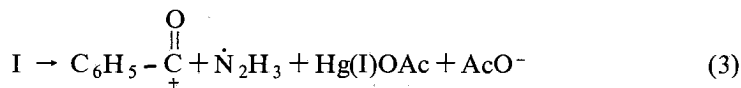
XBAH	$k/\text{mol}^{-1}\text{s}^{-1}$	
	45°C	55°C
p-F-BAH	4.12	9.34
m-Cl-BAH	3.98	9.28
p-Cl-BAH	4.06	9.04
m-Br-BAH	4.18	8.92
p-Br-BAH	4.32	9.42
p-I-BAH	4.20	9.34
m-CH ₃ O-BAH	4.32	9.22
p-CH ₃ O-BAH	4.34	9.20
m-NO ₂ -BAH	4.22	8.98

Reaction mechanism

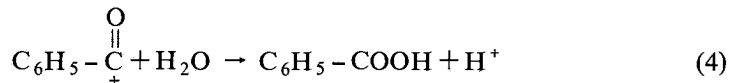
After mixing of the reactants the complex compound I is formed :



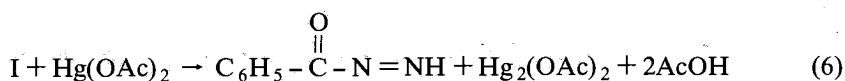
In this complex the amino-group nitrogen acts as a donor. The electron transfer reaction leads to the cleavage of CO-N bond while the formation of the benzoyl ion $\text{C}_6\text{H}_5\overset{+}{\text{C}}=\text{O}$ and the hydrazyle radical $\dot{\text{N}}_2\text{H}_3$ takes place.



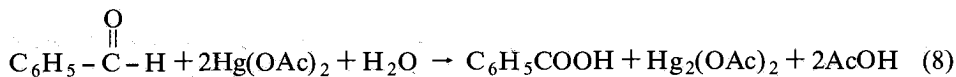
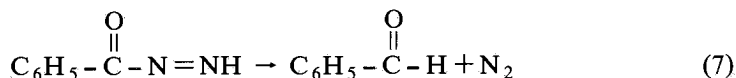
Secondary reactions give the final products :



On the other hand a part of the reaction could take place by the following reaction mechanism :



Secondary reactions give the final products :



The $k/\text{mol}^{-1}\text{s}^{-1}$ values are comparatively³ lower. Thus suggesting that the electron transfer mechanism is hindered by charge or steric effects.

The linear arrangement of the $\text{Hg}(\text{OAc})_2$ molecule and the strongly covalent character of the $\text{Hg}-\text{O}$ bond²⁰ cause a considerable decrease of the electrophilic behaviour of the $\text{Hg}(\text{II})$. Besides the cleavage of the $\text{C}-\text{N}$ bond becomes difficult because of the resonance form due to the charge delocation from the carbonyl-group.

Περίληψη

Κινητική μελέτη της οξειδώσεως του υδραζιδίου του βενζοϊκού οξέος από οξικό υδράργυρο(II)

Μελετήθηκε με τη μέθοδο της φασματοφωτομετρίας η κινητική της οξειδώσεως του υδραζιδίου του βενζοϊκού οξέος από οξικό υδράργυρο(II).

Η μελέτη έγινε σε διαφορετικές θερμοκρασίες, συγκεντρώσεις οξέος και τιμές ιονικής ισχύος απουσία οξυγόνου. Τα προϊόντα της αντιδράσεως είναι βενζοϊκό οξύ, άζωτο, αμμωνία και υδράργυρος(I).

Βρέθηκε ότι η αντίδραση είναι διμοριακή και πρώτης τάξεως για το καθένα από τα αντιδραστήρια (HBAN και $\text{Hg}(\text{OAc})_2$). Η ταχύτητα της αντιδράσεως δεν επηρεάζεται από τη μεταβολή της συγκεντρώσεως του οξέος για περιοχή pH 4.5 - 5.6. Επίσης δεν παρατηρήθηκε επίδραση της ιονικής ισχύος για τιμές αυτής από $5 \cdot 10^{-3}$ έως 1.0 M.

Για τη διερεύνηση της επιδράσεως του επαγωγικού και του συζυγιακού φαινομένου που εισάγει ο υποκαταστάτης χρησιμοποιήθηκαν εννέα υποκατεστημένα στον πυρήνα υδραζιδια του βενζοϊκού οξέος. Και στη περίπτωση αυτή δεν παρατηρήθηκε αξιοσημείωτη επίδραση του υποκαταστάτη στην ταχύτητα της αντιδράσεως.

Με την ανάμιξη των αντιδραστηρίων εννοείται ο σχηματισμός δεσμού $\text{N}-\text{Hg}(\text{II})$. Για την κυρία αντίδραση προτείνεται μηχανισμός μεταφοράς ενός

ηλεκτρονίου με ενδιαμέσο σχηματισμό της ρίζας του υδραζιλίου (N_2H_3). Πιθανή επίσης είναι παράλληλη αντίδραση μεταφοράς τεσσάρων ηλεκτρονίων με ενδιαμέσο σχηματισμό διμιδίου ($\text{C}_6\text{H}_5\text{CO}-\text{N}=\text{NH}$).

References and notes

1. Gogoroshvili P.V., Nagebashvili A.E., Shvelashvili A.E., Machkhoshvili R.I. (USSR): *Issled. Oll. Khim. Kompleksn. Prostykh Soedin, Nek. Pevekhodnykh Redh. Met.* **2**, 174-80 (1974). *Chem. Abstr.*, **82**, 38084m (1975).
2. Nonaka Takamasa, Manono Eiji, Minari Nori, Egawa Hiroaki: *Nippon Kagaku Kaishi* **7**, 1025-31 (1978). *Chem. Abstr.* **89**, 11066K (1978).
3. Haristos D.A., Manoussakis G.E.: *Chim. Chronica*, **10**, 175 (1981).
4. Manoussakis G.E., Haristos D.A., Youri C.E.: *Chim. Chronica* **1**, 182 (1972).
5. Vogel A.I. *Quantitative Inorganic Analysis* p. 487. Third Edition, Longmans, London 1961.
6. Grammatikakis P.: *Bull. Soc. Chim. Fr.* 933 (1970).
7. Manoussakis G.E., Haristos D.A., Youri C.E.: *Can. J. Chem.* **51**, 811 (1973).
8. Britton H.T.S.: *Hydrogen Ions* p. 220 Chapman and Hall, Ltd. London 1932.
9. Weissberger A., editor: *Techniques of Chemistry* Vol. VI p. 131 (Bunett J.F., «Kinetics in solution») John Wiley and Sons, Third Edition. New York 1974.
10. Higginson W.C.E., Wright P.: *J. Chem. Soc.* 1551 (1955).
11. Cahn S.W., Powel R.E.: *J. Am. Chem. Soc.*, **76**, 2568 (1954).
12. Aylward J.B.: *J. Chem. Soc.*, (C) 1663 (1969).
13. Nicholson J., Cohen S.G.: *J. Am. Chem. Soc.*, **88**, 2247 (1966).
14. Littler J.S.: *J. Chem. Soc.* 2190 (1962).
15. Titov E.V., Korzhenevskaya N.G., Rybachenko V.I.: *Ukr. Khim. Zh.*, **34** (12), 1253 (1968).
16. Maguire R.J., Anand S., Chew H., Adams W.A.: *J. Inorg. nucl. Chem.*, **38**, 1659-62 (1976).
17. Long E.G., Kobe A.K.: *Ind. Eng. Chem.*, **43**, 2366 (1951).
18. Weston K.B.Jr., Schwarz H.A.: *Chemical Kinetics*, p. 168, Prentice Hall, New Jersey 1972.
19. Hammett L.P.: *Physical Organic Chemistry*, p. 355, McGraw-Hill, New York 1970.
20. Mahaparta P., Aditya S. Prasad B.: *J. Indian Chem. Soc.* **30**, 509 (1953).

Acknowledgement

The authors thank Professors G.E. Manoussakis and N.E. Alexandrou for their keen interest in the work.

THE CONDUCTANCE AND ASSOCIATION BEHAVIOR OF THE SODIUM BENZENESULFONATE IN DIOXANE-WATER MIXTURES

D. K. PANOPOULOS, D. A. JANNAKOUDAKIS

Laboratory of Physical Chemistry, Faculty of Physics & Mathematics, University of Thessaloniki, Greece

(Received March 9, 1982)

Summary

Conductimetric measurements have been performed on sodium benzenesulfonate solutions in dioxane-water mixtures at 25°C over the range $78.30 \geq D \geq 16.11$. The data have been analysed with the Fuoss-Onsager-Skinner conductivity equations and the resulting parameters are reported.

Association to ion pairs begins to be increasingly visible below to $D = 44.71$. The $\log K_A$ vs $1/D$ plot yields a straight line in agreement with Fuoss' theory of ion-pair formation. The observed complicated behavior of Walden product over the dielectric range covered is discussed in terms of Fuoss-Zwanzig theory and various conclusions are made concerning the applicability of the sphere-in continuum model on the electrolytic solutions studied.

Key Words : Conductimetry, Sodium Benzenesulfonate, Dioxane-Water mixtures, Zwanzig's theory.

Introduction

Studies on the conductance behavior of arenesulfonic electrolytes (salt and acids) in pure and mixed solvents are in progress¹ - the authors' interest being stimulated by the fact that these electrolytes have not been extensively investigated conductimetrically and data reported on them are only sporadic. Furthermore, in what concerns the nature of the factors affecting ionic mobilities, the large enough arenesulfonate anions should better approach Stokes' law, since an inherent requirement of this law - not having received much attention - is that the moving entity must be large enough compared to solvent molecules.

In the present investigation the electrical conductances of sodium benzenesulfonate in dioxane-water mixtures were measured over a large range of values of the dielectric constant $78.30 \geq D \geq 16.11$. The experimental results were analysed by

suitable conductivity equations in order to obtain conductimetric parameters capable of yielding information about the applicability of «sphere-in-continuum» model on ionic association process as well as to allow a deeper insight into the nature of the structural effects affecting the hydrodynamic behavior of the electrolytic systems studied. Association process and hydrodynamic behavior observed have been discussed in terms of Fuoss theory (of ion-pair formation) and of Fuoss-Zwanzig's theory (of dielectric friction) respectively.

Experimental

Sodium benzenesulfonate (Fluka, puriss, 99.5% minimum purity) was repeatedly recrystallized from conductance water and dried at 150°C under reduced pressure. It was stored over phosphorus pentoxide in an evacuated desiccator.

Solvents' purification, instrumentation and experimental procedure were the same as described earlier.¹ Water and dioxane had a specific conductance of about $2 \times 10^{-7} \text{ Ohm}^{-1} \text{ cm}^{-1}$ and $1 \times 10^{-8} \text{ Ohm}^{-1} \text{ cm}^{-1}$ respectively. The conductivity measurements were made at $25 \pm 0.002^\circ \text{C}$. The cell constant was found² to be 0.0270 cm^{-1} and it was repeatedly rechecked during the work. The apparatus used for conductimetric measurements permitted the solvent and solution to be kept in an all glass completely closed system under an inert gas atmosphere at all times. All salt solutions were prepared just before use.

Results and discussion

The measured densities (d), viscosities (η), and low-frequency dielectric constants (D or ϵ_0) as well as the values of infinite-frequency dielectric constants (ϵ_∞) and of relaxation times (τ) evaluated by interpolation from literature¹⁻⁵ are summarized in Table I. The molar conductivities Λ and the concentrations c of the

TABLE I: Properties of solvent mixtures at 25°C

System No	wt-% Dioxane	d (g cm ⁻³)	$10^2 \eta$ (Poise)	$D(\epsilon_0)$	ϵ_∞	$10^{12} \tau$ (sec)
1	0.00	0.9971	0.8903	78.30	5.50	8.30
2	20.25	1.0145	1.2772	61.73	4.80	10.41
3	39.93	1.0286	1.7025	44.71	4.12	13.60
4	49.70	1.0335	1.8701	36.22	3.79	17.17
5	59.42	1.0362	1.9515	28.17	3.46	18.91
6	64.33	1.0369	1.9406	24.01	3.30	23.11
7	69.40	1.0371	1.8988	19.84	3.14	23.92
8	74.33	1.0363	1.8175	16.11	3.01	23.63

salt for the complete range of dioxane-water compositions are listed in Table II.

TABLE II : Molar concentration ($c/mol\ dm^{-3}$) and molar conductivities ($\Lambda/S\ cm^2\ mol^{-1}$) of sodium benzenesulfonate in Dioxane-Water mixtures at $25^\circ C$.

10^4c	Λ	10^4c	Λ	10^4c	Λ
D = 78.30		D = 61.73		D = 44.71	
7.939	85.06	7.939	60.06	7.939	43.88
9.923	84.65	9.923	59.72	9.923	43.59
11.908	84.20	11.908	59.43	11.908	43.42
13.893	83.98	13.893	59.12	13.893	43.21
15.877	83.61	15.877	58.88	15.877	43.01
17.862	83.27	17.862	58.68	17.862	42.85
19.847	83.01	19.847	58.39	19.847	42.70
21.832	82.65	21.832	58.16	21.832	42.59
23.816	82.49	23.816	57.98		
25.801	82.21	25.801	57.81		
27.786	82.04	27.786	57.61		
29.770	81.65	29.770	57.42		
31.754	81.40				
33.739	81.32				
D = 36.22		D = 28.17		D = 24.01	
7.993	38.95	6.946	34.47	5.954	32.07
8.931	38.73	7.939	34.18	6.946	31.72
9.923	38.53	8.931	33.96	7.939	31.48
10.916	38.37	9.923	33.70	8.931	31.25
11.908	38.18	10.916	33.45	9.923	30.99
12.900	38.02	11.908	33.25	10.916	30.80
13.893	37.87	12.900	33.08	11.908	30.60
14.885	37.74	13.893	32.87		
15.877	37.58	14.885	32.71		
16.869	37.40				
17.862	37.34				
D = 19.84		D = 16.11			
5.954	29.36	4.962	26.41		
6.946	28.97	5.954	25.72		
7.939	28.69	6.946	25.15		
8.931	28.34	7.939	24.50		
9.923	28.08	8.931	24.13		
10.916	27.90	9.923	23.80		

In order to obtain the suitable parameters, the results were analysed by the following forms of Fuoss-Onsager-Skinner equation⁶

$$\Lambda = \Lambda_0 - Sc^{1/2}\gamma^{1/2} + E'c\gamma\ln(6E_1c\gamma) + Lc\gamma - K_Ac\gamma f^2\Lambda \quad (1)$$

$$\Lambda = \Lambda_0 - Sc^{1/2} + E'c\ln(6E_1c) + Lc \quad (2)$$

for associated and unassociated electrolytes respectively. (The symbols have their usual significance). The equations were solved using a computer programme by a procedure which is reported in detail elsewhere.¹ The parameters obtained as well as the standard deviations σ_Λ of the individual points from the values predicted by the conductance theory are reported in Table III. The last column numbers identify the equation used in each case according to Fuoss' suggestion.⁶

TABLE III : Derived parameters for sodium benzenesulfonate in Dioxane-Water mixtures at 25°C. The confidence limits of the results are shown in 95% level. (Λ_0/S cm²mol⁻¹; K_A/dm^3 mol⁻¹; α_L /pm; $\Lambda_0\eta/S$ cm²mol⁻¹P)

Syst.N ^o	D	Λ_0	K_A	α_L	σ_Λ	$\Lambda_0\eta$	eqn
1	78.30	87.71 ± 0.09	—		0.06	0.7805	1
2	61.73	62.25 ± 0.05	—		0.03	0.7951	1
3	44.71	45.83 ± 0.05	—	240	0.02	0.7802	1
4	36.22	41.70	30 ± 7	410	0.02	0.7798	2
5	28.17	37.91	63 ± 9	680	0.02	0.7399	2
6	24.01	35.73	132 ± 20	1140	0.02	0.6934	2
7	19.84	34.62	340 ± 34	1620	0.03	0.6574	2
8	16.11	35.78	1128 ± 98	1510	0.08	0.6503	2

Inspection of the derived data shows that there is a slight amount of association up to a dielectric constant of about 44.71 which then increases continuously as the dielectric constant is lowered (as dioxane is added). The plots of $\log K_A$ vs $1/D$ are shown in Fig. 1. In this figure the least square regression line has a correlation coefficient of 0.999. This near unity value indicates the linearity of the $\log K_A$ vs $1/D$ plot. It also suggests for the applicability of the following theoretical Fuoss' expression^{7,8} for the ion-pair formation constant K_A

$$K_A = (4\pi N\alpha^3/3000)e^b \quad (3)$$

$$b = e^2/a_K DkT$$

which - taking logarithms and inserting numerical constants, ion size parameter, a in Å and 25°C for temperature - becomes

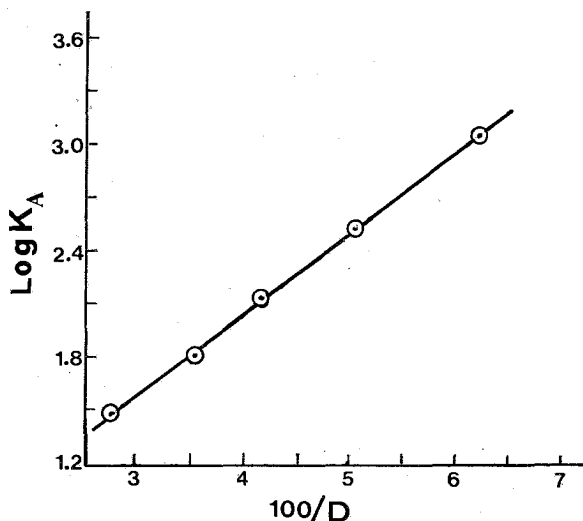


FIG. 1 : Dependence of association constant on dielectric constant.

$$\log K_A = \log(2.523 \times 10^{-3} \bar{a}^3) + (243.335/\bar{a}_K) \frac{1}{D} \quad (4)$$

The various symbols have their usual significance.

The slope and intercept values of the experimental $\log K_A - D^{-1}$ plot were calculated to be 46.2 and 0.1899 respectively. From the theoretical $\log K_A(D^{-1})$ function (4), the slope and intercept, when equated to their corresponding experimental values, lead separately to an average value of the distance of closest approach equal to 527 pm and 850 pm respectively.

Such a discrepancy, between values of the same contact distance, indicates the inadequacy of the simple model of «charged spheres in a continuum» to reach to a comprehensive description of ion-pair formation and further, suggests that structural effects due to microscopic properties of the solvent mixtures must be included in addition to electrostatic attraction.

Such effects have as a main result, the ion-pair formation to be accompanied by a change in the molar free energy of solvation, ΔG_s (molar free energy of solvation of free ions less that of ion pair). Additionally, the variation in the composition of the polar-nonpolar solvent mixture not only does the dielectric constant change, but also does the value of ΔG_s change.

These changes in the difference of free energy of solvation-affecting ion pairing process-should in general lead to a curvature (variable slope) in $\log K_A - D^{-1}$ plot.²⁴ The linearity (constant slope) of the experimental plot reveals, however, that the pairs of ions formed are of the same kind having a constant «slope» distance of closest approach. Therefore, it becomes clear that the «intercept» term of eqn. (4) includes the influence of ΔG_s changes leading, in turn, to an «intercept» distance of

closest approach which is remarkably different from that obtained from the «slope» term.

Furthermore, it must be noted here that the observed systematic increase of a_L values with decreasing dielectric constant (Table III) should also have its origin to similar structural effects mentioned above (ignored by any continuum theory).⁷

From the salt limiting conductance Λ_0 obtained in water and the limiting conductance of the sodium cation (50.10) the limiting conductance of the benzenesulfonate anion as well as the transference numbers of the individual salt ions are calculated to be $\lambda_0^- = 37.61 \text{ S cm}^2 \text{ mol}^{-1}$, $t^+ = 0.57$, $t^- = 0.43$ (water, 25°C).

In dioxane-water mixtures the total salt conductance can not be resolved into separate ionic contributions due to the lack of necessary transference data. However, an application of the extra-thermodynamic assumption that the transference numbers of the salt ions in water are independent of the composition of the dioxane-water mixtures⁹ allows the calculation of the individual limiting ionic conductances and the respective conductance-viscosity products in each solvent composition. These can then be used to estimate the hydrodynamic radii (Stokes radii) of the ions from the following Stokes' law expressions^{10,11}

$$r_{\text{stick}} = N_A e^2 / 6\pi\lambda_0\eta \quad \text{or} \quad r_{\text{stick}} = 82/\lambda_0\eta \quad (\text{in pm}) \quad (5)$$

$$r_{\text{slip}} = N_A e^2 / 4\pi\lambda_0\eta \quad \text{or} \quad r_{\text{slip}} = 123/\lambda_0\eta \quad (\text{in pm}) \quad (6)$$

for the cases of perfect sticking (5) and slipping (6) of the solvent at the surface of the ions. The results obtained are listed in Table IV.

Inspection of the electrolyte limiting conductance-viscosity product as well as of that of single ions shows that its behavior is complicated over the dielectric range covered. A closer scrutiny shows that there must be a maximum in the water-rich region (though not so clear since the measurements have been carried out at too wide a composition interval) after which the conductance decreases to much lower values of the Walden product (as the dielectric constant decreases). A reverse procedure is observed in the variation of Stokes' radii (Table IV).

This complicated behavior will be discussed in terms of the factors affecting ionic mobilities. These factors can be identified by writing the limiting conductance-solvent viscosity product $\lambda_0\eta$ as a sum of the following terms

$$\lambda_0\eta = (\lambda_0\eta)_{\text{CS}} + (\lambda_0\eta)_{\text{CE}} \quad (7)$$

where the term subscripted CS gives the total contribution to the conductance to be expected from a charged sphere. This charged-sphere contribution is written as

$$(1/\lambda_0\eta)_{\text{CS}} = (1/\lambda_0\eta)_{\text{IS}} + (1/\lambda_0\eta)_{\text{DR}} \quad (8)$$

where the term subscripted IS gives the contribution to be expected from an inert sphere and the term subscripted DR gives the contribution to the conductance resulting from a dielectric effect caused by a relaxation of solvent dipoles about the moving ion. The last term of eqn. (7) subscripted CE is a term which reflects the

TABLE IV : Limiting single ion conductance-viscosity products ($\lambda_0\eta/S \text{ cm}^2\text{mol}^{-1}\text{P}$) and Stokes hydrodynamic radii (r/pm) of sodium benzenesulfonate ions in dioxane-water mixtures at 25°C.

Syst.N ^o .	$\lambda_0^+\eta$	$\lambda_0^-\eta$	r ⁺ (stick)	r ⁻ (stick)	r ⁺ (slip)	r ⁻ (slip)
1	0.4455	0.3345	184	245	276	368
2	0.4542	0.3409	180	240	271	361
3	0.4447	0.3355	184	244	276	366
4	0.4445	0.3353	185	245	277	367
5	0.4226	0.3173	194	258	291	387
6	0.3961	0.2973	207	276	311	414
7	0.3755	0.2820	218	291	328	436
8	0.3715	0.2789	221	294	331	441

effects resulting from changes in the solvent in the vicinity of an ion (in its ionic coesphere) due to the presence of either a charged or an inert sphere. It is recalled here that this last factor has been ignored totally by any continuum theory.

The simplest substitution for the inert sphere term comes from an application of Stokes' law (5-6). In order to study the retarding effect resulting from the solvent dipoles relaxation around the moving ions, the experimental data have been analysed using the semi-empirical Fuoss' expression¹², from which the classical Stokes'radius can be derived, written as

$$r = r_\infty + s/D \quad \text{or} \quad rD = s + r_\infty D \tag{9}$$

as well as using Zwanzig's more rigorous derivation^{13,3}

$$\frac{z^2 eF}{\lambda_0 \eta} = A_v \pi r + \frac{A_D z^2}{r^3} \frac{e^2(\epsilon_0 - \epsilon_\infty)}{\epsilon_0(2\epsilon_0 + 1)} \frac{\tau}{\eta} \tag{10}$$

where $A_v = 6$, $A_D = 3/8$ for perfect sticking

$A_v = 4$, $A_D = 3/4$ for perfect slipping

Inserting numerical constants and r in Å, the resulting equation is

$$\frac{15.46}{\lambda_0 \eta} = 18.84 r + \frac{8.64}{r^3} \frac{10^{12}(\epsilon_0 - \epsilon_\infty)}{\epsilon_0(2\epsilon_0 + 1)} \frac{\tau}{\eta} \tag{11}$$

or $L^* = 18.84 r + \frac{8.64}{r^3} P^*$

for perfect sticking and

$$\frac{15.46}{\lambda_0 \eta} = 12.56 \overset{\circ}{r} + \frac{17.28}{\overset{\circ}{r}^3} \frac{10^{12}(\epsilon_0 - \epsilon_\infty)}{\epsilon_0(2\epsilon_0 + 1)} \frac{\tau}{\eta} \quad (12)$$

$$\text{or } L^* = 12.56 \overset{\circ}{r} + \frac{17.28}{\overset{\circ}{r}^3} P^*$$

for perfect slipping.

Essentially, another term inversely proportional to the cube of the ionic radius has been added to the Stokes' radius and the contribution to the total frictional force seems to depend on the ion size. For small ions, dielectric friction dominates while for bulky ions the viscous force is dominant. Furthermore, the dielectric frictional force in a solvent is determined by its P^* value.

In order to visualize the different contribution to the dielectric friction, the relaxation term P^* is considered to be a function of an «effective dynamic radius», r_{ef} , and of a characteristic «equilibrium distance», d_{eq} , of the solvent which are defined by the following expressions¹⁴

$$r_{ef}^3 = \frac{kT}{4\pi} \frac{\tau}{\eta}, \quad d_{eq} = \frac{(ze)^2}{kT} \frac{\epsilon_0 - \epsilon_\infty}{\epsilon_0(2\epsilon_0 + 1)} \quad (13)$$

$$P^* = 0.54 d_{eq} r_{ef}^3 \quad (d, r \text{ in } \text{Å})$$

Furthermore, according to eqn (10), $\lambda_0 \eta$ product for any given solvent has a maximum at a certain value of r . Simple calculation leads to the following expressions¹⁴

<u>«stick»</u>	<u>«slip»</u>
$r_i^{\max} = 1.08 P^{*1/4}$	$r_i^{\max} = 1.43 P^{*1/4}$
$(\lambda_0 \eta)_{\max} = 0.57/P^{*1/4}$	$(\lambda_0 \eta)_{\max} = 0.65/P^{*1/4}$
$r_i^{\max}(\lambda_0 \eta) = 0.62$	$r_i^{\max}(\lambda_0 \eta)_{\max} = 0.93$

All theoretical predictions based on Zwanzig's theory and concerning the solvent mixtures used, have been calculated and listed in Table V. The observed systematic increase of P^* values - yielded from independently measurable solvent parameters ϵ_0 , ϵ_∞ , τ - means that the dielectric frictional force of the solvent system becomes larger, leading to a systematic decrease in ion mobilities, as the dielectric constant decreases (with increasing dioxane content).

TABLE V : Theoretical predictions on solvent mixtures, 25°C (Based on zwanzig's theory).

System N ^o	mole-% Dioxane	P* s poise ⁻¹	r _{ef} pm	d _{eq} pm	r _i ^{max} /pm		(λ _i ^o η) _{max} /S	cm ² mol ⁻¹ P
					stick	slip	stick	slip
1	0.00	5.500	145	331	165	219	0.372	0.425
2	4.93	6.037	139	416	169	224	0.364	0.415
3	11.96	8.016	138	564	182	241	0.339	0.386
4	16.81	11.198	144	684	198	262	0.312	0.355
5	23.04	14.822	147	859	212	281	0.291	0.331
6	26.94	20.955	157	988	231	306	0.266	0.304
7	31.68	26.057	160	1161	244	323	0.252	0.288
8	37.19	31.816	162	1374	257	340	0.240	0.274

However, it must be noted here that Zwanzig's theory, based on a continuum model for solvent, completely ignores the possibility for a change in the size of the moving ion owing to changes in solvation. Thus, it is most successful for large organic ions in solvents where solvation is likely to be minimal and where viscous friction predominates over that caused by dielectric relaxation¹⁴, as already mentioned. The discrepancies becomes more striking the smaller the ionic radius is and the Zwanzig's continuum model fails to account quantitatively for the dependence of ionic mobility on solvent dielectric properties whenever the relaxation term P* becomes large.

A test of eqn. (9) is shown in Fig. 2(B) where the r⁺D and r⁻D experimental values are plotted against D for both extreme cases (of perfect sticking and perfect slipping). The plots are linear with a correlation coefficient of 0.999. (The point of pure water has been omitted and not included in the analysis because it deviated too much from rD-D lines). Inserting the calculated slope-intercept numerical values (r_{∞,s}) in eqn. (9), the following equations are obtained which reproduce with precision the Stokes radii over the D range covered

$$61.73 \geq D \geq 16.11, \quad (r/\text{pm})$$

$$\begin{array}{ll} \text{«stick»} & \text{«slip»} \\ r^+ = 164 + \frac{943}{D} & r^+ = 245 + \frac{1415}{D} \end{array} \quad (15)$$

$$\begin{array}{ll} r^- = 218 + \frac{125}{D} & r^- = 327 + \frac{1830}{D} \end{array} \quad (16)$$

Linear plots of L* vs P* have been obtained only in the dioxane-rich region the deviations being remarkably large in the water-rich region. Fig. 2(A) shows the

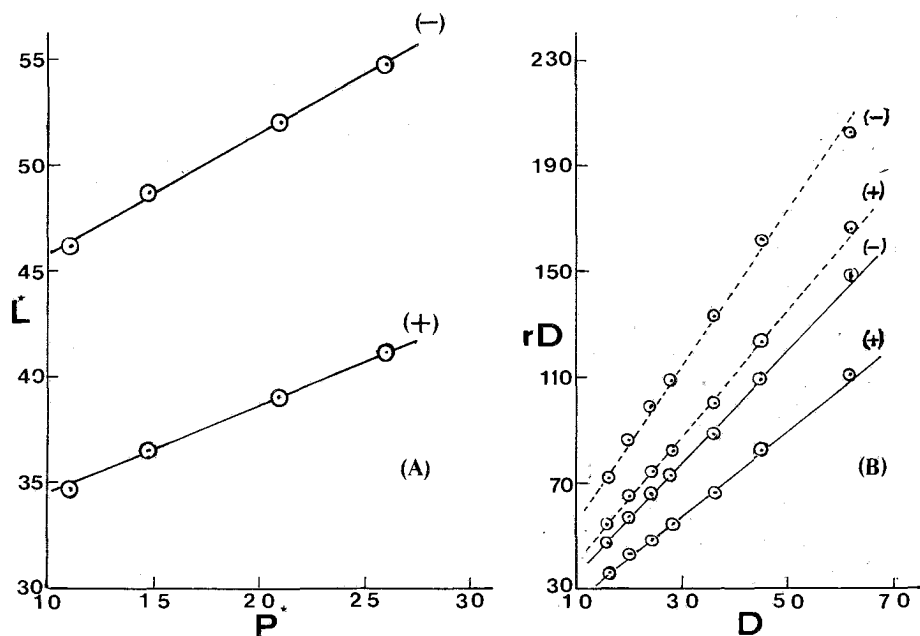


FIG. 2 : (A): A plot of L^* function versus the solvent function P^* Anion, upper plot; Cation, lower plot. (B): Dependence of classical Stokes' radius of anion (-) and cation (+) on dielectric constant. (— : «stick»; --- : «slip»).

$L^* - P^*$ plots, for both cation and anion, covering the range of dielectric constant $36.22 \geq D \geq 19.84$. Both plots are good straight lines with a correlation coefficient of 0.999. The resulting values of hydrodynamic radii are as follows :

	<u>A n i o n</u>		<u>C a t i o n</u>	
	«stick»	«slip»	«stick»	«slip»
Intercept :	213	319	160	239
Slope :	248	312	273	343

It is clearly observable that the values obtained for the anion (intercept, slope) hydrodynamic radii are in good agreement and closer enough to each other in the case of perfect slipping. For the cation the intercept-slope radii values are far from equal in both «stick» and «slip» cases and much higher than its ionic radius of 95 pm. A further interesting comparison can also be made, in each solvent composition studied, between the experimental $\lambda_0\eta$ value (Table IV) and the corresponding value of $(\lambda_0\eta)_{\max}$ (Table V) predicted by either «stick» or «slip» equation (14). It can be seen that Walden product is in every case smaller than the corresponding «maximum» for the anion and always larger in the case of the cation.

According to the results mentioned above, it should be supported that the contribution of $(\lambda_0\eta)_{CE}$ term, which reflects ion-solvent interactions (in eqn.7), appears to be absent or at least negligible in the case of benzenesulfonate anion. The fact that the value of 316 pm (on the average) obtained for «slip» case is satisfactorily close to r_∞ value of 327 pm (concerning an uncharged, inert, unsolvated analog-eqns. 9, 16) could be also considered as a positive evidence that benzenesulfonate anion-solvent interactions are likely to be minimal.

In what concerns the discrepancies observed in cation behavior, it is clear that in this case $(\lambda_0\eta)_{CE}$ term dominates. The fact that the values obtained for cation hydrodynamic radius are, in all cases, larger than its crystallographic size, suggests that it should be strongly solvated. This is a reasonable hypothesis since, as it has repeatedly noted,^{1,15} the smaller and presumably more solvated ions show the greatest deviation. Furthermore, this interpretation receives support from the fact that dioxane-water mixtures appear to form intermolecular hydrogen-bonded complexes of various possible structures^{5,16,21,25,26} which should be immobilized around a cation yielding a firmly held solvation sheath. Thus, the Na^+ experimental mobilities appear to be enhanced against them predicted by the theory since, Zwanzig's equation, overestimating the dielectric friction effect on the solvated cation, lead to lower mobilities.

The difference between the derived distance of closest approach and the average hydrodynamic radius is calculated to be 215 pm and it should be considered as an average hydrodynamic radius of the solvated Na^+ in dioxane-water mixtures. This value remains somewhat lower than the sum of the ionic radius and the solvent's effective dynamic radius obtained for each solvent composition (Table V). Furthermore, this value belongs to a position midway between r_∞^+ values (164-245 pm) obtained from eqn. (15) as well as between the r_{interc}^+ values (160 and 239 pm) obtained from eqn. (11) for both «stick» and «slip» extreme conditions.

The initial increase observed in Walden product, as dioxane is added to water, is likely to be the typical behavior of structure-breaking ions on an enhanced solvent structure. However, such an enhancement is probably absent in dioxane-water mixtures since they appear to form two distinct intermolecular hydrogen-bonded complexes^{1,5,16,21} and further, Na^+ is considered as a poor structure-breaking ion. Therefore, there must be little doubt that what appears to be an enhanced ion mobility in the region of low dioxane contents is actually the result of a dehydration effect occurring upon addition of dioxane^{22,23} rather than a better ion structure-breaking ability on an enhanced water structure. If really a dehydration occurs sharply as dioxane is added and a little dioxanation also occurs²⁰, the size of the moving cation would decrease and a mobility increment would be observed. Furthermore, in what concerns anion behavior, a hydrophobic rather than hydrophilic dehydration may probably occur at the hydrocarbon surface of its benzene ring (considered as a hydrophobic structure-maker surface). Its ability to exhibit hydrophobic effects enforcing the structure of pure water, rapidly disappears as dioxane is added.^{22,23}

Whatever we ascribe the observed hydrodynamic behavior to, it is clear that no definite conclusion can be reached until diffusion data on uncharged molecules-

comparable in size to the ions - become available. By means of these data - containing no contribution from the dipole relaxation or cosphere effects - the inert-sphere term of eqn. (8) could be evaluated with precision and the use of Stokes' law could be avoided.

Περίληψη

Αγωγιμομετρική και ιονική συμπεριφορά του βενζοσουλφονικού νατρίου σε υδατοδιοξανικά διαλύματα

Μελετήθηκε η αγωγιμομετρική και ιονική συμπεριφορά του βενζοσουλφονικού νατρίου σε υδατοδιοξανικά διαλύματα στους 25°C στην ευρεία περιοχή διηλεκτρικής σταθεράς $78.30 \geq D \geq 16.11$. Η ανάλυση των πειραματικών αποτελεσμάτων έγινε με τις αγωγιμομετρικές εξισώσεις των Fuoss-Onsager-Skinner για εταιρισμένους και μη εταιρισμένους ηλεκτρολύτες και προσδιορίστηκαν οι τιμές των αγωγιμομετρικών παραμέτρων.

Διαπιστώθηκε ότι ο εταιρισμός των ιόντων σε ζεύγη αρχίζει να γίνεται αισθητός ($K_A > 10$) από την τιμή διηλεκτρικής σταθεράς 36,22 και αυξάνεται καθώς ελαττώνεται η διηλεκτρική σταθερά του διαλυτικού συστήματος (καθώς δηλ. εμπλουτίζεται αυτό σε διοξάνιο). Η συνάρτηση $\log K_A - 1/D$ προκύπτει ικανοποιητικότερα γραμμική (συντελεστής συσχέτισεως 0,999), γεγονός που βρίσκεται σε πλήρη συμφωνία με τις απόψεις του Fuoss περί εταιρισμού των ιόντων. Από τη γραμμική αυτή σχέση προσδιορίστηκε η ιονική παράμετρος a (ελάχιστη απόσταση προσεγγίσεως των ιόντων).

Παρατηρήθηκε ιδιαίτερα συμπεριφορά στο γινόμενο Walden σε συνάρτηση με τη μεταβολή της διηλεκτρικής σταθεράς του διαλυτικού συστήματος, διακρινόμενη σε δύο περιοχές: Αρχικά, στην πλούσια σε νερό περιοχή του διαλυτικού συστήματος παρατηρείται μιά αύξηση στο γινόμενο Walden, μετά το μέγιστο της οποίας το γινόμενο ελαττώνεται συστηματικά καθώς εμπλουτίζεται το διαλυτικό σύστημα σε διοξάνιο (καθώς δηλ. ελαττώνεται η διηλεκτρική σταθερά). Η αντίθετη πορεία παρατηρείται στη μεταβολή των «υπολογισμένων» υδροδυναμικών ακτίνων των ιόντων. Η συμπεριφορά της αρχικής περιοχής αποδίδεται σε σημαντικές δράσεις διαλύτη-διαλύτη, που οδηγούν στην αφυδάτωση των ιόντων, ενώ η δεύτερη περιοχή μελετήθηκε με βάση τις απόψεις και εξισώσεις των Fuoss και Zwanzig για τη διηλεκτρική τριβή.

References

1. Jannakoudakis D., Panopoulos D.: *Chimika Chronika, New Series*, **10**, 127 (1981).
2. Lind J.E., JR., Zwolenik J.J. and Fuoss R.M.: *J. Phys. Chem.* **81**, 1557 (1959).

3. Atkinson G. and Mori Y.: *J. Phys. Chem.*, **71**, 3523 (1967).
4. Garg S.K. and Smyth C.P.: *J. Chem. Phys.*, **43**, 2959 (1965).
5. Hasted J.B., Haggis G.H., and Hutton P.: *Trans. Faraday Soc.*, **47**, 577 (1951).
6. Fuoss R.M., Onsager L., Skinner J.F.: *J. Phys. Chem.*, **69**, 2581 (1965).
7. Fuoss R.M., and Accascina F.: «*Electrolytic Conductance*» Interscience, New York (1959).
8. Fuoss R.M.: *J. Am. Chem. Soc.*, **80**, 5059 (1958).
9. Lind J.E. and Fuoss R.M.: *J. Phys. Chem.*, **66**, 1727 (1962).
10. Stokes G.G.: Cambridge *Phil. Soc. Trans.*, **9**, 5 (1856).
11. Lamb H., «*Hydrodynamics*» (reprint), p. 602, Dover, New York (1949).
12. Fuoss R.M.: *Proc. Nat. Acad. Sci. (U.S.)*, **45**, 807 (1959); Sadek H. and Fuoss R.M.: *J. Am. Chem. Soc.*, **81**, 4507 (1959).
13. Zwanzig R.: *J. Chem. Phys.*, **38**, 1603, 1605 (1963); **52**, 3625 (1970).
14. Fernández-Prini R. and Atkinson G.: *J. Phys. Chem.*, **75**, 239, (1971).
15. Covington A.K. and Dickinson T.: «*Physical Chemistry of Organic Solvent Systems*», Plenum Press, New York (1973).
16. Greinacher E., Luttke W. and Mecke R.: *Z. Electrochem.*, **59**, 23 (1955).
17. Fratielo A. and Luongo J.R.: *J. Am. Chem. Soc.*, **85**, 3072 (1963).
18. Covington A.K. and Jones P.: «*Hydrogen-Bonded Solvent Systems*» p. 241, Taylor and Francis, London (1968).
19. Hammes G. and Knoche W.: *J. Chem. Phys.*, **45**, 4041 (1966).
20. Gordon J.E. «*The Organic Chemistry of Electrolyte Solutions*» p. 258, J. Wiley, New York (1975).
21. Garg S.K. and Smyth C.P.: *J. Chem. Phys.*, **43**, 2959 (1965).
22. Kay R.L. and Broadwater T.L.: *Electrochim. Acta*, **16**, 667 (1971).
23. Kay R.L.: «*Water-A comprehensive treatise*» Vol. 3 Chapt. 4, Franks F. Ed., Plenum Press, New York-London (1973).
24. Gilkerson W.R.: *J. Phys. Chem.*, **74**, 746 (1970).
25. Jannakoudakis D., Papanastasiou G. and Moumtzis J.: *Chimika Chronika, New Series*, **2**, 73 (1973).
26. Jannakoudakis D., Papanastasiou G. and Mavridis P.: *J. Chim. Phys.*, **73**, 156 (1976).

THE DETERMINATION OF RESIDUAL SOLVENTS IN PLASTICS PACKAGING MATERIALS IN RELATION TO OFF ODORS DEVELOPED IN PACKAGED BAKERY PRODUCTS

MICHAEL G. KONTOMINAS and EMMANUEL VOUDOURIS

Department of Food Chemistry University of Ioannina, Ioannina, Greece

(Received March 16, 1982)

Summary

Measurement of the residual solvents in plastics packaging materials has become increasingly important over the past few years. Such solvents may migrate from the packaging material into the contained product thus causing an off-odor and/or off-taste in the latter. Gas Chromatography and recently G.C-Mass Spectrometry have been successfully used to determine the above migrating species. In this paper three compounds namely, Toluene, Ethanol and Methyl Ethyl Ketone, responsible for an off odor caused in packaged bakery products have been identified and quantified.

Key words : Residual solvents, packaging materials, off odors.

Introduction

Cellophane, one of the most well known food packaging materials today, is seldom being used unconverted in packaging applications. It is usually coated on one or both sides with a polymer such as polyvinylidene chloride (PVDC), Polyvinylchloride (PVC) or Polyethylene (PE). A common method of application of these coatings is to dissolve the polymer in a suitable solvent mixture and then to apply it to the film, after which the solvent is removed by vaporization.¹

It is possible however for any residual solvents remaining in the laminate to migrate from the film into the foodstuff being packaged thus causing: i) off odor and/or off taste problems ii) food safety problems if these solvents are toxic, carcinogenic etc.^{2,3,4}

Similar problems can arise from residual solvents used in the application of inks and adhesives on plastics packaging materials.

A factor which should be seriously considered in such cases is the increased normal storage time for packaged foodstuffs. The «convenience» packages in particular, are designed for long time, ambient temperature storage. Under such conditions even low amounts of residual solvents may migrate and in some cases

accumulate in sufficient quantities to affect the food stuff.^{5,6} The introduction of Gas Chromatography^{7,8} opened a new path to the solution of the above problem. This tool provides the sensitivity and the analytical description needed to measure the volatile residuals in packaging materials.

Two major paths have been followed in the use of this tool :

a) to extract the solvents by a suitable extraneous solvent and analyze the resulting extract.¹

b) to distill off solvents by heat using appropriate collecting devices.^{9,10}

A derivative of this concept proposed by Wilks and Gilbert^{11,12} was used in the present work. Recently the use of Mass Spectrometry in combination with Gas Chromatography has significantly contributed to the positive identification of such compounds.

Materials and Methods

Qualitative and quantitative analysis of retained solvents in film samples was performed by use of the «hot jar» technique^{11,12} in combination with Gas Chromatography (ASTM-72) and Mass Spectrometry:

Samples

The following film samples were provided for analysis

- i) Film A
- ii) Film B
- iii) Film C

All films were laminates consisting of: Cellophane/Saran/PE. According to the supplier, bakery products packaged in the above films developed an objectionable «plastic» off odor which was stronger³ in the case of film C.

Gas Chromatographic Conditions.

A 5750 Hewlett Packard G.C equipped with a dual flame ionization detector was employed for the chromatographic analysis. Stationary phases including SE-30 and Chromosorb 104 were checked for degree of separation of eluting volatiles. The chromosorb 104 column gave better resolution and was thus chosen for the analysis.

The operational conditions used were as follows :

- St. phase : Chromosorb 104 on Anaknom ABS 60-80 Mesh
- Column Temp : 150°C
- Injection Port Temp : 150°C
- Detector Temp : 240°C
- Carrier Gas : Helium 60 ml/min.

Mass Spectrometric Conditions

Temperature programmed analysis was carried out for all three samples. A Hewlett Packard 5992^A G.C-Mass Spec. instrument system was used.

The operational conditions used were as follows :

St. phase : OV-101 10% in a 30m, 0.25mm ID glass capillary column

Initial Column Temp : 30°C

Final » » : 200°C

Injection Port Temp : 210°C

Detector Temp : 240°C

Running Time : 120min

Carrier Gas : Helium 15 ml/min

Analysis of Films

Gas Chromatography Analysis

Two 27 in² pieces of films A,B and C were cut out from the respective rolls. These pieces were cut again into smaller size of 1 × 1 cm and put into serum vials of 120 ml capacity.

TABLE I : Gas Chromatographic Analysis of Film Volatile Compounds

Sample injected	Retention time	Response A	Response B	Response C	Proposed solvents
	2'54''	105	32.0	16.7	Ethanol or 2-propanol
0.5 ml	5'55''	—	75.5	123.8	Methyl Ethyl Ketone
	9'17''	—	198.4	1531.2	Toluene

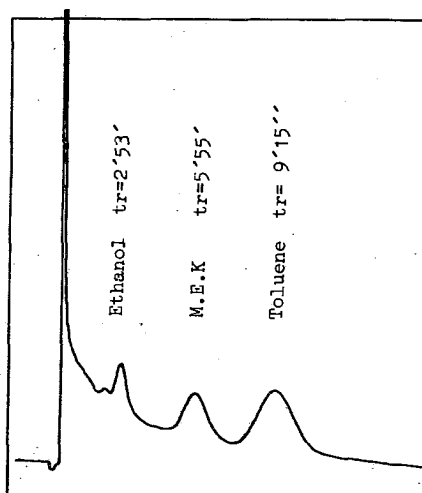
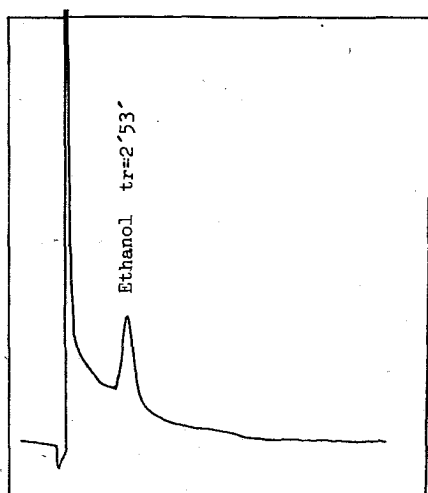


FIG. 1 : Gas Chromatogram of Head space Sample of Film A.

FIG. 2 : Gas Chromatogram of Head space sample of Film B.

The vials were then immediately closed with rubber stoppers, sealed with aluminum crimp caps, evacuated to 15 in. Hg and heated at 100°C for 1 hr.

Using a gas tight 0.5 ml syringe, equipped with a two way luer lock valve, 0.5 ml aliquots were withdrawn from the head space of the vials and injected into the G.C. The response and retention times of the respective peaks are shown in Table I and Figures 1, 2 and 3.

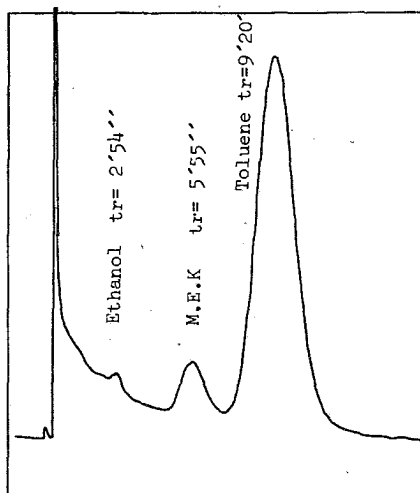


FIG. 3 : Gas Chromatogram of Head space Sample of Film C.

Mass Spectrometry Analysis

The above experimental procedures were repeated and headspace aliquots of the three film samples were introduced into the G.C-Mass Spec system.

Response and retention times of the respective peaks are shown in Figures 4,5, and 6.

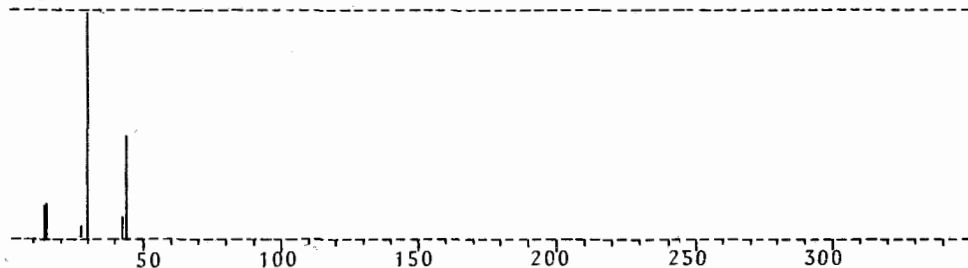
Identification and Quantification of Head Space Volatiles

After careful examination of the Chromatograms, a series of known solvents, 1 μ l of each, were introduced into glass serum vials of 120 cc capacity, using a 5 μ l liquid syringe. Subsequently, the vials were sealed and heated as described above. Using gas tight syringes of 0.25 ml and 0.5 ml capacity, known head space aliquots were withdrawn from the vials and injected into both the G.C and G.C-Mass Spec system. Recovery of method was tested by comparing response of direct injection of liquid solvents and response of head space injection of same solvents.

The retention times and responses of the respective peaks are shown in Table II for the Gas chromatographic analysis and Figures 7, 8 and 9 for the Mass spectrometric analysis.

Standard curves for Toluene, Methyl Ethyl Ketone and Ethanol were subsequently constructed.

Spectrum of Film A. Retention Time=5.8
 Number of peaks detected = 77
 Scanned from 10 to 200 Base Peak=30.6
 Base Peak Abundance=10560 Total Abundance 20201

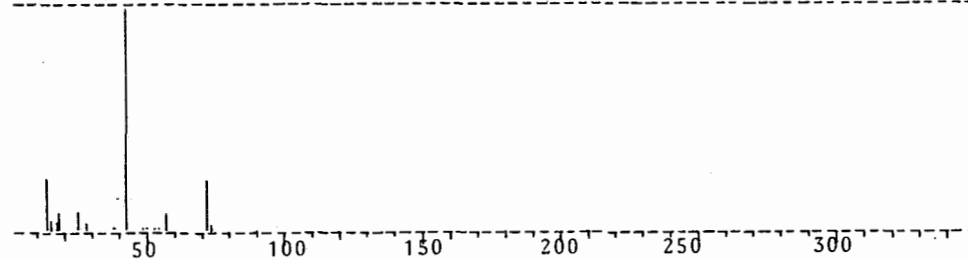


Lower Abundance Cut off Level = 1.0

MASS	ABUNDANCE	MASS	ABUNDANCE
13.8	14.0	30.6	100.0
14.9	15.3	42.6	9.2
27.3	4.5	44.6	43.6

FIG. 4 : Mass Spectrum of Head space sample of Film A.

Spectrum of Film B Retention Time = 7.8
 Number of Peaks detected = 91
 Scanned from 10 to 200 Base Peak =42.6
 Base Peak Abundance = 4876 Total Abundance =9433

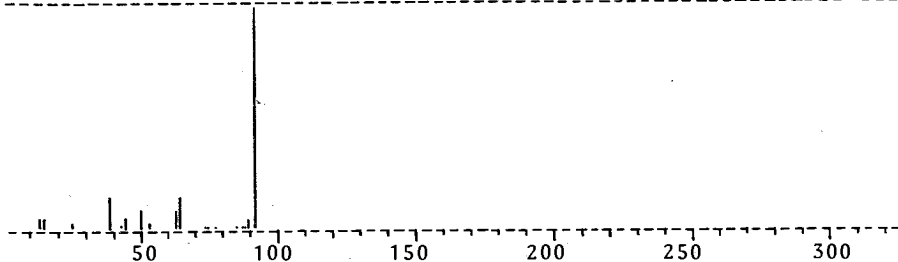


Lower Abundance Cut off Level = 1.0

MASS	ABUNDANCE	MASS	ABUNDANCE
13.5	22.9	27.3	2.6
14.9	4.5	42.6	100.0
16.0	3.3	49.9	1.5
17.3	6.6	56.5	6.9
25.3	7.0	71.5	22.1
		72.7	1.8

FIG. 5 : Mass Spectrum of Head Space Sample of Film B.

Spectrum of Film C Retention Time =12.1
 Number of peaks detected = 89
 Scanned from 10 to 200 Base Peak =90.8
 Base Peak Abundance = 20892 Total Abundance =51334



Lower Abundance Cut off Level = 1.0

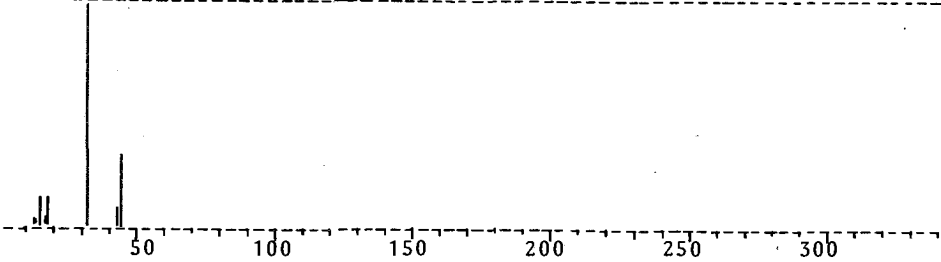
MASS	ABUNDANCE	MASS	ABUNDANCE
13.5	4.5	62.5	8.3
15.0	4.0	64.5	14.1
25.4	1.6	73.5	1.2
38.5	14.5	76.4	1.3
44.7	4.4	88.7	4.2
50.2	6.7	90.8	100.0
50.6	7.7	91.6	64.0
51.8	1.5		

FIG. 6 : Mass Spectrum of Head Space Sample of Film C.

TABLE II : Gas Chromatographic Analysis of Known Compounds

Compound	Retention Time	Response
2-propanol, Ethanol	2'58''	266.6
Methyl Ethyl Ketone	5'55''	302.7
Toluene	9'20''	601.6

Spectrum of Ethanol Retention Time =6.1
 Number of peaks detected 102
 Scanned from 10 to 200 Base Peak = 30.8
 Base Peak Abundance =11424 Total Abundance = 20383

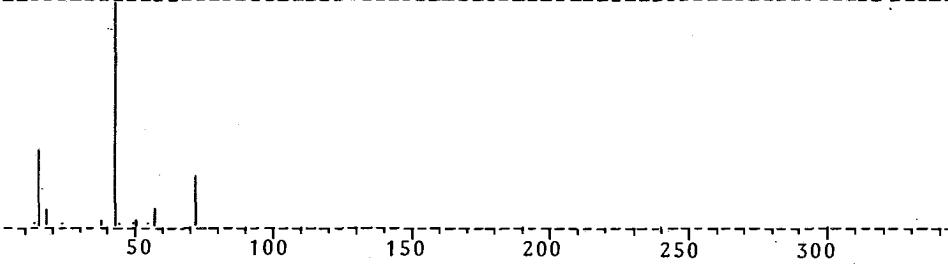


Lower Abundance Cut off Level = 1.0

MASS	ABUNDANCE	MASS	ABUNDANCE
11.9	1.7	17.4	12.3
13.4	2.3	30.8	100.0
14.9	12.2	42.6	7.7
16.0	2.9	44.5	32.4

FIG. 7 : Mass Spectrum of Head Space Sample of Ethanol.

Spectrum of Methyl Ethyl Ketone Retention Time=7.8
 Number of peaks detected = 92
 Scanned from 10 to 200 Base Peak = 42.6
 Base Peak Abundance =2852 Total Abundance =5561



Lower Abundance Cut off Level = 1.0

MASS	ABUNDANCE	MASS	ABUNDANCE
13.4	1.3	49.4	1.4
14.9	32.7	50.6	1.5
17.4	6.7	56.4	6.9
37.0	2.0	71.6	21.6
42.6	100.0	104.6	1.2

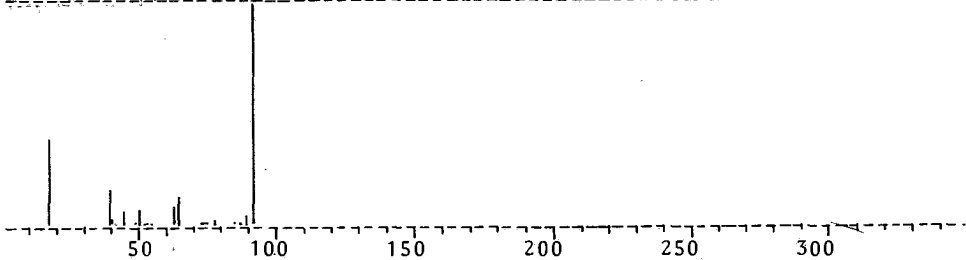
FIG. 8 : Mass Spectrum of Head Space Sample of Methyl Ethyl Ketone.

Spectrum of Toluene

Number of Peaks detected = 81 Retention Time = 12.4

Scanned from 10 to 200 Base Peak = 90.8

Base Peak Abundance = 3556 Total Abundance = 10032



Lower Abundance Cut off Level = 1.0

MASS	ABUNDANCE	MASS	ABUNDANCE
11.9	1.1	62.6	7.5
16.0	39.1	64.5	13.1
37.1	3.3	73.1	1.4
38.9	15.7	76.7	2.1
40.6	2.4	88.7	4.5
44.6	5.6	90.8	100.0
50.5	6.8	91.6	61.1
51.7	1.3		

FIG. 9 : Mass Spectrum of Head Space Sample of Toluene.

By comparison of the retention times and peak areas of the known solvents with those of the unknown components (head space volatiles of the film samples) identification and quantification of the above compounds was accomplished. Results are shown in Table III.

TABLE III : Amounts of Solvents Present in each of the Films

Film Type	Ethanol (mg/m ²)	M.E.K.	Toluene
A	3.04	—	—
B	1.22	1.90	3.84
C	0.85	2.40	33.84

Discussion

From both Gas Chromatographic and Mass spectrometric data it is concluded that the compounds present in the packaging materials examined, are Ethanol, Methyl Ethyl Ketone and Toluene. Toluene was found in excessive amounts in film sample C and is probably responsible for the off taste if transferred into the product.

Περίληψη

Προσδιορισμός καταλοίπων διαλυτών σε πλαστικές συσκευασίες, σε σχέση με δυσοσμίες που προκαλούνται σε συσκευασμένα είδη αρτοποιίας

Τα τελευταία χρόνια έχει δοθεί έμφαση στον προσδιορισμό καταλοίπων διαλυτικών μέσα σε πλαστικά συσκευασίας τροφίμων. Τέτοια διαλυτικά δυνατόν να μεταφερθούν κάτω από ορισμένες συνθήκες από το υλικό συσκευασίας στο περιεχόμενο τρόφιμο, προκαλώντας έτσι δυσοσμία ή και αλλοίωση στη γεύση του τελευταίου. Η Αέρια Χρωματογραφία και πρόσφατα ο συνδυασμός Αέριας Χρωματογραφίας/Φασματοφωτομετρίας Μάζης έχουν χρησιμοποιηθεί επιτυχώς στον προσδιορισμό των πύ πάνω μεταφερομένων ουσιών. Σ' αυτή την εργασία τρεις ενώσεις δηλ. το Τολουόλιο, Μεθυλο-αιθυλοκετόνη και Αιθανόλη, υπεύθυνες για τη δυσοσμία που προκλήθηκε σε συσκευασμένα είδη αρτοποιίας, ταυτοποιήθηκαν και προσδιορίστηκαν ποσοτικά.

References

1. Phifer, L.H.: *Modern Packaging*, Nov. 154 (1964).
2. Wilks, R.A Jr. and Gilbert S.G.: *Food Tech.*, **43** (1), 47 (1969).
3. Wilks R.A. Jr. and Gilbert S.G.: *J. Food Sci.*, **37**, 72 (1971).
4. Fleckenstein J.G.: *Packaging Engineering*, **12**(2), 72 (1967).
5. Peled R. and Manhhein C.H.: *Modern Packaging*, Apr. 45 (1976).
6. Baquet A.: *Dragoco Rep.*, (1), 4 (1979).
7. Adcock C.H.: *Modern Packaging*, Sept. 151 (1962).
8. Gilbert S.G.: *Modern Packaging*, Feb. 129 (1966).
9. Nadeau H.G. and Neumann E.: *Modern Packaging*, Feb. 128 (1964).
10. Gilbert S.G. Oetzel L.I, Asp W. and Brazier I.L.: *Modern Packaging*, May. 167 (1965).
11. Wilks R.A. Jr. and Gilbert S.G.: *Mat. Res. and Stds.* **8** (1), 29 (1968).
12. ASTM F 151-72: 365.

A DIRAC - LIKE EQUATION

P. J. LEMOS

Physics Department North Texas State University Denton, Texas 76203

(Received March 30, 1982)

Summary

A generalization of the Dirac equation is developed both through a van der Waerden-type derivation and from a Dirac-like Lagrangian density. The Lagrangian and equation are invariant with respect to a «gauge-like» transformation out of which the fundamental Weak coupling for leptons falls out. Setting a parameter $m = 0$ results in the corresponding Dirac equation which is not invariant under the transformation in question.

Key Words : Weak Interactions - Ἀδύναται Ἀλληλεπιδράσεις, Gauge Interactions - Ἀλληλεπιδράσεις Βαθμίδων, Elementary Interactions - Στοιχειώδεις Ἀλληλεπιδράσεις, Electrons - Ἡλεκτρόνια, Myons - Μυόνια.

Introduction

The Dirac equation is known to describe the kinematics of leptons and believed to also describe the kinematics of quarks¹. However, it does not describe gauge interactions in a natural way, except for these derived from the gauge group U (1) of electromagnetism; for example in describing the leptonic Weak Interaction, it necessitates the ad hoc elimination of the $\Psi_a \gamma_\nu (1 - \gamma_5) \Psi_b$ and $\Psi_b \gamma_\nu (1 \pm \gamma_5) \Psi_a$ transition amplitudes. Still it has met with amazing success in describing electromagnetic interactions as mediated by a gauge field and this has led to the attempt to describe all interactions as mediated by gauge fields, which has resulted in the brilliant gauge theories of the last fifteen years². Such gauge field theories have used the Higgs mechanism³ to overcome the problem that, if the vacuum is invariant under a gauge group, the masses of the particles are identically equal to zero. The Higgs mechanism permits some of the gauge bosons to acquire non-vanishing and, in general, different from each other masses; observable consequences of this mass splitting have been experimentally verified². Similarly, consequences of the invariance of quarks under SU (3) and of leptons under SU (2) have been tested quite successfully⁴. But there are also experimental results that apparently can only be derived from quark models making contradictory assumptions about the physical properties of the constituent quarks⁵. Moreover gauge

symmetries by themselves do not predict everything we would wish a complete theory to predict, for an obvious example, the masses of the quarks and leptons.

We are perhaps at the stage where it would be profitable to be more specific. One way to do so is to study different generalizations of the Dirac equation with an eye toward the degree of fitness to experimental results and naturalness with which gauge interactions can be introduced into the resulting theories. It is in such a spirit that this series of research papers is undertaken.

We begin by developing a Dirac-like equation, namely

$$\gamma_\nu P^\nu \Psi = M \Psi \quad (1.1)$$

where

$$M = m + \gamma_5 \mu \quad (1.2)$$

γ_ν , γ_5 being the Dirac matrices, P^ν the momentum-energy operator and m , μ real numbers. The equation is «derived» and its plainwave solutions are found to satisfy.

$$E^2 - \mathbf{p} \cdot \mathbf{p} = m^2 - \mu^2 \quad (1.3)$$

and therefore it is reasonable to assume that $(m^2 - \mu^2)^{1/2}$ is the (rest) mass; as should be the case in any relativistic theory⁶, the mass commutes with the generators of the Lorentz group.

It can be shown that the equation can be made invariant with respect to a transformation similar to the gauge transformation of the electromagnetic potential, it can be formally derived from a Langrangian density also invariant under the transformation and it naturally excludes interactions of the form $\Psi_\alpha (1 \pm \gamma_5) \Psi_\alpha \cdot fF(x^\mu)$. In fact it gives the fundamental Weak coupling of the lepton fields and should be considered as a candidate for the equation that describes leptons. However we find that, for the invariance to hold, m and μ must be functions of the space-time coordinates with the restriction that $(m^2 - \mu^2)^{1/2}$ be a constant.

A Dirac-like equation

The Dirac equation may be derived from a special case of the system of two two-component equations

$$(P_0 - \sigma \cdot \mathbf{P}) \Phi_L = (m + \mu) \Phi_R \quad (2.1A)$$

$$(P_0 + \sigma \cdot \mathbf{P}) \Phi_R = (m - \mu) \Phi_L, \quad (2.1B)$$

namely the case $\mu=0$. Here P_0 is the energy and \mathbf{P} the momentum operators, σ the Pauli matrices and both m and μ are assumed real. Adding and subtracting the equations, we derive the following generalization of the Dirac equation:

$$\gamma_\nu P^\nu \Psi = (m + \gamma_5 \mu) \Psi, \tag{2.2}$$

where

$$\gamma_0 = \begin{pmatrix} I & O \\ O & -I \end{pmatrix},$$

$$\gamma_i = \begin{pmatrix} O & \sigma_i \\ -\sigma_i & O \end{pmatrix}, \quad i = 1, 2, 3 \tag{2.3B}$$

$$\gamma_5 = \begin{pmatrix} O & I \\ I & O \end{pmatrix} = i\gamma_1\gamma_2\gamma_3\gamma_4 \tag{2.3C}$$

are specific representation of the Dirac gamma matrices and

$$\Psi = \begin{pmatrix} \Phi_R + \Phi_L \\ \Phi_R - \Phi_L \end{pmatrix} \tag{2.4}$$

is a Dirac-like spinor. In fact the Dirac equation was derived by B. L. van der Waerden⁷ from the special case $\mu = 0$ of eq. (2.1) above.

The transformation

$$\Psi' = S\Psi \tag{2.5}$$

leaves the equation invariant if S is invertible and there exists another representation of the Dirac matrices γ_ν , γ_5 , a vector P'^ν and scalars m' , μ' such that

$$\gamma_\nu P'^\nu - m' - \gamma_5 \mu' = S(\gamma_\nu P^\nu - m - \gamma_5 \mu)S^{-1}. \tag{2.6}$$

Since the continuous Lorentz transformations are expressible in terms of such matrices, namely⁸ products of S_{Rot^n} and S_{Boost} (i, j can take the values 1, 2, 3, with $i \neq j$) given by

$$S_{\text{Boost}} = \cosh(\theta) + \gamma_0 \gamma_i \sinh(\theta), \tag{2.7A}$$

and

$$S_{\text{Rot}^n} = \cos(\Phi) + \gamma_i \gamma_j \sin(\Phi), \tag{2.7B}$$

the equation is invariant under the continuous Lorentz transformations.

If the theory is to lead to the same predictions for the primed as for the unprimed spinor, equation (2.2) must permit the probability of covariant quantities (i.e. tensors and spinors) to remain covariant and of the same tensorial/ spinorial rank as the quantities themselves; and equation (2.5) must result in transformed probability amplitudes whose relationship to the original ones is consistent with the interpretation of the theory. The two most commonly mentioned examples of eq. (2.2) are given by $S = e^{-ieE(x^\mu)}$ resulting in a gauge transformed equation and the S of eq. (2.7) resulting in a Lorentz transformed equation. For the gauge transforming S , the transition amplitude of a physical i.e. measurable quantity, say a Lorentz vector must remain unaltered; but this need not be true of the electromagnetic potential because it is not directly measurable; also the amplitude of P^ν must transform into the amplitude of $P'^\nu = P^\nu - ie^\nu (\ln S)$ and therefore P^ν is not a measurable vector; the amplitude of $(m^2 - \mu^2)^{1/2}$ must remain unchanged (see eq. (1.3)), but that of $m + \gamma_5 \mu$ need not be. For the S given by eq. (2.7), the transition amplitude of the same Lorentz vector P^ν must also transform as a Lorentz vector. We see by these examples that different assumptions about what is physically measurable would place different restraints on our freedom to choose S . In the case of equation (2.2), this requirement and the usual assumptions about which quantities are physical necessitate the usual interpretation of the Dirac covariants as the bilinear covariants of the theory.

The free-particle Hamiltonian

$$H = -\gamma_0 \gamma_i P^i + \gamma_0 m + \gamma_0 \gamma_5 \mu \quad (2.8)$$

commutes with the operator

$$x^i P^j - P^i x^j + \frac{i}{2} \gamma^i \gamma^j \quad (2.9)$$

(again i and j range over 1, 2, 3 and $i \neq j$) from which we conclude that our equation describes a spin 1/2 particle.

Gauge invariance

By analogy with the gauge theory of electromagnetism, we note that eq. (1.1) is invariant under the transformation

$$\Psi(x^\mu) \rightarrow \Psi'(x^\mu) = e^{iF(x^\mu)(1+\gamma_5)} \Psi(x^\mu), \quad (3.1)$$

where f is a real constant and $F(x^\mu)$ a real function, if P^ν is generalized to

$$P^\nu = i\partial^\nu - i\gamma_5 f B^\nu(x^\mu) - iC^\nu(x^\mu), \quad (3.2)$$

and the additional transformations

$$B^\nu(x^\mu) \rightarrow B'^\nu(x^\mu) = B^\nu(x^\mu) + \partial^\nu(F(x^\mu)) \tag{3.3A}$$

$$C^\nu(x^\mu) \rightarrow C'^\nu(x^\mu) = C^\nu(x^\mu) + \partial^\nu(F(x^\mu)) \tag{3.3B}$$

and

$$M \rightarrow M' = Me^{-2\gamma_5 fF(x^\mu)} \tag{3.3C}$$

are simultaneously performed.

It is reasonable but not necessary, in view of these equations, to assume that $B^\nu = C^\nu$ and we shall make this assumption until circumstances suggest otherwise. Also M , which up to now was implicitly assumed to be constant, is seen to be a variable field; but the quantity $(m^2 - \mu^2)^{1/2}$ remains invariant. There remains one final task: specifying under what conditions the free-particle Hamiltonian H , eq. (2.8), commutes with the angular momentum operator, eq. (2.9). It is obvious from the form of H that this will be the case when M is spherically symmetric. If the generalized gauge transformation, (3.1) - (3.3), is to preserve this, the generalized gauge functions $F(x^\mu)$ must all be spherically symmetric about the same center of symmetry.

Considering now the quantity

$$\mathcal{L}_{a,b} = \Psi_a \{ \gamma_\nu [i\partial^\nu - i(1 + \gamma_5)fB^\nu(x^\mu)] - (m + \gamma_5 m) \} \Psi_b \tag{3.4}$$

an obvious extension of the Dirac Langrangian density, the only exception being that the bra and ket spinors are not Langrangian we get the equations of motion

$$\{ \gamma_\nu [i\partial^\nu - i(1 + \gamma_5)fB^\nu(x^\mu)] - (m + \gamma_5 m) \} \Psi_b = 0 \tag{3.5A}$$

and

$$\{ \gamma_\nu [i\partial^\nu + i(1 + \gamma_5)fB^\nu(x^\mu)] - (m - \gamma_5 m) \} \Psi_a = 0 \tag{3.5B}$$

which show that Ψ_a and Ψ_b belong to states that couple to the field B^ν with opposite charges. The Langrangian density is invariant under the transformations (3.3) and

$$\Psi_a(x^\mu) \rightarrow \Psi'_a(x^\mu) = e^{fF(x^\mu)(1 + \gamma_5)} \Psi_a(x^\mu), \tag{3.6A}$$

$$\Psi_b(x^\mu) \rightarrow \Psi'_b(x^\mu) = e^{-fF(x^\mu)(1 + \gamma_5)} \Psi_b(x^\mu), \tag{3.6B}$$

and it gives a fundamental coupling of the form

$$H = -ifL_\nu(x^\mu)B^\nu(x^\mu), \tag{3.7A}$$

where

$$L_\nu(x^\mu) = \bar{\Psi}_a(x^\mu)\gamma_\nu(1 + \gamma_5)\Psi_b(x^\mu). \tag{3.7B}$$

This of course is the coupling of the electronic (or alternatively the muonic) lepton field to a vector boson field⁹. We may further choose the sum of two Langrangian densities, one coupling the electron to the electronic neutrino and the other coupling the muon to the muonic neutrino, to be the leptonic Langrangian density, i.e.

$$\mathcal{L}_{\text{LEPT}} = \mathcal{L}_{e,\nu_e} + \mathcal{L}_{\mu,\nu_\mu} \quad (3.8)$$

In fact, since \mathcal{L} is not Hermitian, we must add it to its Hermitian conjugate to get the full leptonic Langrangian density

$$\mathcal{L}_{\text{LEPT}} = \mathcal{L} + \mathcal{L}^\dagger \quad (3.9)$$

\mathcal{L}^\dagger will give the equations of motion for the Dirac conjugates of the spinors that enter in \mathcal{L} , however this redundancy is unavoidable here as much as with the Dirac Langrangian, since the spinors Ψ_a and $\bar{\Psi}_a$ are treated as distinct fields by the formalism.

The τ lepton can also be incorporated in exactly the same way.

Plane wave solutions

We now look for solutions of the form

$$\Psi = \begin{pmatrix} A \\ B \end{pmatrix} e^{-iEt + iP \cdot x} \quad (4.1)$$

which, when inserted into equation (2.2), gives

$$(E - m)A = (-\sigma \cdot P + \mu)B \quad (4.2A)$$

$$(E + m)B = (-\sigma \cdot P - \mu)A \quad (4.2B)$$

Pre-multiplying the first of these by $E + m$, we find

$$\begin{aligned} (E^2 - m^2)A &= (-\sigma \cdot P + \mu)(E + m)B \\ &= (-P \cdot P - \mu^2)A, \end{aligned}$$

i.e. the momentum-energy vector is constrained to satisfy

$$E^2 - P \cdot P = m^2 - \mu^2, \quad (4.3)$$

so it is reasonable to identify $m^2 - \mu^2$ with the square of the physical mass, and therefore also positive.

One set of solutions is, up to a normalization constant, the following :

$$\Psi_1 = \begin{pmatrix} 1 \\ 0 \\ -(P_3 + \mu)/(E + m) \\ -(P_1 + iP_2)/(E + m) \end{pmatrix} e^{-iEt + iP \cdot x} \quad (4.4A)$$

$$\Psi_2 = \begin{pmatrix} 0 \\ 1 \\ -(P_1 - iP_2)/(E + m) \\ -(P_3 - \mu)/(E + m) \end{pmatrix} e^{-iEt + iP \cdot x} \quad (4.4B)$$

$$\Psi_3 = \begin{pmatrix} -(P_3 - \mu)/(E - m) \\ -(P_1 - iP_2)/(E - m) \\ 1 \\ 0 \end{pmatrix} e^{-iEt + iP \cdot x} \quad (4.4C)$$

$$\Psi_4 = \begin{pmatrix} -(P_1 + iP_2)/(E - m) \\ -(P_3 - \mu)/(E - m) \\ 0 \\ 1 \end{pmatrix} e^{-iEt + iP \cdot x} \quad (4.4D)$$

Since $|E|$ can vary continuously from less than $|m|$ to greater than $|m|$, as equation (4.3) shows, avoiding singular solutions requires that $E/m > 0$ for the first two solutions and $E/m < 0$ for the other two. We note that setting $\mu=0$ gives the usual plane-wave Dirac spinors.

Another set of plane-wave solutions, which gives quite different, but related, values for the bilinear covariants, is the following

$$\Psi'_1 = \begin{pmatrix} m + \mu P_3/(E \mp n) \\ \mu(P_1 + iP_2)/(E + n) \\ -\mu - mP_3/(E + n) \\ -m(P_1 + iP_2)/(E + n) \end{pmatrix} e^{-iEt + iP \cdot x} \quad (4.5A)$$

$$\Psi'_2 = \begin{pmatrix} \mu(P_1 - iP_2)/(E + n) \\ m - \mu P_3/(E + n) \\ -\mu(P_1 + iP_2)/(E + n) \\ -\mu + mP_3/(E + n) \end{pmatrix} e^{-iEt + iP \cdot x} \quad (4.5B)$$

$$\Psi'_3 = \begin{pmatrix} -mP_3/(E - n) - \mu \\ m(P_1 + iP_2)/(E - n) \\ \mu P_3/(E - n) + m \\ \mu(P_1 + iP_2)/(E - n) \end{pmatrix} e^{-iEt + iP \cdot x} \quad (4.5C)$$

$$\Psi'_4 = \begin{pmatrix} -m(P_1 - iP_2)/(E - n) \\ -\mu + mP_3/(E - n) \\ \mu(P_1 - iP_2)/(E - n) \\ m - \mu P_3/(E - n) \end{pmatrix} e^{-iEt + iP \cdot x} \quad (4.5D)$$

where

$$n = (m^2 - \mu^2)^{1/2} \quad (4.6)$$

and here the first two solutions satisfy $E/n > 0$ while the last two satisfy $E/n < 0$.

Conclusion

The equation we developed has several appealing features. It describes a spin 1/2 particle and couples to a field which we have attempted to identify with the one that describes the Weak Interaction. It naturally describes particles with a Weak charge of value $\pm f$, and equi-charged particles do not interact with each other through this field. The equation is susceptible to further generalization and we intend to see how far this can go and whether more interesting groups such as $SU(2) \times SU(3)$ can lead us to a differential equation that describes a larger portion of the realm of elementary particle interactions.

The equation also has several drawbacks. It is derived from a Lagrangian density that is not invariant with respect to the gauge group of electromagnetism*. It couples two leptons of the same mass-squared (in our notation the same $m^2 - \mu^2$). The choice $(1 - \gamma_5)fF(x^\mu)$ for a gauge function is a possibility that we only excluded by our choice of the gauge function and it can not be excluded on principle. Of these drawbacks only the last one can not be dealt with by resorting to the Higgs mechanism and therefore is the more serious one; it is however a drawback that also exists in the Dirac equation.

In subsequent papers we intend to proceed along two parallel paths. One is the development of the theory derivable from equation (1.1) particularly such aspects of it as the study of the bilinear covariants, second quantization and classification of the fields described by the equation, derivation of physically relevant, closed-form and approximate solutions and the relationship to experimental results. The other is the generalization of the equation as indicated in the first paragraph of this section.

* It can be made invariant but only by giving Ψ_a and Ψ_b electric charge of equal magnitude in contradiction of the identifications in eq. (3.8).

Περίληψη

Μία εξίσωσις Τύπου Dirac

Εἰς αὐτό τό ἄρθρον ἀναπτύσομεν μίαν γενίκευσιν τῆς ἐξισώσεως τοῦ Διράκ, πρῶτον ἀπό μίαν παραγωγὴν τύπου Βάν ντέρ Βέρντεν (Van der Waerden) καί δεύτερον μέσω μιᾶς πυκνότητος Λανγκράνζ (Langrange) τοῦ εἴδους Διράκ. Ἡ πυκνότης Λανγκράνζ καί ἡ ἐξίσωσις εἶναι ἀναλλοίωτοι ὑπὸ ἓνα μετασχηματισμὸν βαθμίδος ἐκ τοῦ ὁποίου παράγεται ἡ βασικὴ Ἀσθενὴς Σύζευξις τῶν Λεπτονίων. Θέτοντες τὴν παράμετρον τῆς ἐξισώσεως ἴσην τοῦ «μηδέν» λαμβάνομεν τὴν ἐξίσωσιν τοῦ Διράκ, ἡ ὁποία ὁμοῦ δέν εἶναι ἀναλλοίωτος ὑπὸ τὸν μετασχηματισμὸν βαθμίδος τὸν ὁποῖον ἀναφέραμε προηγουμένως.

References

1. Fonda, L., and Ghirardi, G. C.: *Symmetry Principles in Quantum Physics*, Marcel Dekker, Inc., N. Y. 1970, pp. 502-503.
2. Salam, A.: *Rev. Mod. Phys.*, **52**, 525 (1980).
Glashow, S.L.: *Rev. Mod. Phys.*, **52**, 539 (1980).
Weinberg, S.: *Rev. Mod. Phys.*, **52**, 515 (1980).
Weinberg, S.: *Rev. Mod. Phys.*, **46**, 255 (1974).
3. Higgs, P. W.: *Phys. Rev. Lett.*, **12**, 132 (1964); **13**, 508 (1964); *Phys. Rev.*, **145**, 1156 (1966);
Kibble, T. W. B.: *Phys. Rev.*, **155**, 1554 (1967); Gurainik, G. S., Hagen, C. R. and Kibble, T. W. B.: *Phys. Rev. Lett.*, **13**, 321 (1964).
4. Lichtenberg, D. B.: *Unitary Symmetry and Elementary Particles*, Academic Press, New York and London, 1970 pp. 152-183, 206-224; Fonda, L., and Ghirardi, G. C. Ibid pp. 483-503.
5. Lichtenberg, D. B.: Ibid pp. 224-226.
6. Bailin, D.: *Weak Interactions*, Sussex University Press, London Troonto and New York, 1977, pp. 12-22.
7. Sakurai, J. J.: *Advanced Quantum Mechanics*, Addison-Wesley, Reading, Massachusetts, 1967, pp. 79-80.
8. Sakurai, J. J.: Ibid, pp. 97-99.
9. Bailin, D.: Ibid, p. 94.

SYNTHESIS AND STRUCTURE ELUCIDATION OF A NEW SERIES OF (TRIPHENYLPHOSPHINE) (N-ALKYLDITHIOCARBAMATE) (NITROSYL) NICKEL COMPLEXES

CONSTANTINOS A. TSIPIS, DIMITRIOS Ph. KESSISOGLOU and GEORGE E. MANOUSSAKIS.

Laboratory of Inorganic Chemistry, University of Thessaloniki, Thessaloniki, Greece

(Received May 19, 1982)

Summary

A new series of (triphenylphosphine) (N-alkyldithiocarbamate) (nitrosyl)nickel complexes of the general formula, $\text{Ni}(\text{NO})(\text{S}_2\text{CNHR})(\text{PPh}_3)$, $\text{R} = \text{Me, Et, i-Pr, n-Bu, s-Bu, t-Bu, i-Bu, C}_6\text{H}_5, \pi\text{-ClC}_6\text{H}_4$ and $\pi\text{-CH}_3\text{OC}_6\text{H}_4$, have been prepared and studied. The structures of the new complexes are discussed in relation to their spectroscopic (IR, $^1\text{H-NMR}$, UV-Vis and MS) and magnetic data. All the complexes were found to be of the $\{\text{NiNO}\}^{10}$ type with a pseudo-tetrahedral geometry containing a bending Ni-N-O group. The bending of the Ni-N-O group is relatively small and slightly depended on the nature of the dithiocarbamate ligands. These new nitrosyl-complexes do not oxidized to the corresponding nitro-complexes and therefore could not support O-transfer reactions.

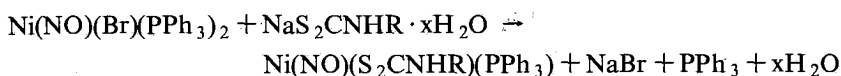
Key Words : (triphenylphosphine) (N-alkyldithiocarbamate) (nitrosyl)nickel complexes, bending Ni-N-O group, O-transfer reactions, pseudo-tetrahedral geometry.

Introduction

Transition metal nitro-nitrosyl redox couples have attracted considerable interest in the last few years, because of their use to the catalytic air oxidation of inorganic and organic substrates, such as CO, NO, PR_3 , olefins and isonitriles.¹⁻⁴ In the course of a research program in our laboratory to further develop new nitro-nitrosyl redox couples we have prepared and studied some new mixed-ligand nickel nitro- and nitrosyl-complexes.^{5,6} Some of these complexes were found to be potential homogeneous catalysts for the reaction between atmospheric oxygen and carbon monoxide. This catalytic O-transfer reaction takes place rapidly under mild conditions (room temperature and atmospheric pressure). Continuing our interest on the chemistry of nickel nitrosyl complexes we report on our results concerning the synthesis and study of some new (triphenylphosphine) (N-alkyldithiocarbamate)(nitrosyl)nickel complexes.

Results and discussion

The new (triphenylphosphine)(N-alkyldithiocarbamate)(nitrosyl)nickel complexes were prepared by the reaction of the bis(triphenylphosphine)(bromo)(nitrosyl)nickel complexes with the sodium or ammonium N-alkyldithiocarbamates according to the following general equation



where Ph = phenyl and R = Me, Et, *i*-Pr, *n*-Bu, *s*-Bu, *i*-Bu, *t*-Bu, C₆H₅, π -ClC₆H₄ and π -MeOC₆H₄.

The analytical data, as well as the melting points and the colors of the new compounds are shown in Table I.

These new nitrosyl-nickel complexes, which were obtained in nearly quantitative yields, were remarkably stable in the atmosphere either in solid state or in solution. However, on standing in the atmosphere for a long period (more than two weeks) showed decomposition, which was evident from the gradual change of their color from deep-blue to greenish-gray. All the complexes are soluble in most of the common organic solvents, such as chloroform, acetone, benzene, methylene chloride, but are insoluble in petroleum ether and water.

The structures of the complexes under investigation were established by spectroscopic methods (IR, UV-Vis, ¹H NMR and MS) as well as by magnetic susceptibility measurements.

Table II lists some of the most important infrared absorption bands of the new compounds along with their assignments.

The nitrosyl ligand showed in the infrared spectra a very strong and broad band in the region of 1720-1750 cm⁻¹. The $\nu(\text{NO})$ stretching frequency strongly suggest⁷⁻⁹ the existence of a bending Ni-N-O moiety in the complexes under investigation. Formally the nitrosyl-complexes can be regarded as containing the NO ligand in the form of NO⁺ with a considerable π -back bonding of the type Ni_(d) \rightarrow (NO)_(π^*), which has as a result the bending of the Ni-N-O group. As the π -back bonding increases the N \equiv O bond order decreases and consequently the $\nu(\text{NO})$ stretching frequency decreases as well. This is reflected from the lower $\nu(\text{NO})$ stretching frequencies observed in the complexes under investigation compared with those of the corresponding (triphenylphosphine)(nitrosyl)(O-alkyldithiocarbamate)nickel complexes.⁵ This observation could be explained on the basis of the stronger electron releasing ability of the N-alkyldithiocarbamate ligands relative to that of the O-alkyldithiocarbamate ligands, which enhances the π -back bonding phenomenon. Also, by substitution of the triphenylphosphine ligand with the stronger Lewis-base tri-*n*-butylphosphine ligand one could expect an enhancement of the π -back bonding and consequently a decrease of the $\nu(\text{NO})$ stretching frequencies. In fact this is the case.⁶ It is also worthwhile to be noticed that the $\nu(\text{NO})$ stretching frequencies of the studied compounds is only slightly affected from the nature of the alkyl group of the dithiocarbamate moiety.

TABLE I : Elemental analysis results and some physical properties of the (triphenylphosphine)(N-alkyldithiocarbamate)(nitrosyl) nickel complexes.

Compound	color	m.p. (°C)	M.W.	%C	%N	%H	%Ni
Ni(NO) (S ₂ CNHCH ₃) (PPh ₃)	blue	115-118	448 (457)	52.45 (52.51)	6.10 (6.12)	4.10 (4.15)	12.50 (12.84)
Ni(NO) (S ₂ CNHC ₂ H ₅) (PPh ₃)	blue	118-122	476 (471)	53.48 (53.50)	5.90 (5.94)	4.40 (4.45)	12.30 (12.46)
Ni(NO) [S ₂ CNH (n-C ₄ H ₉)] (PPh ₃)	blue	121-125	489 (499)	55.25 (55.31)	5.10 (5.61)	5.00 (5.01)	11.60 (11.76)
Ni(NO) [S ₂ CNH (i-C ₄ H ₉)] (PPh ₃)	blue	117-121	507 (499)	55.30 (55.31)	5.55 (5.61)	4.91 (5.01)	11.65 (11.76)
Ni(NO) [S ₂ CNH (s-C ₄ H ₉)] (PPh ₃)	blue	100-104	480 (499)	55.15 (55.31)	5.50 (5.61)	4.90 (5.01)	11.50 (11.76)
Ni(NO) [S ₂ CNH (t-C ₄ H ₉)] (PPh ₃)	blue	70- 75	482 (499)	55.18 (55.31)	5.53 (5.61)	4.96 (5.01)	11.70 (11.76)
Ni(NO) (S ₂ CNHC ₆ H ₅) (PPh ₃)	blue-green	128-130	522 (519)	56.90 (57.80)	5.85 (5.39)	4.02 (4.04)	11.11 (11.36)
Ni(NO) [S ₂ CNH (π-C ₁₀ H ₈)] (PPh ₃)	green-blue	130-134	557 (555)	53.60 (54.05)	5.00 (5.04)	3.60 (3.60)	10.20 (10.23)
Ni(NO) [S ₂ CNH (π-CH ₃ OC ₆ H ₄)] (PPh ₃)	green-blue	92	540 (549)	56.80 (56.88)	5.00 (5.10)	4.16 (4.18)	10.50 (10.74)

TABLE II : Relevant IR frequencies (cm^{-1}) of the (triphenylphosphine)(N-alkyldithiocarbamate)(nitrosyl)nickel complexes.

Compound	ν (N-H)	ν (N=O)	ν (C-S-N)	ν (C-S)	δ (Ni-NO)	ν (Ni-N)
Ni(NO) (S_2CNHCH_3) (PPh_3)	3280m,br	1750vs,br	1525s,br	970m	570m	430m
Ni(NO) ($\text{S}_2\text{CNHC}_2\text{H}_5$) (PPh_3)	3280m,br	1740vs,br	1512s,br	972m	572m	422m
Ni(NO) [$\text{S}_2\text{CNH}(n\text{-C}_4\text{H}_9)$] (PPh_3)	3240m,br	1752vs,br	1521s,br	941m	570m	420m
Ni(NO) [$\text{S}_2\text{CNH}(s\text{-C}_4\text{H}_9)$] (PPh_3)	3230m,br	1725vs,br	1512s,br	958m	565m	429m
Ni(NO) [$\text{S}_2\text{CNH}(i\text{-C}_4\text{H}_9)$] (PPh_3)	3230m,br	1722vs,br	1520s,br	989m	567m	430m
Ni(NO) [$\text{S}_2\text{CNH}(t\text{-C}_4\text{H}_9)$] (PPh_3)	3232m,br	1730vs,br	1502s,br	978m	569m	430m
Ni(NO) ($\text{S}_2\text{CNHC}_6\text{H}_5$) (PPh_3)	3200m,br	1740vs,br	1350s,br	995m	581m	440m
Ni(NO) [$\text{S}_2\text{CNH}(\pi\text{-ClC}_6\text{H}_4)$] (PPh_3)	3160m,br	1721vs,br	1345s,br	998m	576m	420m
Ni(NO) [$\text{S}_2\text{CNH}(\pi\text{-CH}_3\text{OC}_6\text{H}_4)$] (PPh_3)	3170m,br	1729vs,br	1400s,br	995m	623m	435m

The bending of the Ni-N-O moiety is further supported by the examination of the region of $400\text{-}600\text{ cm}^{-1}$ in the infrared spectra of the studied compounds. In this region the weak skeletal vibrations of the Ni-N-O group occur together with some other bands due to the other ligands in the complexes.^{10,11} The $400\text{-}600\text{ cm}^{-1}$ region of the infrared spectra of some representative nitrosyl-complexes under question is shown in Figure 1.

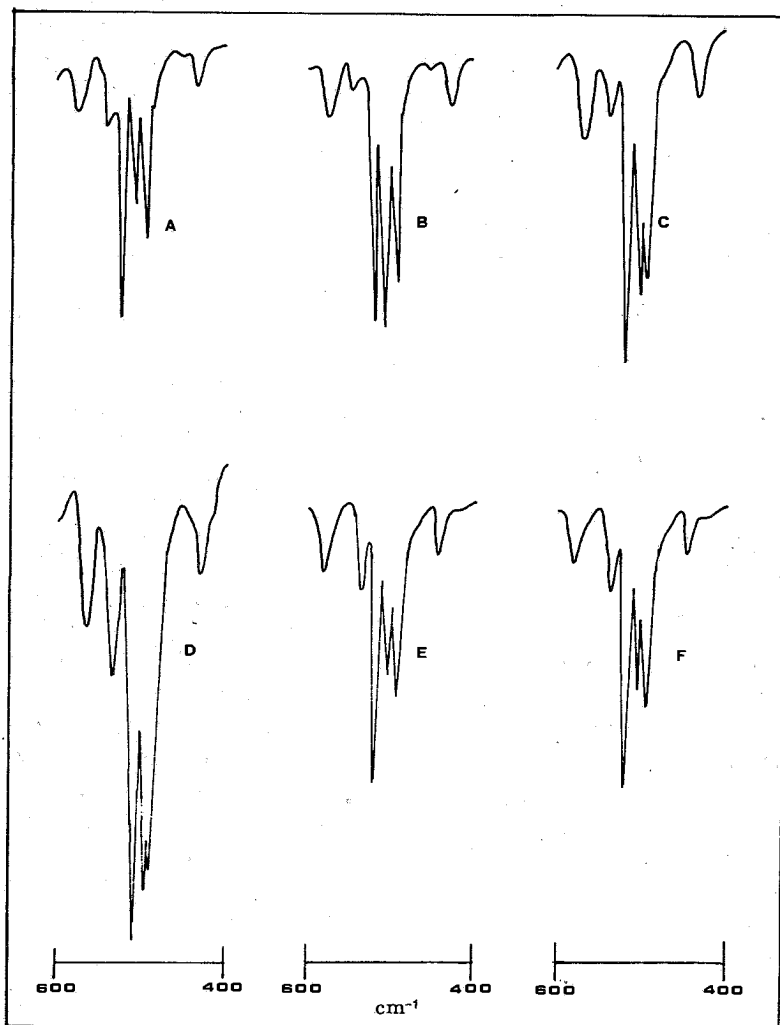


FIG. 1

From figure 1 it is evident that the two bands at $420\text{-}440\text{ cm}^{-1}$ and $570\text{-}620\text{ cm}^{-1}$, which are attributed^{10,11} to $\nu(\text{Ni-NO})$ and $\delta(\text{Ni-NO})$ normal modes of vibration, respectively, are weak for our nitrosyl-complexes with about the same intensity. This pattern of the two bands is indicative for the existense of a bending Ni-N-O

group, since it is well known^{10,11} that in linear MNO moieties the degenerate bending vibration $\delta(\text{M-NO})$ is more intense than the $\nu(\text{M-NO})$ vibration. On the other hand in the strongly bent MNO moieties the intensity of the $\nu(\text{M-NO})$ band is increased while that of the $\delta(\text{M-NO})$ band is decreased and only one bending vibration is expected because $\delta(\text{M-NO})$ is nondegenerate in strongly bent MNO moieties.

Of interest and considerable importance is also the region of $1350\text{--}1550\text{ cm}^{-1}$ of the i.r. spectra of the compounds under consideration. In this region the very intense thioureide band occurs.¹² The position of the thioureide band indicates that the $\text{C}\equiv\text{N}$ bond in the N-alkyldithiocarbamate ligand has a significant double bond character. This strongly suggest the bidentate character of the dithiocarbamate ligand.

From the above discussion of the infrared spectra we can conclude that the nitrosyl-complexes studied are four-coordinated nickel complexes containing the $[\text{NiNO}]^+$ unit. Such complexes must be of the $\{\text{NiNO}\}^{10}$ type which are complexes of the zerovalent nickel (d^{10}) containing the NO^+ ligand and a heteroallyl type η^3 -bonded dithiocarbamate ligand. It is obvious that the structure of these complexes must be tetrahedral with no unpaired electrons on the nickel atom. In fact, magnetic measurements by the Faraday technique showed that the complexes were diamagnetic which is in agreement with the d^{10} electron configuration of the central atom. The square-planar structure expected for the nitrosyl-complexes of the $\{\text{NiNO}\}^8$ type containing $\text{Ni}^{2+}(d^8)$ and NO^- ligand, which correspond to diamagnetic complexes as well, can be excluded on the basis of the infrared spectra, since no I.R. absorption bands characteristic for the coordinated NO^- ligand in the region of c.a. 1100 cm^{-1} were observed.⁷⁻⁹ On the other hand, as it is well known¹³ the tetrahedral $\{\text{MNO}\}^{10}$ complexes contain a linear MNO moiety which can be bent if the symmetry of the complexes is lowered. The bending of the Ni-N-O group in our complexes indicates a low symmetry and therefore their structure must be a distorted tetrahedral or in other words a pseudo-tetrahedral. Recent X-ray structure investigation¹⁴ of the analogous complex (triphenylphosphine)(O-cyclopentylthiocarbonato)(nitrosyl)nickel, which gave the $\nu(\text{NO})$ stretching frequency at 1780 cm^{-1} , showed that the complex adopts a pseudo-tetrahedral geometry with a bending Ni-N-O moiety (Ni-N-O angle = 167°). The pseudo-tetrahedral structure of the new nitrosyl-complexes is further supported from their electronic spectra. The positions of the band maxima and of discernible shoulders, as well as their $\log \epsilon_{\text{mol}}$ values are given in Table III.

In the ultraviolet region of the electronic spectra a number of intense bands occur, which can be assigned to intraligand transitions ($\pi^* \leftarrow \pi$ and $\pi^* \leftarrow n$). In the visible region of the spectra three low intensity bands occur, which on the basis of their intensity could be assigned to charge-transfer transitions. The high extinction coefficient of the band at c.a. 17.5 kK ($\approx 500\text{--}800$) is characteristic for tetrahedral complexes. Crystal-field transitions (d-d) are not expected for tetrahedral complexes of central atoms with d^{10} electron configuration, and were not observed in the nitrosyl complexes studied.

The ^1H NMR chemical shifts (τ , ppm) of the complexes described herein are given in Table IV.

TABLE III : Electronic spectra of the (triphenylphosphine)(N-alkyldithiocarbamate)(nitrosyl)nickel complexes in CH_2Cl_2 solutions.

Compound	Ultraviolet region	Visible region
	ν (kK) ($\log \epsilon_{\text{mol}}$)	ν (kK) ($\log \epsilon_{\text{mol}}$)
Ni(NO) (S ₂ CNHCH ₃) (PPh ₃)	41.32sh(4.25), 37.59(4.01)	23.69sh(2.83)
	35.46 (3.95), 31.44(3.85)	21.50sh(2.49)
	26.17 (3.32)	17.48 (2.70)
Ni(NO) (S ₂ CNHC ₂ H ₅) (PPh ₃)	40.81sh(4.05), 37.33(3.98)	23.64sh(2.75)
	35.08 (3.90), 31.44(3.78)	21.50sh(2.59)
	25.77 (3.04)	17.54 (2.98)
Ni(NO) [S ₂ CNH(i-C ₄ H ₉)] (PPh ₃)	40.65sh(4.04), 37.73(3.99)	23.52sh(2.82)
	34.72 (3.83), 31.44(3.83)	21.50sh(2.58)
	26.10 (3.25)	17.54 (2.74)
Ni(NO) [S ₂ CNH(t-C ₄ H ₉)] (PPh ₃)	40.98sh(4.15), 37.59(4.00)	23.52sh(2.74)
	35.08sh(3.95), 31.54(3.90)	21.50sh(2.58)
	25.70 (3.17)	17.54 (2.71)
Ni(NO) [S ₂ CNH(s-C ₄ H ₉)] (PPh ₃)	40.98sh(4.20), 37.59(4.04)	23.64sh(2.76)
	35.33sh(3.98), 31.54(3.95)	21.50sh(2.50)
	25.70 (3.13)	17.63 (2.92)
Ni(NO) [S ₂ CNH(n-C ₄ H ₉)] (PPh ₃)	40.81sh(4.15), 37.59(4.10)	23.64sh(2.80)
	35.33sh(4.02), 31.54(3.98)	21.50sh(2.50)
	25.90 (3.21)	17.63 (3.01)
Ni(NO) (S ₂ CNHC ₆ H ₅) (PPh ₃)	40.81sh(4.10), 37.73(4.05)	23.64 (3.58)
	35.08sh(4.00), 31.25(3.95)	21.18sh(2.83)
		17.48 (2.73)
Ni(NO) [S ₂ CNH(π -C ₁₀ H ₈)] (PPh ₃)	40.65sh(4.15), 37.73(4.10)	23.64 (3.40)
	35.08sh(4.00), 31.26(3.90)	21.41sh(2.78)
		17.70 (2.57)
Ni(NO) [S ₂ CNH(π -CH ₃ OC ₆ H ₄)] (PPh ₃)	41.00sh(4.10), 37.73(4.05)	23.62 (3.50)
	35.06sh(4.01), 31.25(3.90)	21.30sh(2.75)
		17.70 (2.61)

TABLE IV : ^1H NMR spectral Data of the (triphenylphosphine)(N-alkyldithiocarbamate)(nitrosyl)nickel complexes.

Compound	τ (ppm)
Ni(NO) (S ₂ CNHCH ₃) (PPh ₃)	7,26 (d, 3H, CH ₃ , J _{HH} =5,0) : 2,68 (m, 15H, C ₆ H ₅)
Ni(NO) (S ₂ CNHC ₂ H ₅) (PPh ₃)	9,03 (t, 3H, CH ₃ , J _{HH} =7,0) : 6,5-7,02 (m, 2H, CH ₂) : 2,67 (m, 15H, C ₆ H ₅)
Ni(NO) [S ₂ CNH(i-C ₄ H ₉)] (PPh ₃)	9,21 (d, 6H, CH ₃ , J _{HH} =6,5) : 8,02-8,72 (m, 1H, CH) : 6,91 (t, 2H, CH ₂ , J _{HH} =6,5) : 2,60 (m, 15H, C ₆ H ₅)
Ni(NO) [S ₂ CNH(n-C ₄ H ₉)] (PPh ₃)	9,16 (t, 3H, CH ₃ , J _{HH} =6,5) : 8,35-8,90 (m, 4H, -CH ₂ -CH ₂) : 6,53-7,00 (m, 2H, CH ₂ -NH-) : 2,61 (m, 15H, C ₆ H ₅)
Ni(NO) [S ₂ CNH(s-C ₄ H ₉)] (PPh ₃)	8,40-9,50 (m, 9H, CH ₃ -CH ₂ -CH ₃) : 5,80-6,50 (m, 1H, CH-NH) : 2,61 (m, 15H, C ₆ H ₅)
Ni(NO) [S ₂ CNH(t-C ₄ H ₉)] (PPh ₃)	8,53 (s, 9H, (CH ₃) ₃ -C) : 2,42 (m, 15H, C ₆ H ₅)

The chemical shifts and the multiplicity of the peaks observed are in accordance with the formulation of the new compounds. For the complexes (triphenylphosphine)(N-aryldithiocarbamate)(nitrosyl)nickel the peaks due to the aryl group of the dithiocarbamate moiety are obscured by the peaks due to the phenyl groups of the triphenylphosphine ligand and therefore no information could be obtained for their chemical shifts. This is the reason for the exclusion of these complexes in Table IV.

The most important peaks in the mass spectra of the studied nitrosyl-complexes are given in Table V.

The salient feature of the mass spectra of the studied compounds is the absence of the peak due to the molecular ion. This fact may be due to the pyrolytic decomposition, which these complexes undergo at elevated temperatures (170-250°C). All the compounds gave the base peak at $m/e = 262$. This peak corresponds to the $[PPh_3]^+$ ion. Another peak with high relative intensity was observed at $m/e = 294$ and corresponds to the $[SPPH_3]^+$ ion. This fragment is probably formed during the pyrolytic decomposition of the complexes, or through an intramolecular sulfur elimination from the dithiocarbamate ligand by the phosphine ligand, since it is well known that phosphines react easily with sulfur either bonded or free. Based on literature data¹⁵⁻²⁵ concerning the fragmentation pattern of phosphines and dithiocarbamate complexes we can propose the fragmentation scheme showed in figure 2 for our new nitrosyl-complexes of nickel.

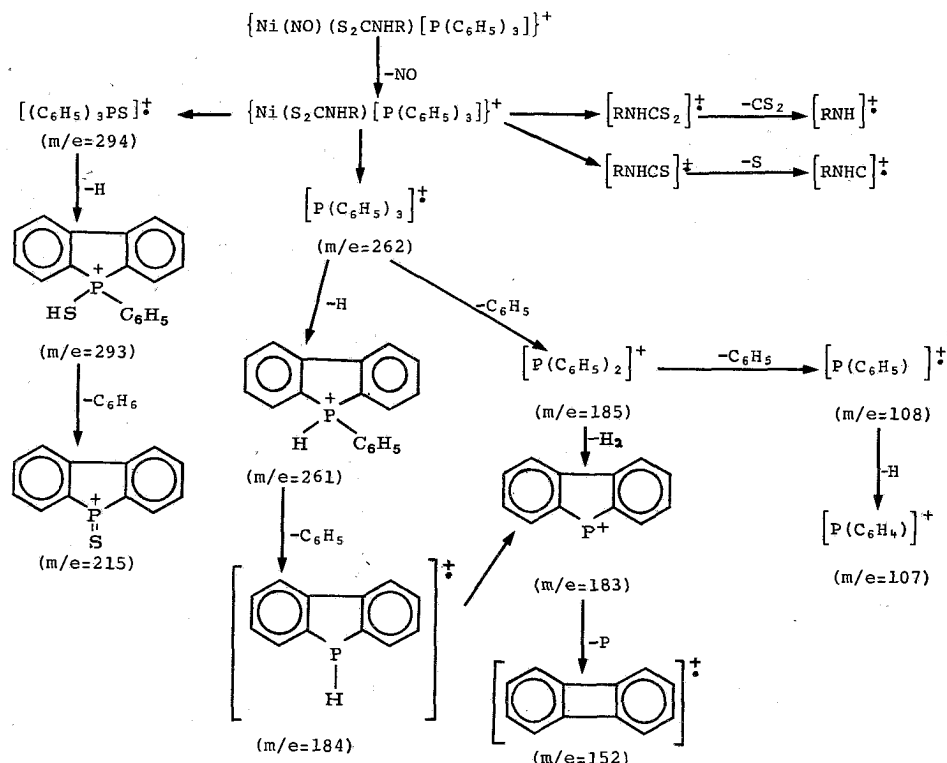


FIG. 2

TABLE V : Most relevant mass spectral peaks of the (triphenylphosphine)(N-alkyldithiocarbamate)(nitrosyl)nickel complexes.

Compound	m/e (R.I)
Ni(NO) (S ₂ CNHC ₂ H ₅) (PPh ₃)	27 (6) : 30 (39) : 32 (9) : 33 (5) : 34 (16) : 41 (50) : 44 (17) : 73 (66) : 74 (9) : 75 (6) : 76 (7) : 77 (12) : 107 (20) : 108 (42) : 131, 5 (2) : 152 (16) : 183 (87) : 184 (24) : 185 (61) : 215 (7) : 217 (5) : 261 (25) : 262 (100) : 277 (27) : 278 (17) : 293 (61) : 294 (92)
Ni(NO) (S ₂ CNHC ₂ H ₅) (PPh ₃)	27 (5) : 29 (5) : 30 (5) : 41 (7) : 43 (7) : 55 (7) : 77 (4) : 107 (12) : 108 (33) : 131, 5 (2) : 152 (8) : 183 (63) : 184 (16) : 185 (16) : 261 (16) : 262 (100) : 277 (7) : 278 (4) : 293 (8) : 294 (13) : 426 (0, 05)
Ni(NO) [S ₂ CNH(i-C ₄ H ₉)] (PPh ₃)	27 (6) : 29 (7) : 30 (8) : 41 (25) : 43 (17) : 55 (9) : 56 (8) : 57 (18) : 71 (4) : 72 (4) : 73 (4) : 77 (3) : 83 (4) : 84 (2) : 107 (8) : 108 (20) : 115 (16) : 131, 5 (1) : 149 (8) : 152 (6) : 183 (52) : 184 (13) : 185 (17) : 236 (2) : 261 (14) : 262 (100) : 277 (5) : 278 (3) : 293 (13) : 294 (22)
Ni(NO) [S ₂ CNH(t-C ₄ H ₉)] (PPh ₃)	27 (23) : 29 (70) : 30 (34) : 32 (13) : 41 (24) : 43 (8) : 44 (30) : 55 (20) : 56 (25) : 57 (97) : 59 (6) : 72 (16) : 83 (4) : 84 (9) : 107 (4) : 108 (11) : 115 (100) : 116 (8) : 149 (8) : 152 (2) : 183 (20) : 184 (15) : 185 (4) : 261 (5) : 262 (31) : 293 (1) : 294 (1)
Ni(NO) [S ₂ CNH(s-C ₄ H ₉)] (PPh ₃)	27 (12) : 29 (22) : 30 (63) : 32 (25) : 41 (32) : 55 (19) : 56 (25) : 57 (26) : 76 (10) : 77 (3) : 83 (2) : 107 (8) : 108 (24) : 115 (30) : 149 (11) : 152 (6) : 183 (50) : 184 (12) : 185 (11) : 261 (13) : 262 (100) : 277 (5) : 278 (3) : 293 (3) : 294 (6)
Ni(NO) (S ₂ CNHC ₆ H ₅) (PPh ₃)	27 (5) : 30 (31) : 32 (8) : 33 (5) : 34 (14) : 40 (16) : 41 (32) : 44 (7) : 45 (14) : 72 (28) : 73 (55) : 76 (4) : 77 (12) : 81 (3) : 107 (18) : 108 (41) : 131, 5 (6) : 152 (16) : 183 (25) : 184 (16) : 185 (57) : 215 (6) : 261 (24) : 262 (100) : 277 (32) : 278 (22) : 293 (50) : 294 (82)
Ni(NO) [S ₂ CNH(η-C ₁₀ H ₈)] (PPh ₃)	27 (4) : 30 (14) : 32 (4) : 34 (5) : 35, 5 (2) : 44 (7) : 45 (7) : 72 (11) : 73 (44) : 77 (9) : 107 (12) : 108 (25) : 131, 5 (1) : 152 (12) : 183 (78) : 184 (17) : 185 (34) : 215 (4) : 261 (9) : 262 (100) : 277 (29) : 278 (20) : 293 (31) : 294 (52)

Finally, it is worthwhile to be noticed that the new nitrosyl-complexes studied do not react with dioxygen to give the corresponding nitro-complexes. Therefore, our attempts to use these complexes as homogeneous catalysts in O-transfer reactions were unsuccessful. Comparing the new nitrosyl-complexes with the corresponding (tri-n-butylphosphine)(N-alkyldithiocarbamate)(nitrosyl)nickel complexes, which were found to be potential homogeneous catalysts in O-transfer reactions⁶, we can attribute their catalytic inertness to the lower bending of the Ni-N-O moiety as it is reflected from the $\nu(\text{NO})$ stretching frequencies. This idea is supported from the fact that the mechanism of the oxygenation of nitrosyl-complexes²⁶ includes an attack of the nitrogen atom of the nitrosyl ligand by the dioxygen through a HOMO-LUMO interaction. Thus as the bending of the Ni-N-O moiety increases, also the electron density on the nitrogen atom increases and the nucleophilic attack of the dioxygen is enhanced. Of course some more results concerning the mechanism of these catalytic O-transfer reactions are necessary to be obtained in order to find out the relation between the extent of the bending of the Ni-N-O moiety and the catalytic activity of the nitrosyl-complexes. Such studies are at present under investigation and the results will be published soon.

Experimental

Physical Measurements

Infrared spectra were recorded in the region of 4000-250 cm^{-1} on a Perkin-Elmer 467 spectrophotometer using KBr discs or nujol mulls. ^1H NMR spectra were obtained on a Varian A 60A (60 Mc/s) instrument in CDCl_3 solutions using TMS as an internal standard. Electronic spectra were obtained on a Perkin-Elmer-Hitachi 200 spectrophotometer with freshly prepared acetone or methylene chloride solutions. Mass spectra were measured on an RMU-6L Hitachi Perkin-Elmer mass spectrometer with ionisation source of AT-2P type operating at 70eV. Magnetic susceptibility measurements in solution were done by the Evans method using chloroform solutions 2% v/v in TMS and in solid state by the Faraday technique using $\text{Hg}[\text{Co}(\text{SCN})_4]$ as the calibrant. Carbon, hydrogen and nitrogen were determined using a Perkin-Elmer 240 Elemental Analyzer.

Preparation of the complexes

All manipulations were done under argon atmosphere and the reactions were carried out into Schlenk tubes. The solvents used were all of reagent grade and were used without further purification in synthetic work. For the preparation of the new (triphenylphosphine)(N-alkyldithiocarbamate)(nitrosyl)nickel complexes the following general method was employed :

To a solution of 0.693g (1.0 mmol) of the complex bromobis(triphenylphosphine)(nitrosyl)nickel prepared by published method²⁷ in 20 ml of acetone, a solution containing 1.0 mmol of the appropriate sodium or ammonium salt of the dithiocarbamate ligand in 20 ml of acetone was added slowly under continuous magnetic stirring. The reaction mixture was kept for 1 hr at room temperature and then the solvent was removed by evaporation under reduced pressure. The resulting

solid material was treated with diethyl ether (c.a. 30-40 ml) and the undissolved sodium or ammonium bromide was removed by filtration. The deep blue filtrate was condensed up to a small volume (c.a. 5 ml) and was diluted by addition of 5.0 ml of methanol. After cooling the new solution at -20°C the desired complex was separated as a deep blue crystalline material. After removing the solvent by filtration the solid compounds were washed several times with small portions of methanol and were dried under vacuum. Purification of the complexes was carried out by repeated recrystallizations from a mixture of diethylether and methanol.

Περίληψη

Σύνθεση και διεκρίνιση της δομής μιας νέας σειράς (τριφαινυλοφωσφίνο)(N-αλκυλοδιθειοκαρβαμιδικών)(νιτροζυλο)συμπλόκων του νικελίου.

Στην εργασία αυτή παρουσιάζονται τα αποτελέσματα που αφορούν τη σύνθεση και τη μελέτη της δομής μιας νέας σειράς (τριφαινυλοφωσφίνο)(N-αλκυλοδιθειοκαρβαμιδικών)(νιτροζυλο)συμπλόκων του νικελίου του γενικού τύπου $\text{Ni}(\text{NO})(\text{S}_2\text{CNHR})(\text{PPh}_3)_3$, όπου $\text{R} = \text{Me}, \text{Et}, i\text{-Pr}, n\text{-Bu}, s\text{-Bu}, t\text{-Bu}, i\text{-Bu}, \text{Ph}, p\text{-ClC}_6\text{H}_4$ και $p\text{-CH}_3\text{OC}_6\text{H}_4$.

Η δομή των νέων συμπλόκων διεκρινίζεται με βάση τα φασματοσκοπικά τους δεδομένα (IR, ^1H NMR, UV-Vis και MS), καθώς επίσης και με μετρήσεις των μαγνητικών τους ιδιοτήτων. Όλα τα σύμπλοκα που μελετούνται βρέθηκε, ότι περιέχουν τη δομική μονάδα $(\text{NiNO})^+$ και το N-αλκυλοδιθειοκαρβαμιδικό ligand ως διδραστικό ligand. Τέτοια σύμπλοκα είναι του γενικού τύπου $\{\text{NiNO}\}^{10}$ και είναι σύμπλοκα του μηδενοσθενούς νικελίου (d^{10}), που περιέχουν το ιόν του νιτροζωνίου, NO^+ , ως ligand και το N-αλκυλοδιθειοκαρβαμιδικό ligand με τη μορφή ενός η³-δεσμευμένου ετεροαλλυλικού τύπου ligand. Η διαμαγνητική φύση των μελετούμενων συμπλόκων συνηγεί για μια τετραεδρική διαμόρφωση γύρω από το κεντρικό άτομο του Ni^0 . Είναι, όμως, γνωστό ότι τα τετραεδρικά σύμπλοκα του γενικού τύπου $\{\text{MNO}\}^{10}$ περιέχουν γραμμική M-N-O ομάδα, η οποία μπορεί να παρουσιάσει κάμψη όταν η συμμετρία του συμπλόκου ελαττωθεί. Τα μελετούμενα σύμπλοκα βρέθηκε ότι περιέχουν κεκαμένη ομάδα Ni-N-O και επομένως η στερεοχημική του δομή θα πρέπει να είναι παραμορφωμένη τετραεδρική ή ψευδο-τετραεδρική. Πράγματι, αυτό διαπιστώθηκε και από μελέτες με ακτίνες-X ανάλογου συμπλόκου που περιέχει, αντί του N-αλκυλοδιθειοκαρβαμιδικού ligand το O-αλκυλοδιθειοκαρβονικό ligand. Η εξίσου πιθανή επίπεδη-τετραγωνική δομή για σύμπλοκα του $\text{Ni}^{2+}(d^8)$ με τό ligand NO ως NO^- αποκλείεται με βάση τα φάσματα I.R., αφού δεν παρατηρείται η χαρακτηριστική ταινία απορρόφησης $\nu(\text{NO}^-)$ στα 1100 cm^{-1} περίπου. Επίσης, δίνεται πιθανό πρότυπο διασπάσεως των συμπλόκων στα φάσματα μαζών.

Τέλος, τα μελετούμενα σύμπλοκα σε αντίθεση με τα αντίστοιχα σύμπλοκα της τρι-n-βουτυλοφωσφίνης, δεν οξειδώνονται προς τα αντίστοιχα νιτρο-σύμπλοκα, με αποτέλεσμα να μη μπορούν να χρησιμοποιηθούν ως καταλύτες σε αντιδράσεις μεταφοράς οξυγόνου.

References

1. Booth, G. and Chatt, J.: *J. Chem. Soc.*, 2099 (1962).
2. Feltham, R.D. and Kriege, J.C.: *J. Am. Chem. Soc.*, **101**, 5064 (1979).
3. Doughty, D.T., Gordon, G. and Stewart Jr. R.D.: *J. Am. Chem. Soc.*, **101**, 2645 (1979).
4. Andrews, M.A. and Kelly, K.P.: Abstracts of the X International Conference on Organometallic Chemistry, Toronto, Canada, p. 117 (1981).
5. Kessissoglou, D.Ph., Tsipis, C.A. and Manoussakis, G.E.: *J. Inorg. Nucl. Chem. Letters*, **16**, 245 (1980).
6. Tsipis, C.A., Kessissoglou, D.Ph. and Manoussakis, G.E.: *Inorg. Chim. Acta*, in press.
7. Lewis, J., Irving, R.J. and Wilkinson, G.: *J. Inorg. Nucl. Chem.* **7**, 32 (1958).
8. Griffith, W.P., Lewis, J. and Wilkinson, G.: *J. Inorg. Nucl. Chem.*, **7**, 38 (1958).
9. Gans, P.: *J. Chem. Soc., Chem. Commun.*, 144 (1965).
10. Quinby, M.S. and Feltham, R.D.: *Inorg. Chem.*, **11**, 2468 (1972).
11. Quinby-Hunt, M. and Feltham, R.D.: *Inorg. Chem.*, **17**, 2515 (1978).
12. Coucouvanis, D.: *Progress Inorg. Chem.*, **11**, 321 (1970).
13. Enemark, J.H. and Feltham, R.D.: *Coord. Chem. Rev.*, **13**, 339 (1974).
14. Phanariotis, P., Christidis, P.C. and Rentzeperis, P.J.: *Z. fur. Crystallography*, was submitted for publication.
15. Williams, D.H., Ward, R.S. and Cooks, R.G.: *J. Am. Chem. Soc.*, **90**, 966 (1968).
16. Bublitz, D.E. and Baker, A.N.: *J. Organometal. Chem.*, **9**, 363 (1967).
17. Miller, J.M.: *J. Chem. Soc.*, A 828 (1967).
18. Colton, R. and Porter, Q.N.: *Austr. J. Chem.*, **21**, 2215 (1968).
19. Rake, A.T. and Miller, J.M.: *J. Chem. Soc.*, A 1881 (1970).
20. Bowie, J.M. and Nussey, B.: *Org. Mass. Spectr.*, **3**, 933 (1970).
21. Rake, A.T. and Miller, J.M.: *Org. Mass. Spectr.*, **3**, 237 (1970).
22. Fraser, I.W., Garnett, J.L., Gregor, I.K. and Jessop, K.J.: *Organic. Mass. Spectrometry*, **10**, 69 (1975).
23. Manoussakis, G.E., Micromastoras, E.D. and Tsipis, C.A.: *Z. Anorg. Allg. Chem.*, **403**, 87 (1974).
24. Given, K.W., Mattson, B.M. and Pignolet, G.H.: *Inorg. Chem.*, **15**, 3152 (1977).
25. Given, K.W., Mattson, B.M., Miessler, G.I. and Pignolet, L.H.: *J. Inorg. Nucl. Chem.*, **39**, 1309 (1977).
26. Ugo, R., Bhaduri, S., Johnson, B.F.G., Khair, A., Pickard, A. and Benn-Taarit, Y.: *J.C.S. Chem. Comm.*, 694 (1976).
27. Feltham, R.D.: *Inorg. Chem.*, **3**, 116 (1964).

FLUORESCENT PROPERTIES OF AROMATIC COMPLEXES WITH RARE EARTHS AND OTHER ELEMENTS OF THE IIIa-GROUP

GEORGE KALLISTRATOS

Technical assistance : U. KALLISTRATOS and H. MÜNDNER

Department of Experimental Physiology, Faculty of Medicine, University of Ioannina, Ioannina Greece

(Received May 24, 1982)

Summary

A number of aromatic complexes with rare earths (Lanthanides) and other elements of the IIIa Group of the periodical system have been synthesized. Many of these complexes exhibit a strong monochromatic fluorescence when excited with ultra-violet light. The formation of complexes is indicated through their physico-chemical properties. Three mechanisms which could be responsible for the enhancement of the fluorescence have been investigated. The complexes reported possess very important physical, chemical and biological properties which could be applied in several fields of science.

Key words : Monochromatic fluorescence, aromatic complexes, rare earths, Actinides, Scandium, Yttrium, Intramolecular Energy Transport.

Introduction

Some elements, especially these of the IIIa group of the periodical system such as Scandium, Yttrium, Lanthanides (rare earths) and Actinides, form complexes which in their electronic excited state, exhibit strong fluorescence of varying monochromatic properties^{1,2}. Also some organic compounds possess fluorescent properties which can be enhanced in presence of the above mentioned elements.³ The mechanism of the fluorescent enhancement is probably due to the following possibilities.⁴

- I. The fluorescence of the reagent is enhanced in the presence of the elements.
- II. The fluorescence of the elements is enhanced by the presence of the reagent.
- III. Through the so called «Intramolecular Energy Transport» the excitation energy is absorbed from the organic part of the complex; The energy is then intramolecularly transferred to the rare earth ion⁵⁻¹⁰.

Furthermore, the potential lasing ability of rare earth chelates was reported two decades ago.¹¹⁻¹³

It must be pointed out that some aromatic heterocyclic reagents investigated have a very important practical application in solar energy conversion for the photochemical cleavage of water in Hydrogen and Oxygen.¹⁴ For example 2,2-bipyridine forms transition metal complexes with Ruthenium which can serve as both electron acceptors and electron donors.¹⁵⁻¹⁹ In the present paper some fluorescent reactions of aromatic complexes with Lanthanides and other elements of the IIIa group are reported.

Materials and Methods

Except Promethium which exists in radioactive form, all other rare earths (Lanthanides) as well as Scandium, Yttrium, Thorium and Uranium in form of their oxides, chlorides or nitrates, were purchased from Auer-Remy Hamburg, Fluka Buchs, and other International Chemical Companies. Their purity was 99.9 %.

The chlorides and nitrates of the investigated elements were dissolved according to their solubility in water, ethyl alcohol or pyridine. For the quantitative determination of the sensitivity of the reaction of the elements with the chosen reagent, increased amounts from 0.5 to 30 micrograms/element were plotted on a Schleicher and Schüll No 2043a paper at 2-3 cm intervals, by means of a micro-apparatus (Desaga Mikrometer-Dosiergerät). The paper stripes were dried at 100°C for 5-10 minutes. The dry papers were then sprayed with an aqueous or alcoholic solution of 0.1 - 0.5 % of the selected reagent, dried again at 100°C and observed under the Ultra-Violet light with two UV-lamps of a wave length of 254 nm and 366 nm (UFANALYS). The fluorescence intensity of the reaction was registered in relation to the amount present as a weak fluorescence sensitivity (+), medium (++) or strong fluorescence (+++). The fluorescence spectra of the complexes were recorded either from the chromatographic stripes or from solutions, by means of a ZEISS PMQ II Spectral fluorimeter using varying excitations wave-length.

For the above mentioned investigations only microgram amounts were necessary. For further studies on the nature and properties of the complexes, greater amounts of substances were required. The synthesis of many lanthanide complexes is a relatively easy procedure. For example, 100 mg of EuCl_3 or TbCl_3 are dissolved in 10 ml pyridine or ethyl alcohol. The corresponding reagent is also dissolved in pyridine or ethyl alcohol and mixed together with the lanthanide solution at a ratio of Lanthanide/Reagent 1:1, 1:2, 1:3, and 1:4. A precipitate is formed either immediately or after refluxing the reaction products for a few minutes up to some hours, depending upon the nature of the complexes formed. After filtration, the solid phase (precipitate) is washed several times with different solvents in order to remove impurities and dried in an excicator.

The infrared spectra of the complexes were recorded with a Beckman IR-4 spectrographic apparatus.

The melting points of the complexes were determined with a Mettler FP-I apparatus (sensitivity $\pm 0.1^\circ\text{C}$).

Results and Discussion

The formation of complexes between the rare earths (and other elements) and some organic compounds, is indicated through the changes of the following physico-chemical properties of the reacting components²⁰.

1. Changes of solubility after the reaction of the Lanthanide solution and the reagent solution and the formation of precipitates.
2. The characteristic intensive fluorescence produced after the excitation of the complex with ultra-violet light.
3. The comparison of the infrared spectra of the reacting components and the Lanthanide complex formed (Figure 1).

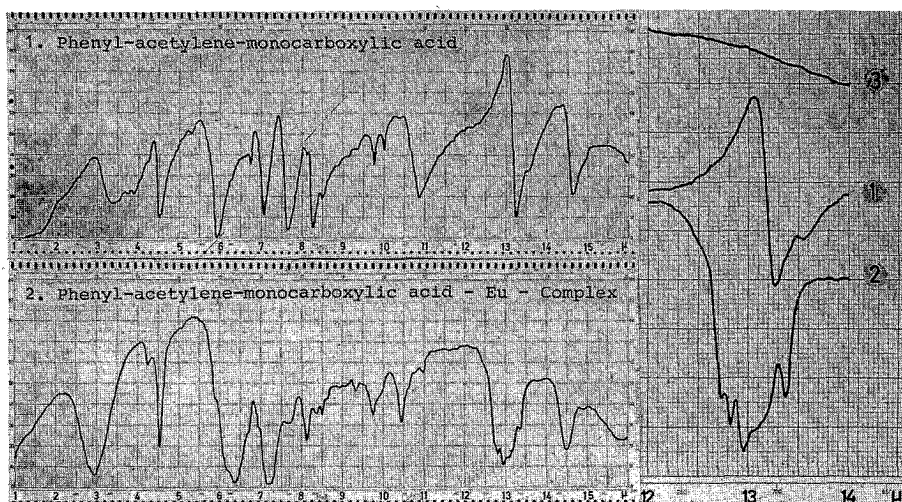


FIG. 1 : Infrared spectra of: (1) Phenyl-acetylene-monocarboxylic acid (above), and (2) Phenyl-acetylene-monocarboxylic acid Europium complex (below). Notice the different absorption bands, especially between 12-14 μ resulting from the formation of a complex. (3) EuCl_3 .

4. Changes of the melting point of the new complex derivative formed in comparison to the reacting components.

Concerning the possible mechanism of the fluorescence enhancement either of the reagents or of the elements, it was found experimentally that :

I. The weak fluorescence of some organic compounds such as Reserpine or Testosterone can be intensified in presence of Thorium or Terbium ions respectively (Figures 2 and 3). The fluorescence intensity is proportional to the concentration of the ions present in the investigating solution (Figure 4).

II. The weak fluorescence of some elements of the IIIa group can be intensified in presence of suitable reagents (Figure 5).

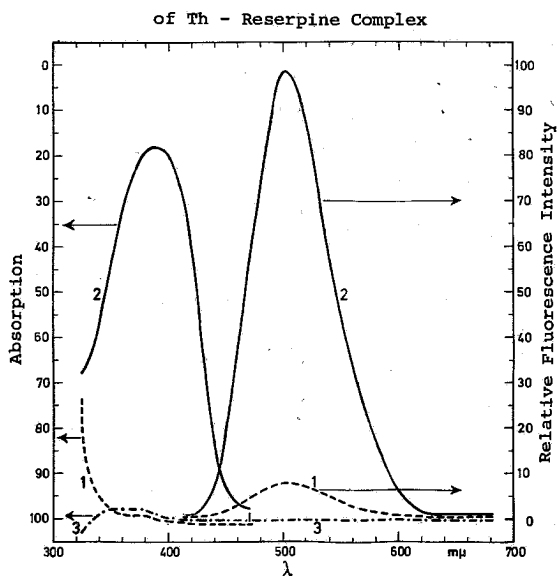


FIG. 2 : Absorption and fluorescence spectra of: (1) Reserpine 0.5 mg/ml; (2) Reserpine 0.5 mg/ml + ThCl_4 0.5 mg/ml, and (3) ThCl_4 0.5 mg/ml in ethyl alcohol. Excitation 393 nm. Fluorescence maximum 500 nm.

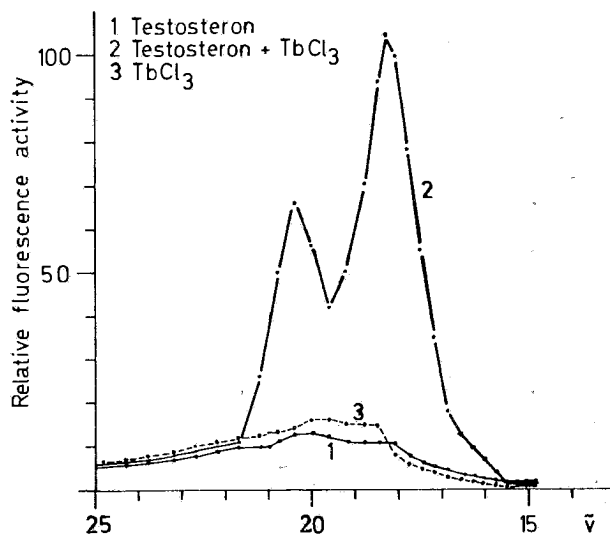


FIG. 3 : Fluorescence spectra of (1) Testosterone 1 mg/ml, (2) Testosterone 1 mg/ml + TbCl_3 0.5 mg/ml and (3) TbCl_3 0.5 mg/ml in ethyl alcohol. Excitation energy 278 nm. Fluorescence maxima 542 and 490 nm. Notice the increased intensity of the fluorescence of the Tb-Testosterone-complex.

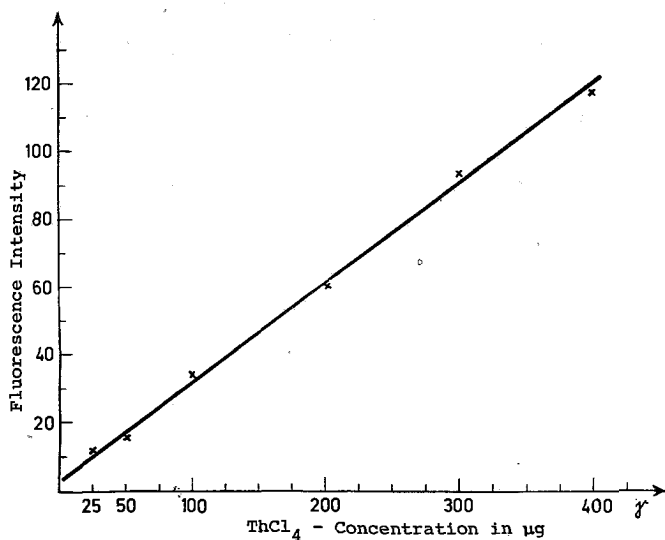


FIG. 4 : Fluorescence intensity of constant amount of 0.5 mg/ml Reserpine (ordinates) in relation to increased concentration of Thorium ions (Abscissas). Notice the enhancement of the Reserpine fluorescence from 4 RFI-units (Relative Fluorescence Intensity) without Thorium ions, to 120 RFI-units in presence of 0.4 mg ThCl₄/ml. (Excitation wavelength 392 nm. Fluorescence maximum 500 nm).

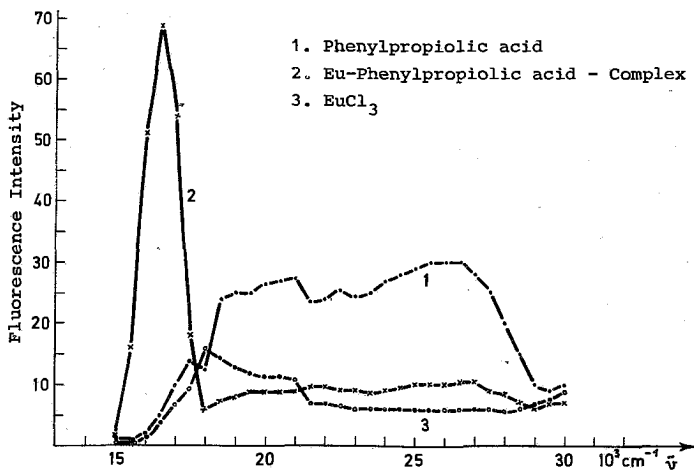
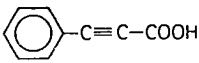


FIG. 5 : Fluorescence spectra of: (1) Phenylpropionic acid (Phenylacetylene-monocarboxylic acid), (2) Eu-phenylpropionic acid complex, and (3) EuCl₃ registered from paper chromatographic stripes (1 × 4 cm) with a Zeiss spectral fluorimeter RMQ II, ZFM 4. (Europium concentration ca 40 micrograms/cm². Excitation energy 312.5 nm (32 × 10³ cm⁻¹).

III. For studying the «Intramolecular Energy Transport» a number of aromatic complexes of rare earths have been synthesized which are classified in eleven groups (Tables I-XI).

I. Group : Acetylene derivatives : (Table I)

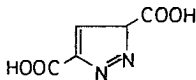
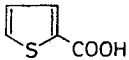
TABLE I : Acetylene derivatives

Chemical formula	Substance	Element	/ Fluorescence	/ Intensity
$\text{HC}\equiv\text{C}-\text{COOH}$	Acetylene-monocarboxylic acid	Y	green	+++
		Lu	green	+++
		Gd	green	++
	Phenyl-acetylene-mono carboxylic acid (Phenylpropionic acid)	Eu	red	+++
		Tb	green	+++

Acetylene derivatives form complexes with Yttrium and several Lanthanides. For example; acetylene monocarboxylic acid forms with Yttrium and Lutetium complexes which exhibit a strong green fluorescence in UV-light. The complexes with Gadolinium possess a less intensive green fluorescence. Europium and Terbium complexes exhibit a weak red and yellow fluorescence respectively. The red and the yellow-green fluorescence of Europium and Terbium can be enhanced when the Hydrogen of the acetylene group is substituted with a phenyl group, i.e. phenylpropionic acid.

II. Group : Five member heterocyclic rings (Table II)

TABLE II : Five membered heterocyclic rings

	Pyrazol-3,5-dicarboxylic acid	Eu	red	+++
		Tb	green	+++
		Gd	blue	++
	Thiophen-2-carboxylic acid	Eu	red	++
		Tb	green	+++

Pyrazol-3,5-dicarboxylic acid forms complexes with Europium, Terbium and Gadolinium which exhibit a strong red green and blue fluorescence respectively.

Thiophen-2-carboxylic acid forms complexes with Europium and Terbium with a red and green fluorescence in UV-light.

III. Group : Benzoic acid derivatives (Table III)

TABLE III : Benzoic acid derivatives

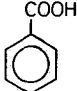
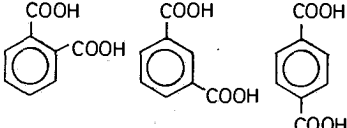
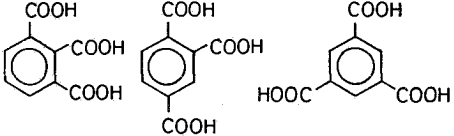
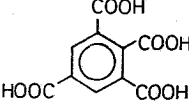
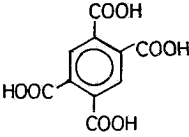
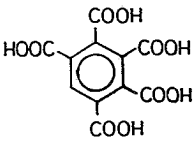
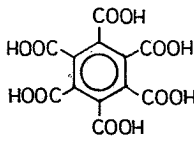
Chemical formula	Substance	Element	/ Fluorescence	/ Intensity
	Benzoic acid	Tb	green	+++
	ortho-, meta-, and para-phthalic acid (Phthalic, Isophthalic and Terephthalic acids)	Tb	green	+++
	1,2,3-, 1,2,4- and 1,3,5-Benzene-tricarboxylic acids (Hemimellitic, Trimellitic and Trimesic acids)	Tb	green	+++
	1,2,3,5-Benzene-tetracarboxylic acid (Prenitic acid)	Tb	green	+++
	1,2,4,5-Benzene-tetracarboxylic acid (Pyrromellitic acid)	Eu Tb	red green	++ +++

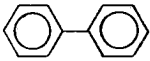
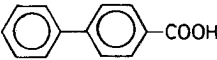
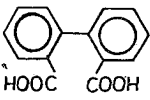
TABLE III : Benzoic acid derivatives (continue)

Chemical formula	Substance	Element	/ Fluorescence	/ Intensity
		Tb	green	+++
1,2,3,4,5-Benzenepenta-carboxylic acid	1,2,3,4,5,6-Benzenhexa-carboxylic acid			

All benzoic acid derivatives from mono- up to hexacarboxylic acids form complexes mainly with Terbium which exhibit a strong green fluorescence. The position of the carboxylic groups in the benzene molecule may influence the intensity of the green fluorescence of Terbium in UV-light. The strongest green fluorescence under the experimental conditions mentioned, was observed with the 1,2,4,5-tetracarboxylic acid derivative, the Pyromellitic acid-Terbium complex.

IV. Group : Biphenyl derivatives (Table IV).

TABLE IV : Biphenyl derivatives

Chemical formula	Substance	Element	/ Fluorescence	/ Intensity
	Biphenyl	Eu Tb	red green	+ +
	Biphenyl-4-carboxylic acid	Eu Tb	red green	+++ +++
	Biphenic acid	Eu Tb	red green	+ +++

Biphenyl forms complexes with Europium and Terbium, possessing a weak red and green fluorescence in UV-light respectively. The fluorescence of both complexes is enhanced when a Hydrogen of the aromatic ring is substituted with a

carboxylic group, i.e. in case of Biphenyl-4-carboxylic acid. A further enhancement of the green fluorescence intensity of the Terbium complex may occur, when a second Hydrogen atom from the second aromatic ring is substituted with a carboxylic group, i.e. in case of Biphenic acid. In that case, a reduction of the red fluorescent intensity of the Eu-biphenic acid complex takes place. This example indicates the importance of the substitution for the enhancement or reduction of the fluorescent intensity of the complexes.

V. Group : Pyridine derivatives (Table V).

TABLE V : Pyridine derivatives

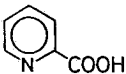
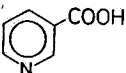
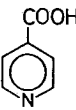
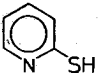
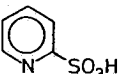
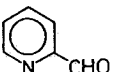
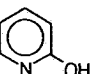
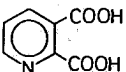
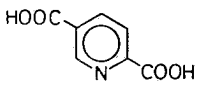
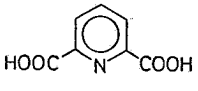
Chemical formula	Substance	Element	Fluorescence	Intensity
	Pyridine-2-carboxylic acid (2-Picolinic acid)	Eu Tb U	red green green	+++ +++ +++
	Pyridine-3-carboxylic acid (Nicotinic acid)	Eu Tb U	red green green	+++ +++ +
	Pyridine-4-carboxylic acid (Isonicotinic acid)	Eu Tb	red green	++ +++
	2-Mercaptopyridine	Tb	green	+++
	2-Pyridine-2-sulfonic acid	Eu Tb Gd	red green green	+ +++ +
	Pyridine-2-aldehyde	Tb	green	+++
	2-Hydroxypyridine	Tb	green	+++
	Pyridine-2,3-dicarboxylic acid (quinolinic acid)	Eu Tb	red green	++ +++

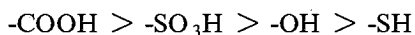
TABLE V : Pyridine derivatives (continue)

Chemical formula	Substance	Element	Fluorescence	Intensity
	Pyridine-2,5-dicarboxylic acid	Eu	red	+++
		Tb	green	+++
	Pyridine-2,6-dicarboxylic acid (Dipicolinic acid)	Eu	red	+++
		Tb	green	+++

Pyridine itself exhibits no fluorescence with the rare earths. It is mainly used as a solvent for many reactions of lanthanides and reagents.

Its substituted derivatives are very important compounds because they form complexes with a number of elements. For example, Pyridine-2-carboxylic acid (2-picolinic acid) form complexes with Europium, Terbium and Uranium with an intensive red, green and green fluorescence respectively when stimulated with UV-light. The strong green fluorescence of Uranium is reduced when the distance of the carboxylic group from the Nitrogen of the heterocyclic ring is increased, as in the case of pyridine-3-carboxylic acid (Nicotinic acid) and pyridine-4-carboxylic acid (Isonicotinic acid).

The groups in the α -substituted position also influence the intensity of the fluorescence. For example, the different acidic groups may selectively reduce the red fluorescent intensity of Europium in the following order :



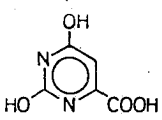
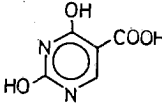
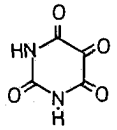
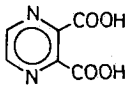
The intensity of the green fluorescent complex of Terbium with the above groups remains almost unchanged.

A strong green fluorescence exhibits the Tb-pyridine-2-aldehyde complex. Pyridine-dicarboxylic acids: Pyridine-2,3-dicarboxylic acid (quinolinic acid), Pyridine-2,5-dicarboxylic acid and Pyridine-2,6-dicarboxylic acid (dipicolinic acid) form also complexes with Europium and Terbium producing a strong red and green fluorescence respectively under the UV-light. Furthermore, Eu-dipicolinate was used in the TREES (Time-Resolved Eu Excitation Spectroscopy) technic for elucidating details of Eu (III) binding to macromolecules, for example zinc endoprotease thermolysin.²¹

VI. Group : Pyrimidine and Pyrazine derivatives (Table VI).

Orotic acid forms fluorescent complexes with Europium, as well as green and blue fluorescent complexes with Terbium and Gadolinium respectively.^{2,22,23} The green fluorescence of Terbium is enhanced when instead of orotic acid, the iso-

TABLE VI : Pyrimidine and pyrazine derivatives

	Orotic acid	Eu Tb Gd	red green blue	++ +++ +
	Iso-orotic acid	Eu Tb	red green	+ +++
	Alloxan	Tb	green	+++
	Pyrazine-2,3-dicarboxylic acid	Eu Tb	red green	+++ +++

orotic acid is used as complexing agent. In this case, the red fluorescence of Eu-iso-orotic acid complex is reduced in comparison to Eu-orotic acid complex. Alloxan forms complexes with Terbium exhibiting a strong green fluorescence in UV-light.

Pyrazine-2,3-dicarboxylic acid forms complexes with Europium and Terbium with a strong red and green fluorescence in UV-light.

VII. Group : Di- and tripyridyl derivatives (Table VII).

a,a'-Dipyridyl forms complexes with several rare earths such as Europium, Terbium and Gadolinium exhibiting red, green and green fluorescence in the UV-range.^{2,4,25}

The isomer γ,γ' -dipyridyl forms also complexes with Europium and Terbium but the fluorescence intensity is weaker in comparison to Eu-*a,a'*-dipyridyl complex.

Very interesting monochromatic fluorescent derivatives forms *a,a',a''*-tripyridyl with Europium and Gadolinium (red), Terbium (green) as well as Scandium Yttrium and Lanthan (blue) when excited with UV-light. Terpyridyl complexes with Europium and Terbium have been reported since 1965.²⁶

VIII. Group : Quinoline derivatives (Table VIII).

Unsubstituted quinoline forms complexes with Scandium, Yttrium, Lanthanum, Cerium and Thorium. Substituted derivatives such as 8-hydroxy-quinoline forms also complexes with Scandium, Yttrium, and Lutetium as well, possessing a strong fluorescence.

TABLE VII : Di- and tripyridyl derivatives

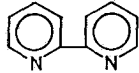
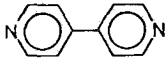
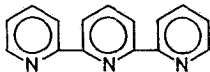
Chemical formula	Substance	Element	/Fluorescence	/ Intensity
	α,α'-Dipyridyl	Eu	red	+++
		Tb	green	+++
		Gd	green	+
	γ,γ'-Dipyridyl	Eu	red	+
		Tb	green	+++
	α,α',α''-Tripyridyl	Eu	red	+++
		Tb	green	+++
		Y	blue	+++
		La	blue	+++
		Sc	blue	++
		Gd	red	++

TABLE VIII : Quinoline derivatives

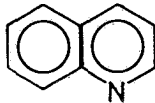
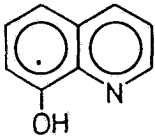
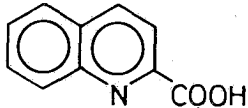
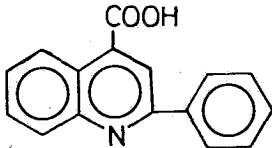
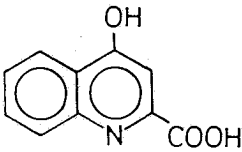
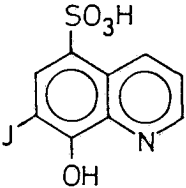
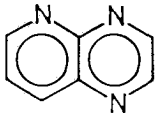
Chemical formula	Substance	Element	/ Fluorescence	/ Intensity
	Quinoline	Th	blue	+++
		Sc	green-yellow	+++
		Y	green-yellow	++
		La	green-yellow	++
		Ce	green-yellow	++
	8-Hydroxyquinoline	Sc	green	+++
		Y	green	++
		Lu	green	+++
	Quinoline-2-carboxylic acid (quinaldinic acid)	Eu	red	+++
		La	blue	++
	Phenyl-quinoline-4-carboxylic acid (Atophan)	Eu	red	+++
		Sc	yellow	+

TABLE VIII : Quinoline derivatives (continue)

Chemical formula	Substance	Element	Fluorescence	Intensity
	4-hydroxy-quinoline-2-carboxylic acid (Kynurenic acid)	Eu	red	+++
		Tb	green	+++
		Gd	green	+++
		Sc	blue	++
		Y	blue	++
	7-Jodo-8-hydroxyquinoline-5-sulfonic acid (Chiniofon)	Y	blue	+++
		Lu	blue	+++
		Gd	orange	++
	1,4,5-Triaza-naphthalene	Eu	red	+
		Tb	green	+++

Quinoline-2-carboxylic acid (quinaldinic acid) forms fluorescent derivatives with Europium (red) and Lanthanum (blue). The pharmacologically active drug Atophan (phenyl-quinoline-4-carboxylic acid) forms complexes with Europium, exhibiting a strong red fluorescence while Scandium gives a weak yellow fluorescence.^{2,27}

Some metabolic products such as kynurenic acid (4-hydroxy-quinoline-2-carboxylic acid) forms complexes with a characteristic monochromatic strong fluorescence in the UV-range with Europium (red) Terbium and Gadolinium (green) Scandium and Yttrium (blue). Another substituted quinoline derivative, the Chiniofon (7-Jodo-8-hydroxyquinoline-5-sulfonic acid) forms complexes with Yttrium and Lutetium exhibiting a strong blue fluorescence while Gadolinium gives an orange fluorescence.

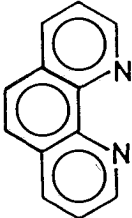
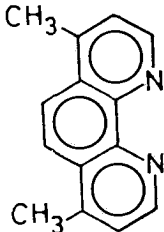
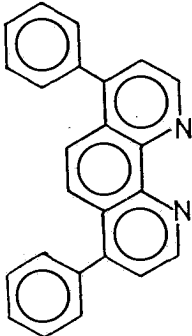
1,4,5-Triazanaphthalene reacts with Terbium and the complex exhibits a strong green fluorescence in UV-range, and a weak red fluorescence with Europium.

IX. Group : Phenanthroline derivatives (Table IX).

1,10-Phenanthroline forms fluorescent complexes with Europium, Terbium and Uranium exhibiting a strong red, green and green fluorescence respectively, in UV-range.^{2,4,27,36}

Some physico-chemical properties such as LASER action, fluorescence analysis, etc, of Europium, Terbium and Gadolinium-1,10-phenanthroline complexes have been reported.^{25,28,29}

TABLE IX : Phenanthroline derivatives

Chemical formula	Substance	Element	Fluorescence	/ Intensity
	1,10-Phenanthroline	Eu	red	+++
		Tb	green	+++
		U	green	+++
	4,7-dimethyl-1,10-phenanthroline	Eu	red	+++
		Tb	green	+
		U	green	+++
	4,7-diphenyl-1,10-phenanthroline (Bathophenanthroline)	Eu	red	+++
		Tb		-
		U	green	+
		Th	blue	+++
		La	blue	++

Similar results were obtained with the 4,7-dimethyl substitution of the 1,10-phenanthroline. More interesting is the 4,7-diphenyl substitution of 1,10-phenanthroline (Bathophenanthroline) because the red fluorescence of Europium is enhanced and the green fluorescence of Terbium and Uranium is diminished. Bathophenanthroline forms also complexes with Thorium and Lanthanum possessing a blue fluorescence in the UV-range.

X. Group : Cytostatic derivatives of Aza-uracil (Table Xa).

Europium and Terbium-5-aza-uracil complexes exhibit a red and green fluorescence in UV-region. The intensity of the green fluorescence of the Terbium complex can be enhanced if the 6-aza-uracil isomer is used.

Xb : Cytostatic purine derivatives (Table Xb).

Allopurinol forms complexes with Terbium and Uranium possessing a weak green fluorescence in UV-region. A stronger green and blue fluorescence exhibit the 8-azaxanthine complexes of Terbium and Gadolinium respectively.

TABLE Xa : Cytostatic Aza-uracil derivatives

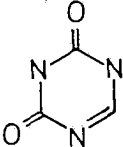
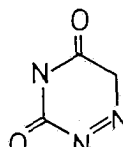
Chemical formula	Substance	Element	Fluorescence	Intensity
	5-Aza-uracil	Eu Tb	red green	+ ++
	6-Aza-uracil	Eu Tb	red green	+ +++

TABLE Xb : Cytostatic purine derivatives

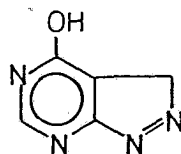
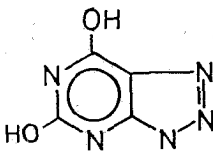
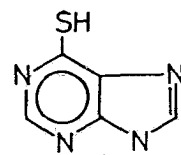
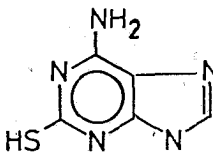
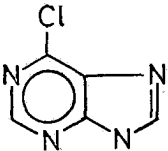
Chemical formula	Substance	Element	Fluorescence	Intensity
	Allopurinol	Tb U	green green	+ +
	8-Azaxanthine	Tb Gd	green blue	+++ +++
	6-Mercaptopurine	Tb	green	+++
	6-Aminopurine- 2-thiol	Tb	green	+++

TABLE Xb : Cytostatic purine derivatives (continue)

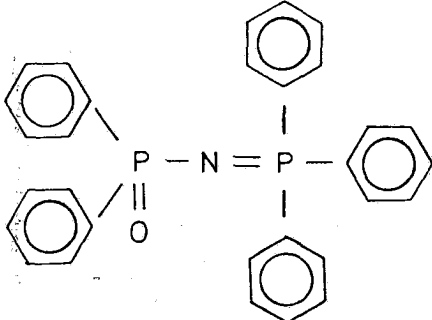
Chemical formula	Substance	Element	Fluorescence	Intensity
	6-Chloropurine	Tb	green	+++

The compounds 6-mercaptapurine, 6-chloropurine, and 6-aminopurine-2-thiol form complexes with Terbium exhibiting a strong green fluorescence in UV-region.³⁰

Lanthanide-cytostatic complexes possessing both tumor growth inhibitory effect and malignant cells photosensitive properties may be useful for the selective destruction of cancer cells.³¹

XI. Group : Organic phosphonimido derivatives (Table XI)

TABLE XI : Organic phosphonimido derivatives

Chemical formula	Substance	Element	Fluorescence	Intensity
		Eu	red	+++
		Tb	green	+++
		U	green	+++

Diphenyl-phosphonimido-triphenyl-phosphoran

Diphenyl-phosphonimido-triphenyl-phosphoran forms complexes with Europium, Terbium and Uranium. These complexes exhibit a strong red, green and green fluorescence respectively, when excited with ultra-violet light.

Many of the above mentioned reactions have also a practical application in several fields of science and have been used in the analytical chemistry for the detection of Lanthanides and other elements,^{32,33,34} for fluorimetric analysis³⁵ for the enhancement of sensitivity in microanalysis³ etc.

Also in Physics, i.e. monochromatic fluorescence, intramolecular energy

transport, LASER, etc. In biology and Medicine, for example the combination of both cytostatic and photosensitive properties in one compound with the target of selective killing of malignant cells, etc. Furthermore, many of the aromatic compounds mentioned form also complexes with Ruthenium and other elements which could be useful derivatives for the important research projects of the solar energy conversion for the photochemical cleavage of water, in order to increase their efficacy and yield of Oxygen and Hydrogen.

Περίληψη

Φθορίζουσες ιδιότητες αρωματικών συμπλόκων ενώσεων σπανίων γαιών, και άλλων στοιχείων της ομάδος IIIa.

Παρασκευάστηκαν διάφορες σύμπλοκες ενώσεις σπανίων γαιών (Λανθανιδίων), Σκανδίου, Υτρίου, Θορίου και Ουρανίου, με αρωματικές ουσίες. Η σύμπλοκη μορφή αυτών των ενώσεων αποδεικνύεται από την μελέτη των φυσικοχημικών των ιδιοτήτων, όπως π.χ. διαφορές των υπερύθρων φασμάτων, έντασις φθορισμού, σημείον τήξεως, διαλυτότης κλπ. Πολλές από τις παρασκευασθήσες σύμπλοκες ενώσεις ευρέθη ότι εκπέμπουν έντονο μονοχρωματικό φθορισμό (πράσινο, κυανού και ερυθρό) όταν διεγερθούν με υπεριώδη ακτινοβολία. Επίσης μελετήθηκαν οι εξής τρεις μηχανισμοί οι οποίοι δύνανται να αυξήσουν την ένταση του φθορισμού :

I. Ο ασθενής φθορισμός του οργανικού αντιδραστηρίου μπορεί να αυξηθή παρουσία ενός εκ των προαναφερθέντων στοιχείων π.χ. ο φθορισμός μερικών βιολογικώς δρώντων ουσιών όπως της Ρεζερπίνης ή Τεστοστερόνης ημπορεί να αυξηθή παρουσία ιόντων Θορίου και Τερβίου αντιστοιχώς. Κατ' αυτόν τον τρόπον επιτυγχάνεται η αύξησις της ευαισθησίας του χημικού προσδιορισμού των ανωτέρω ενώσεων.

II. Ο ασθενής φθορισμός ενός εκ των στοιχείων της ομάδος IIIa ημπορεί να αυξηθή παρουσία ενός καταλλήλου οργανικού αντιδραστηρίου. Π.χ. ο ασθενής φθορισμός του Ευρωπίου παρουσία του Φαινυλο-ακετυλενο-μονοκαρβοξυλικού οξέος.

III. Δι' ενός «Ενδομοριακού μηχανισμού μεταφοράς ενεργείας». Εις αυτήν την περίπτωσιν, η ενέργεια διεγέρσεως απορροφάται από το οργανικό μέρος της συμπλόκου ενώσεως και μεταφέρεται εις το ανόργανον ιόν.

Οι παρασκευασθήσες σύμπλοκες ενώσεις ταξινομήθησαν εις ένδεκα ομάδες και περιγράφονται οι φθορίζουσες ιδιότητες εις τους αντίστοιχους πίνακες.

References

1. Kallistratos G. Pfau A. and Ossowski B.: *Anal. Chim. Acta* **22**, 195 (1960).
2. Kallistratos G. Pfau A. and Ossowski B.: *Naturwiss.* **47**, 468 (1960).
3. Kallistratos G.: *J. Less Common Metals* **29**, 226 (1972).

4. Sinha S.P.: *Complexes of rare earths*, Pergamon, Oxford (1966).
5. Weissman S.I.: *J. Chem. Phys.* **10**, 214 (1942).
6. Sevchenko A.N. and Morachevskii A.G.: *Izv. Akad. Nauk CCCP, Ser. Fiz.* **15**, 628 (1951).
7. Sevchenko A.N. and Trofimov A.K.: *Zh. Eksper. Teor. Fiz.* **21**, 220 (1951).
8. Crosby G.A. and Kasha M.: *Spectrochim. Acta* **10**, 377 (1958).
9. Crosby G.A. and Whan R.E.: *J. Chem. Phys.* **32**, 614 (1960).
10. Crosby G.A.: *Mol. Crystal* **1**, 37 (1966).
11. Whan R.E. and Crosby G.A.: *J. Mol. Spectrosc.* **8**, 315 (1962).
12. Rieke F.F. and Allison R.: *J. Chem. Phys.* **37**, 3011 (1962).
13. Bykov V.P.: *Zh. Eksper. Teor. fiz.* **43**, 2313 (1962).
14. Sprintschnik G. et al.: *J. Am. Chem. Soc.* **98**, 2337 (1976).
15. Demas J.N. and Adamson A.W.: *J. Am. Chem. Soc.* **95**, 5159 (1973).
16. Bock C.R., Meyer T.J. and Whitten D.G.: *J. Am. Chem. Soc.* **96**, 4710 (1974).
17. Navon G. and Sutin N.: *Inorg. Chem.* **13**, 2159 (1974).
18. Lawrence G. and Balzani V.: *Inorg. Chem.* **13**, 2976 (1974).
19. Gray H. and Maverick A.: *Science* **214**, 120 (1981).
20. Kallistratos G. and Mündner H.: *J. Less Common Metals* **27**, 426 (1972).
21. Horrocks W. and Sudnik D.: *Science* **206**, 1194 (1979).
22. Kasimova L.V., Burjulina V.N. and Serebrenikov V.V.: *Zh. Obst. Chimii* **48**, 1433 (1978).
23. Sarpotdar A. and Burr J.G.: *J. Inorg. nucl. Chem.* **41**, 549 (1979).
24. Sinha S.P.: *Spectrochim. Acta* **20**, 879 (1964).
25. Filipescu N. Hurt C.R. and McAvoy N.: *Nature* **217**, 631 (1968).
26. Sinha S.P.: *Z. Naturforsch.* **20**, 164 (1965).
27. Kononenko L.I., Vitkun R.A. and Drobyazko V.N.: *Russ. J. Inorg. Chem.* **17**, 649 (1972).
28. Butter E., Seifert W. and Kreher K.: *Z. Chem.* **6**, 269 (1966).
29. Sinha S.P. and Butter E.: *Mol. Phys.* **16**, 285 (1969).
30. Kallistratos G. and Pfau A.: *J. Less Common Metals* **19**, 68 (1969).
31. Kallistratos G. and Faske E.: *Folia Biochim. Biol. Graeca* **17**, 4 (1980).
32. Hais I.M. and Macek K.: *Handbuch der Papierchromatographie*, Jena (1963).
33. Anderson R.G. and Nickless G.: *The Analyst* **92**, 207 (1967).
34. Jung K. and Specker H.: *Fresenius Z. Anal. Chem.* **289**, 48 (1978).
35. Weissler A.: *Anal. Chem.* **46**, 500 (1974).
36. Melby L.R. et al.: *J. Am. Chem. Soc.* **86**, 5117 (1964).